GRAN SASSO SCIENCE INSTITUTE

Thesis defence
XXXIV PhD cycle

Optimisation of amplification and gas mixture for directional Dark Matter searches with the CYGNO/INITIUM project

Candidate : Giorgio Dho

Supervisor: Prof.ssa Elisabetta Baracchini

14 – 04 – 2023

Istituto Nazionale di Fisica Nucleare

www.gssi.it

Summary

- Directional Dark Matter (Intro)

- Amplification Stage Optimisation

- Negative Ion Drift Operation

    Atmospheric Pressure

    Lower Pressure

- Directionality Studies

    CYGNO-30 Limits

    DM Discrimination

Summary

- Directional Dark Matter (Intro)
- Amplification Stage Optimisation
- Negative Ion Drift Operation
  - Atmospheric Pressure
  - Lower Pressure
- Directionality Studies
  - CYGNO-30 Limits
  - DM Discrimination

GSSI

Dark Matter

- Standard Model and General Relativity are the most succesful theories of modern physics
- Astrophysical and cosmological measurements indicate that the picture is still incomplete and some ingredients are still missing
- Deviations from expectations are observed across all scales
- All these measurements are related to gravitational effects
- Dark matter (DM) considered an established paradigm of modern physics (84% of all matter)

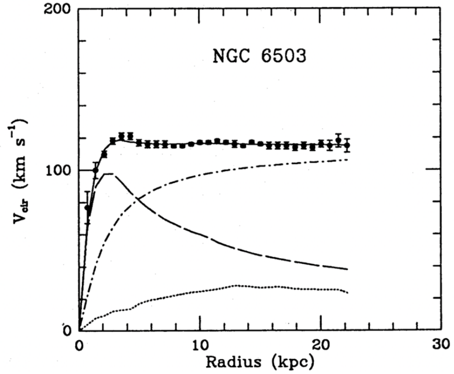

Begeman et al, R.A.S., 249 (3) (1991)

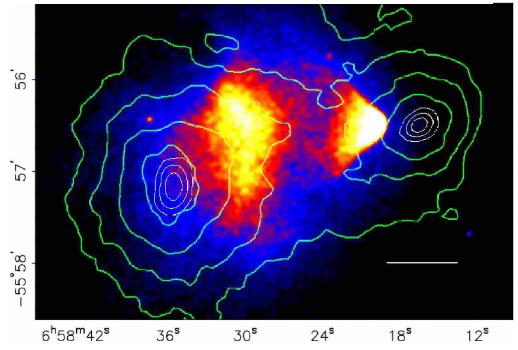

Clowe et al, AJ, 648 (2) (2006)

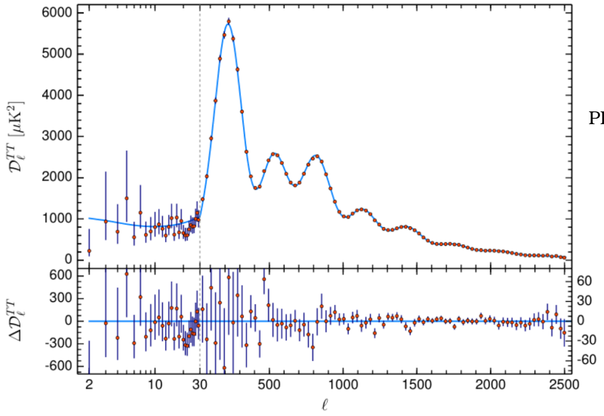

PLANCK, A.A., 641 (2020)

Dark Matter Candidates

Our knowledge of gravity is incomplete → **MOND** $R_{\mu\nu}+\frac{1}{2}g_{\mu\nu}R+\alpha f_{\mu\nu}(g_{\mu\nu}) = \frac{8\pi G}{c^4}T_{\mu\nu}$

Dark Matter Candidates

Our knowledge of gravity is incomplete → **MOND** $R_{\mu\nu} + \frac{1}{2} g_{\mu\nu} R + \alpha f_{\mu\nu}(g_{\mu\nu}) = \frac{8\pi G}{c^4} T_{\mu\nu}$

Unobserved astrophysical object cause the gravitational effects measured → **PBH**

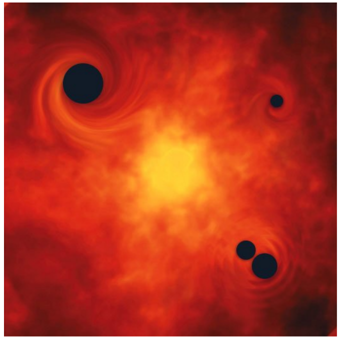

Dark Matter Candidates

Our knowledge of gravity is incomplete → **MOND** $R_{\mu\nu}+\frac{1}{2}g_{\mu\nu}R+\alpha f_{\mu\nu}(g_{\mu\nu}) = \frac{8\pi G}{c^4}T_{\mu\nu}$

Unobserved astrophysical object cause the gravitational effects measured → **PBH**

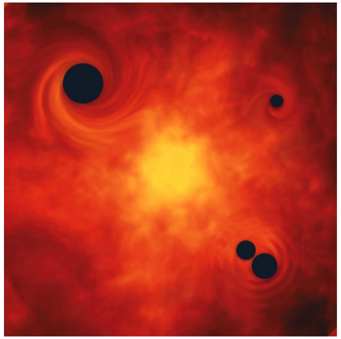

New particle or set of them is responsible →

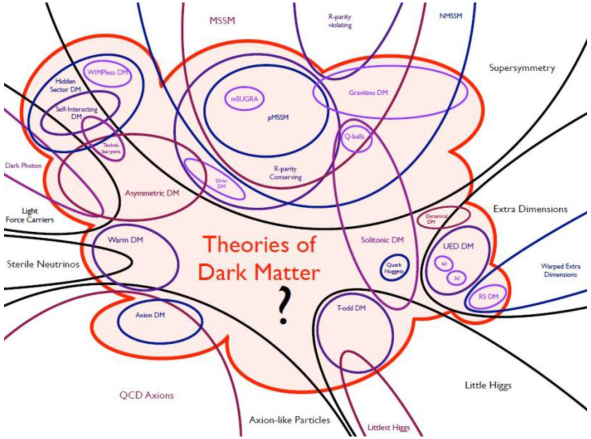

Dark Matter Candidates

Our knowledge of gravity is incomplete → **MOND** $R_{\mu\nu}+\frac{1}{2}g_{\mu\nu}R+\alpha f_{\mu\nu}(g_{\mu\nu}) = \frac{8\pi G}{c^4}T_{\mu\nu}$

Unobserved astrophysical object cause the gravitational effects measured → **PBH**

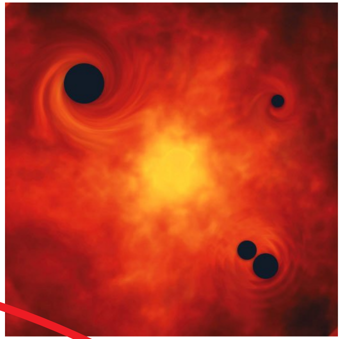

New particle or set of them is responsible →

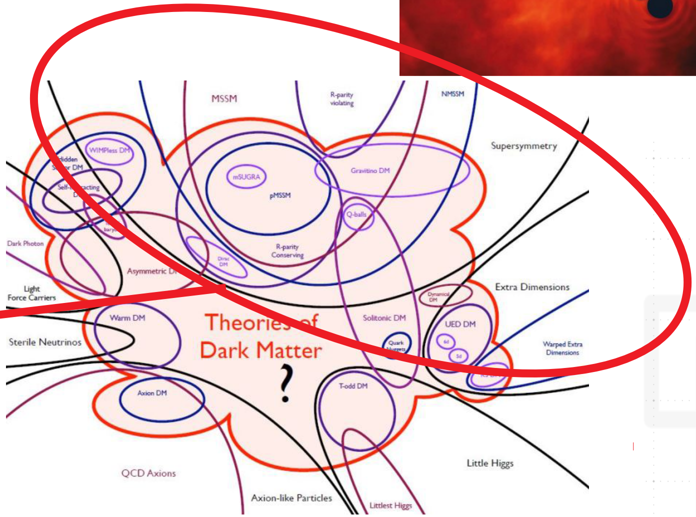

WIMPs

WIMPs

- To be consistent with the measurements particles need to be:
  - Non baryonic
  - Neutral and colour-free
  - Stable
  - Abundant (Ω = 0.26)
  - Weakly interacting
  - Warm or cold

- Weakly Interactive Massive Particles (WIMPs) are excellent candidates for DM
  - Naturally predicted by many SM extensions
  - Freeze-out mechanism allows to reproduce current abundance
  - **Cold** candidate
  - Mass **O(1) GeV/c²** to **O(1) TeV/c²**

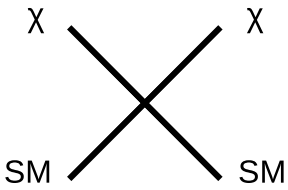

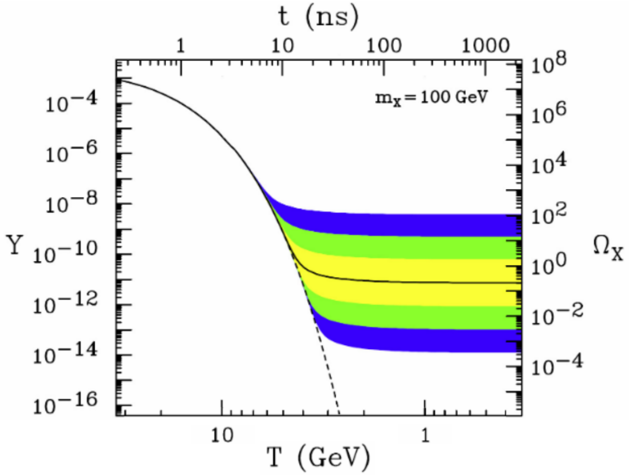

Feng, A,R., 48 (1) (2010)

Direct Detection

- WIMPs are expected to populate the Galaxy with an almost **isothermal halo (Standard Halo Model)**
- This weak interaction can be exploited to detect recoils of regular matter → **Direct detection**

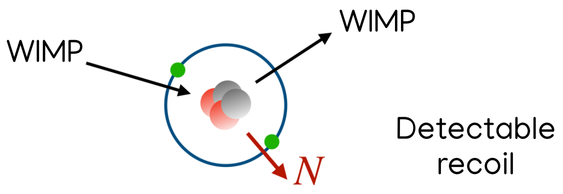

Nuclei preferred to electrons for better kinematic coupling

Differential rate per unit mass

$$\frac{dR}{dq^2 d\Omega} \propto \frac{N_0}{A_{mol}} \frac{\rho_0}{m_\chi} \frac{d\sigma}{dq^2} \int \delta\left(\cos\theta - \frac{q}{2\mu_A v}\right) v f(v) d^3 v$$

Target material chosen:
- Abundance of target
- Kinematic coupling with DM

Nuclear physics:
- Differential cross section of the process
- Interaction considered elastic
- Spin independent or dependent interactions assumed

$$\sigma_{WA} = \sigma_{WA,SI} + \sigma_{WA,SD}$$

Astronomical parameters:
- Standard Halo Model for the velocity distribution structure
- DM density at Earth position
- Earth's relative motion with Respect to Galaxy

Rare Event Search and Backgrounds

- Current limits point at less than 1 event/kg/y with energies well below 100 keV

Rare searches

- The quest can be hindered by many backgrounds:

Cosmic Rays

–High energetic secondary cosmic rays can overwhelm signal

Solution:

– Underground operation to shield aginst them

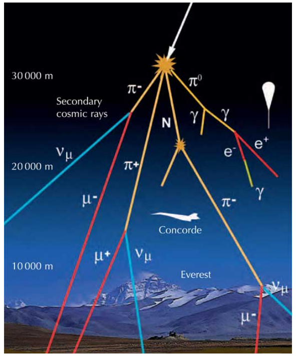

Rare Event Search and Backgrounds

- Current limits point at less than 1 event/kg/y with energies well below 100 keV

Rare searches

- The quest can be hindered by many backgrounds:

Cosmic Rays

–High energetic secondary cosmic rays can overwhelm signal

Solution:

– Underground operation to shield aginst them

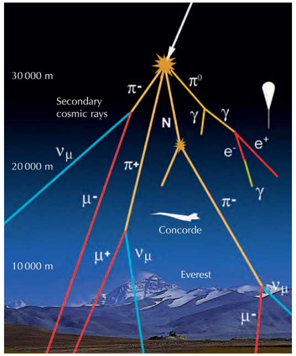

Gamma rays

– Interact in the detector inducing electron recoils (ERs)

– At low energy hard to distinguish from NRs

– Come from natural radiactivity of both laboratory and detector materials

Solution:

– Shield (high Z) against environment, radiopure material

– Exploit detector feature to distinguish NR from ER

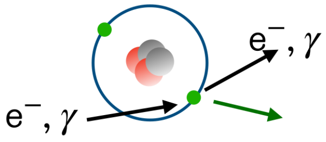

Rare Event Search and Backgrounds

- Current limits point at less than 1 event/kg/y with energies well below 100 keV

Rare searches

- The quest can be hindered by many backgrounds:

Cosmic Rays

–High energetic secondary cosmic rays can overwhelm signal

Solution:

– Underground operation to shield aginst them

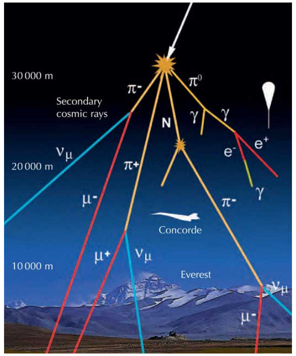

Gamma rays

– Interact in the detector inducing electron recoils (ERs)

– At low energy hard to distinguish from NRs

– Come from natural radiactivity of both laboratory and detector materials

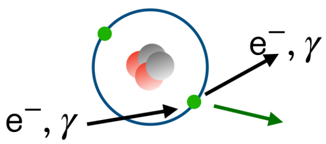

Solution:

– Shield (high Z) against environment, radiopure material

– Exploit detector feature to distinguish NR from ER

Neutrons

– Interact in the detector inducing NRs

–Originated by muon spallation in rocks or by (α,n) phenomenon

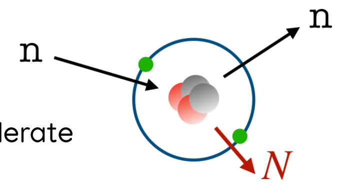

Solution:

– Shield with hydrogen rich materials to moderate and capture them

– Radiopure materials

Rare Event Search and Backgrounds

- Current limits point at less than 1 event/kg/y with energies well below 100 keV

Rare searches

- The quest can be hindered by many backgrounds:

Cosmic Rays

–High energetic secondary cosmic rays can overwhelm signal

Solution:

– Underground operation to shield aginst them

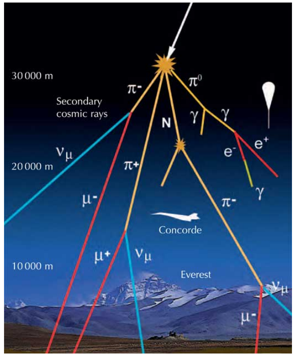

Gamma rays

– Interact in the detector inducing electron recoils (ERs)

– At low energy hard to distinguish from NRs

– Come from natural radiactivity of both laboratory and detector materials

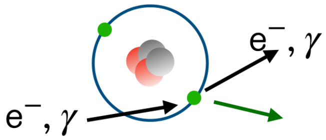

Solution:

– Shield (high Z) against environment, radiopure material

– Exploit detector feature to distinguish NR from ER

Neutrons

– Interact in the detector inducing NRs

–Originated by muon spallation in rocks or by (α,n) phenomenon

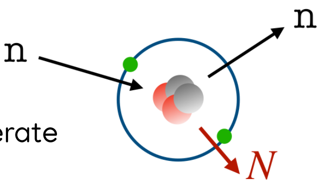

Solution:

– Shield with hydrogen rich materials to moderate and capture them

– Radiopure materials

Neutrinos

– Cross any type of shield and produce both ERs and NRs

– Origin from Sun, atmosphere, extragalactic

– Strongly harden the direct search:

Neutrino floor and fog

O'Hare, P.R.L., 127 (25) (2021)

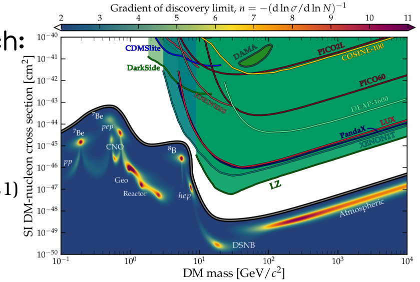

Directional Search

- Most of the experiment can only measure the energy of the recoils
- Nuclear recoils have also an angular distribution that could be measured → **1 more degree of freedom**

Only wave intensity

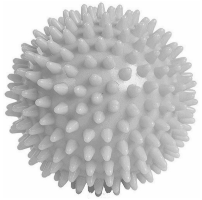

Directional Search

- Most of the experiment can only measure the energy of the recoils
- Nuclear recoils have also an angular distribution that could be measured → **1 more degree of freedom**

Coloured

Adding wavelength ←

Only wave intensity

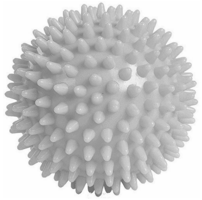

Directional Search

- Most of the experiment can only measure the energy of the recoils

- Nuclear recoils have also an angular distribution that could be measured → **1 more degree of freedom**

Coloured

← Adding wavelength

Only wave intensity

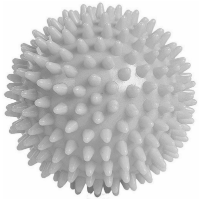

Adding phase →

Hologram

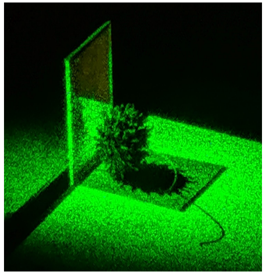

Directional Search

- Most of the experiment can only measure the energy of the recoils

- Nuclear recoils have also an angular distribution that could be measured → **1 more degree of freedom**

Coloured

Adding wavelength ←

Only wave intensity

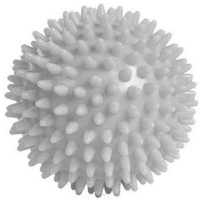

→ Adding phase

Hologram

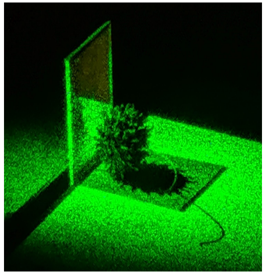

- WIMP expected recoil distribution is expected highly anisotropical thanks to Sun and Earth's motion

$$\frac{dR}{d\cos\gamma} \propto \int_{E_{thr}}^{E_{max}} e^{-\frac{(v_{lab}\cos\gamma - v_{min})^2}{v_p^2}}$$

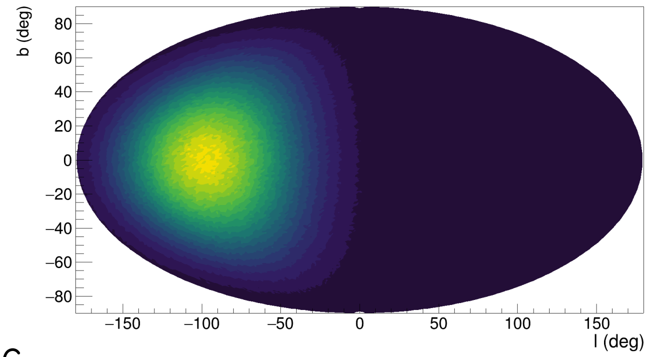

Galactic coord

10 GeV WIMP

Fluorine target

Directional Advantages I

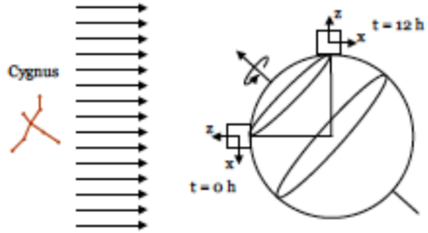

Vahsen et al., Annual review

- The strongly anisotropic signal in contrast to an expected **flat** background enhances the power of limits or discovery of DM interactions
- Directional information is more powerful than energy one

Energy	Angle	
Exponential signal over **exponential** background	**Peaked dipole** signal over **flat** background →	In case no signal is statistically different from expected background BETTER LIMITS

- How well can the dipole be seen?

Head-tail (HT)

3D/2D

angular resolution

Billard, Mayet, Santos (Physical Review D ,85(3) (2012)

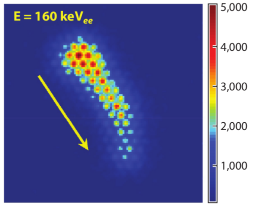

Vahsen et al., Annual review

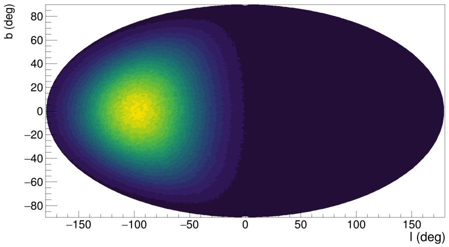

Full HT

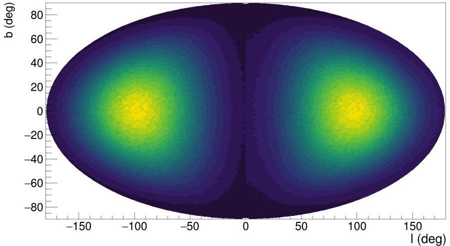

no HT

Directional Advantages II

- Akin to limits, an excess over background can be found with same significance with less exposure (factor ~ 100 with perfect head-tail and background recognition)

Billard, Mayet, Santos (Physical Review D ,85(3) (2012)

- The neutrino fog can be sidestepped (almost completely for Solar neutrinos) with nice directional performances (HT>75%, ang res>20°)

- A measured arrival direction of WIMPs can lead to a **positive claim** of Galactic DM

- High performance directional detector will be able to estimate the **3D structure of the velocity distribution,** actively probing DM theories

Vahsen et al., Annual review,71 (1) (2021)

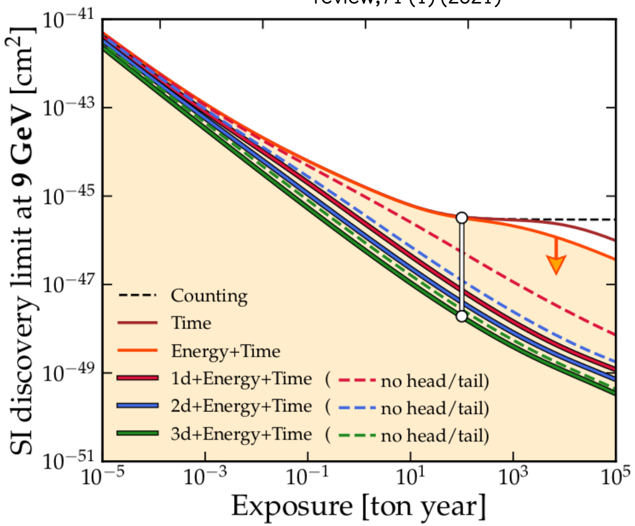

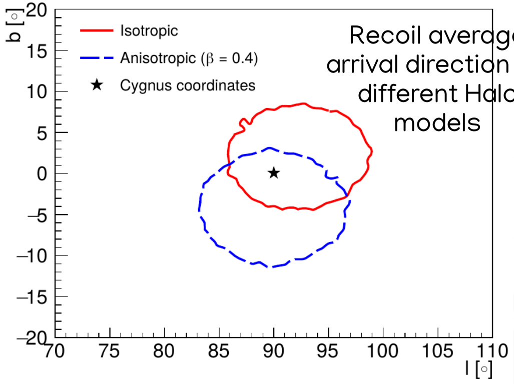

Recoil average arrival direction for different Halo models

Mayet et al., P.R., 627 (2016)

Gas TPCs as Directional Detectors

- Gaseous Time Projection Chambers (TPCs) provide the best architecture directional searches at low energy

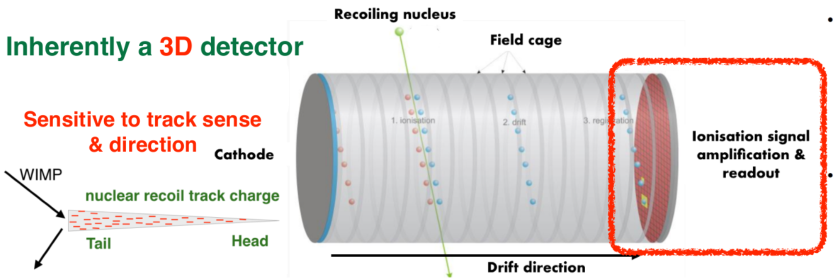

- Advantages:
  - Axial Directionality
  - **Head/tail**
  - Background rejection
  - Particle ID
  - 3D fiducialization
- Technologically challenging, but now achievable via multiple technologies

- Gas medium allows multiple element target and longer recoils, O(1) mm, than solid (O(1) nm) or liquids (O(1) μm)

- Exploits ionization of the gas with a potential energy threshold of >20 eV

- Imaging the recoils grants directional information and ER/NR rejection

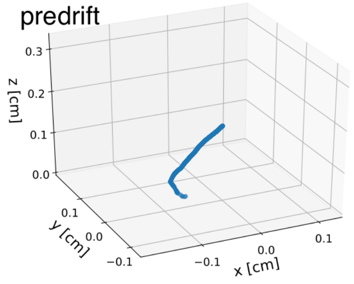

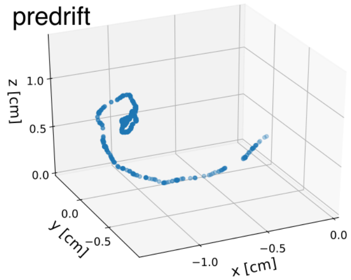

CYGNUS white paper: https://arxiv.org/abs/2008.12587

CYGNUS

- Proto-collaboration which aims for the construction of a multi-target, multi-site Galactic Observatory at the tonne scale to probe DM and measure Solar neutrinos based on the gas TPC technology

Drift coll., J.C.A.P., 2021 (7) (2021)

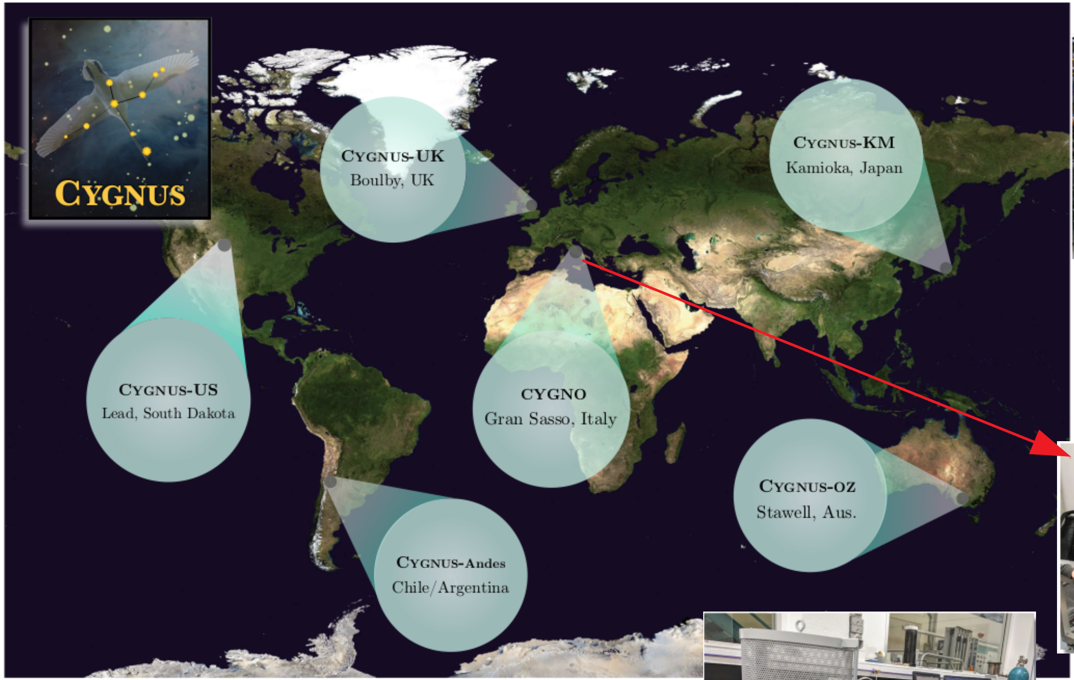

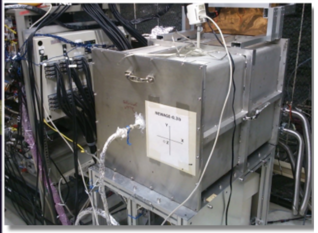

Ikeda et al, Prog. T. E.P., 2021 (6) (2021)

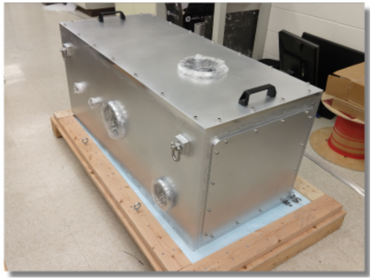

Vahsen et al, NIM A 788 (2015)

CYGNUS white paper: https://arxiv.org/abs/2008.12587

Amaro et al, Instruments 6 (1) (2022)

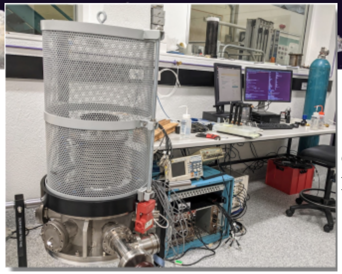

CYGNUS white paper: https://arxiv.org/abs/2008.12587

- Foreseen operation with both electron and negative ion drift charge and optical readout

CYGNO Experiment

- CYGNO project aims to construct a large directional detector, O(10–100) m^3, for rare event searches (DM, Solar neutrinos)

TPC

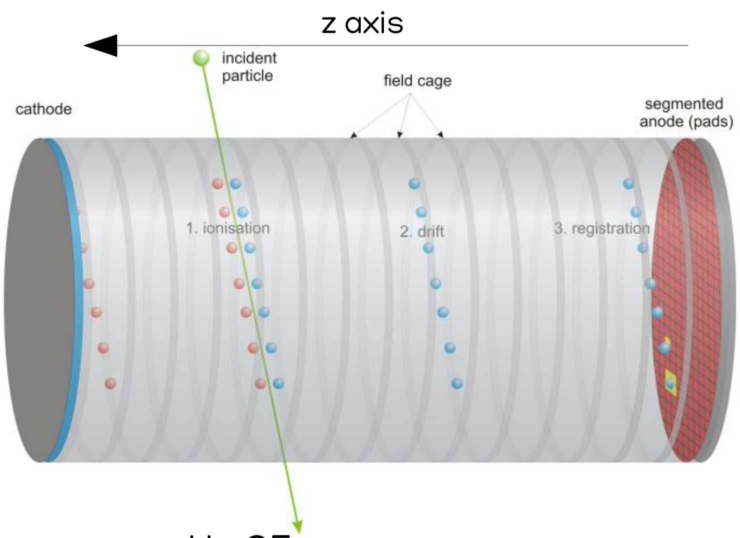

He:CF_4 gas
room temperature
atmospheric pressure

Amplification Stage

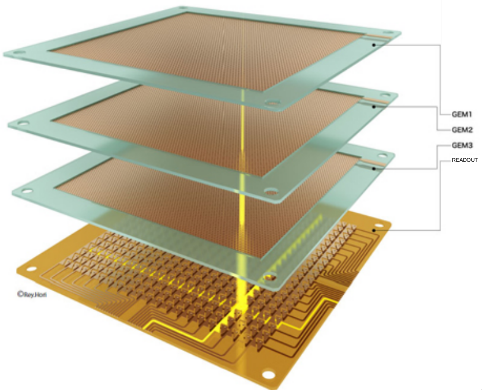

Gas Electron Multipliers (GEMs)

Grants large gains with high granularity

Optical readout

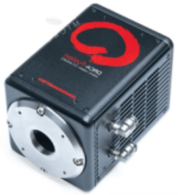

PMT
sCMOS cameras

Decoupled from gas,
less contamination
less noise

Gas: He:CF_4

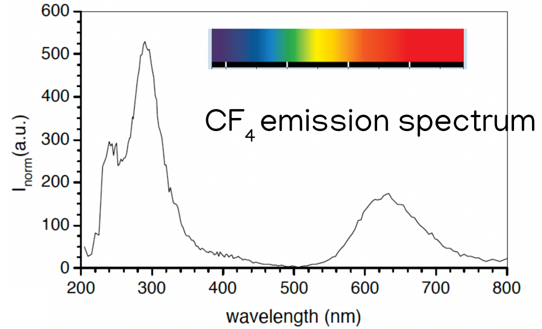

Morozov et al., J.I., 7 (02) (2012)

- Combination of a light noble gas with molecular scintillating gas (CF_4)

- Optimised to a **60/40** He:CF_4 mixture

Density:
~ 1,59 kg/m^3

W-value:
~ 38 eV

- CF_4 is a **cold gas**

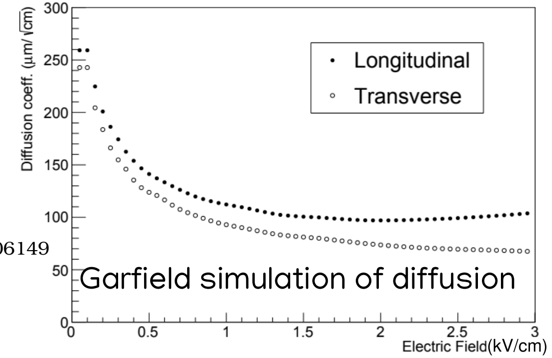

Veenhof, Conf Proc., 9306149 (1993)

Low diffusion:
Transverse ~100μm/$\mathrm{cm}^{1/2}$ at 1 kV/cm

- Light He is excellent for **low WIMP mass** searches (down to 1 GeV/c^2)

$$E_{max} = \frac{1}{2} r m_{\chi} v^2 \quad 0 < r < 1$$

r maximum with WIMP and target mass equal

- **Fluorine** has spin odd nucleus with high sensitivity to **SD coupling**

Amplification: GEM

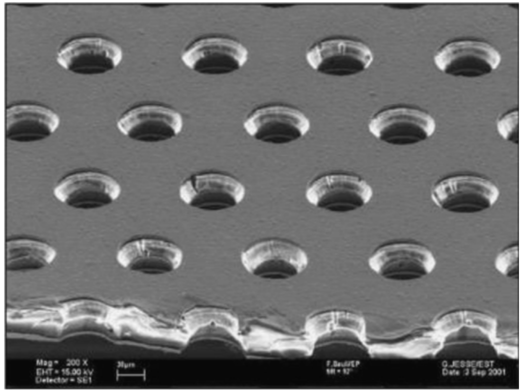

- Insulator cladded in copper conductor with plenty of small holes (~5000/cm^2)
- The strong electric fields in the holes generate electron avalanches

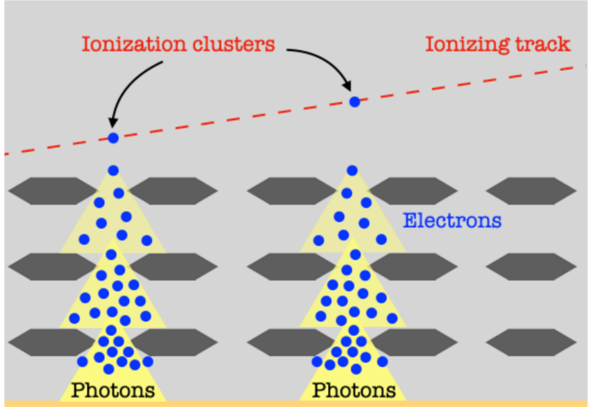

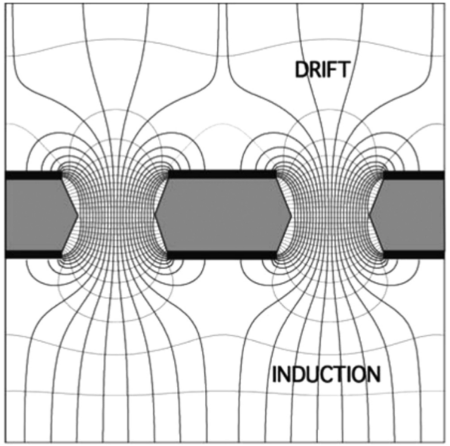

- Triple structure of 50 μm thin GEMs to grant high gains (up to 10^6)
- Production of photons during amplification due to neutral and charged fragmentation of CF_4 (0.07 ph/e$^-$)

Readout: Optical

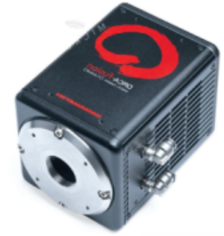

PMT

- Fast light detector
- Provides
  - Energy information from number of photons
  - Z direction topology and development

sCMOS Camera

- Highly sensitive and granular sensor
  (1 camera can image a 35x35 cm^2 area with 155x155 μm^2 granularity)
- Low noise per pixel (modern below 0,7 e^- RMS)
- Market pulled
- Provides
  - Energy information from number of photons
  - dE/dx on X-Y plane
  - X-Y positionand topology

QE

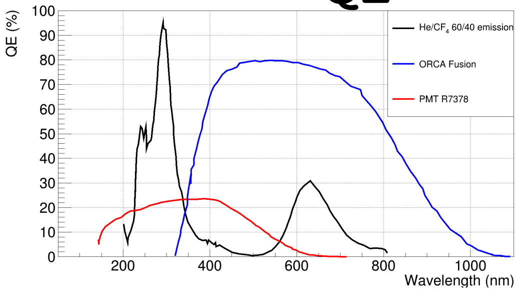

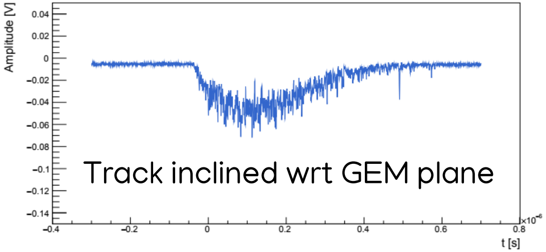

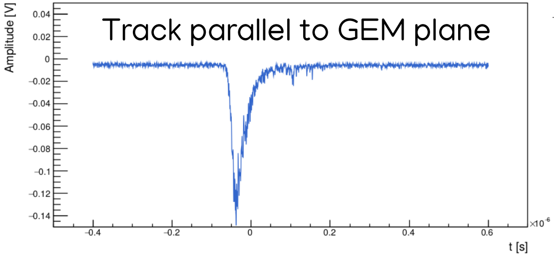

The combination allows energy and 3D topological measurement of each track

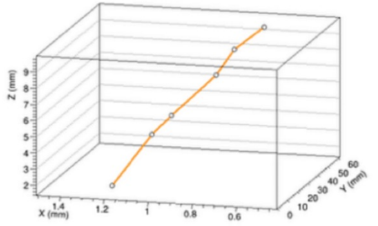

Readout: Optical

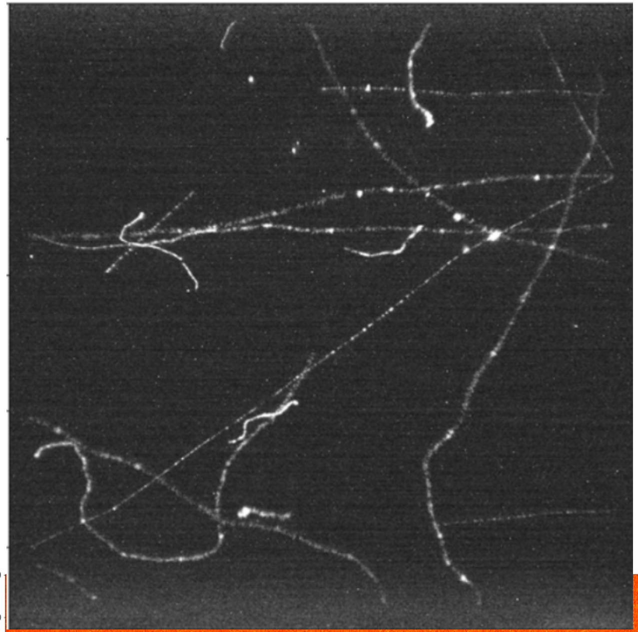

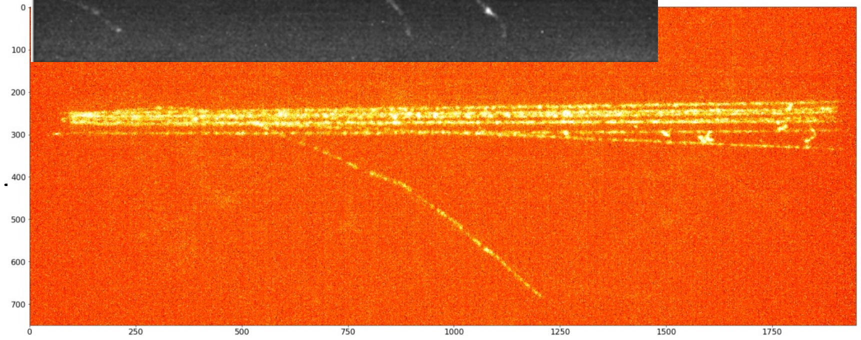

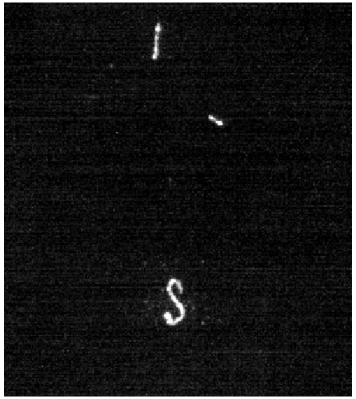

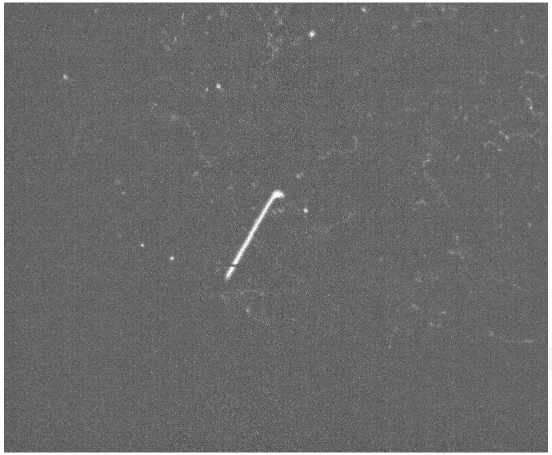

TIMELINE

FUNDED

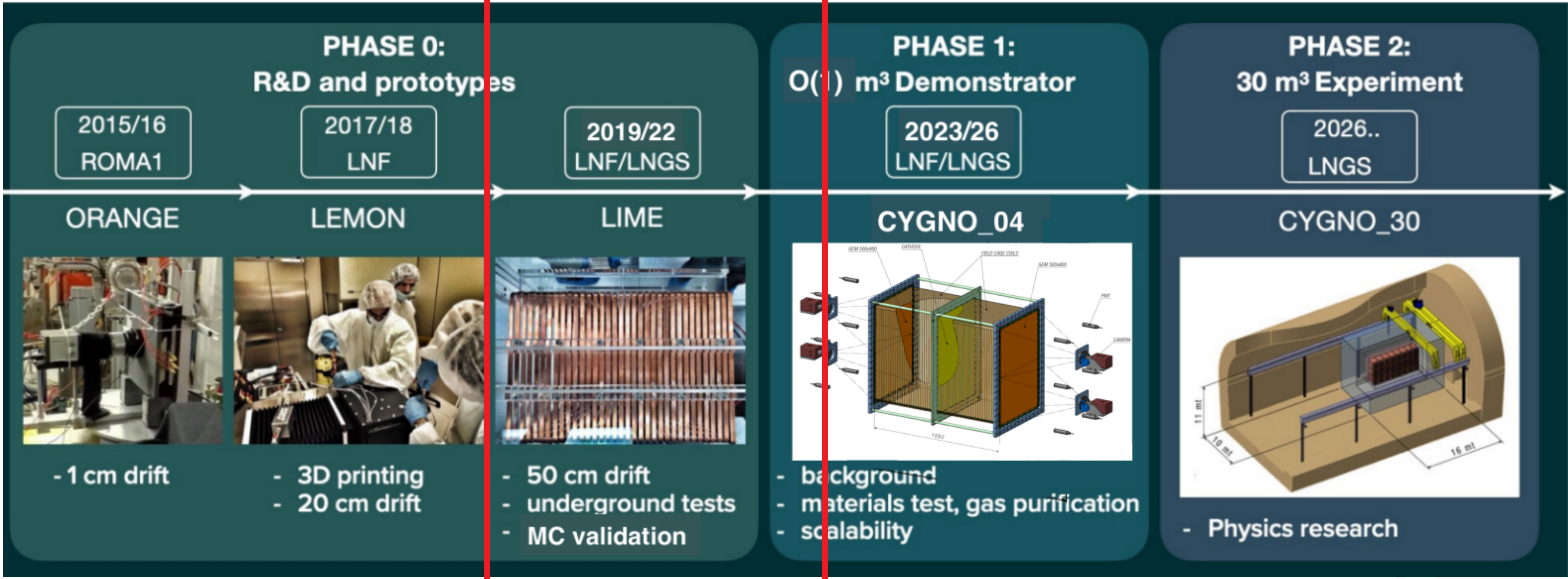

NOW

LIME

- Long IMaging Module
- Large readout area (33x33 cm^2) imaged by 4 PMTs and 1 sCMOS
- 50 l volume, with 50 cm drift
- Nice linearity in the low energy band (3–45 keV$_{ee}$)
- Underground at LNGS to validate MC simulation of the background

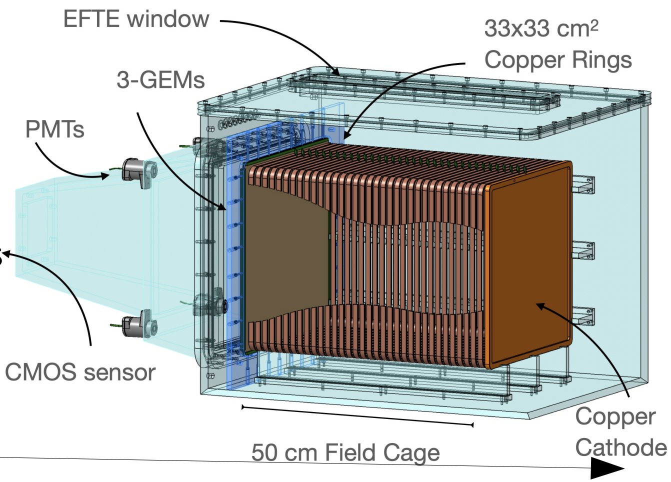

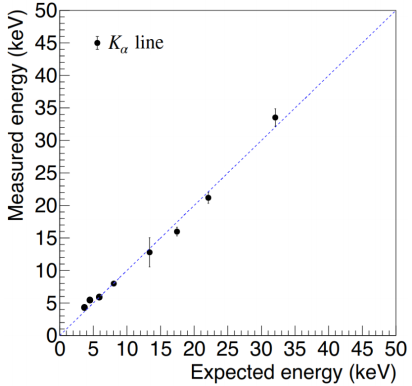

LIME in copper shield

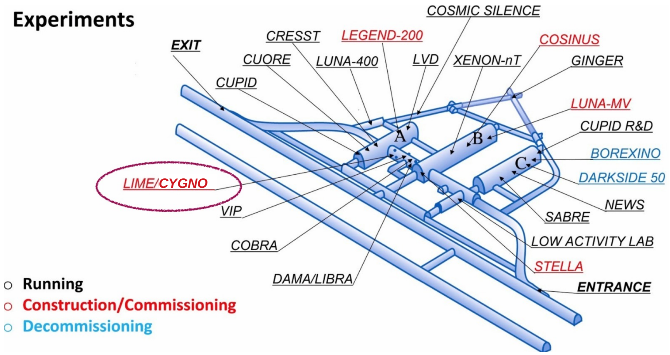

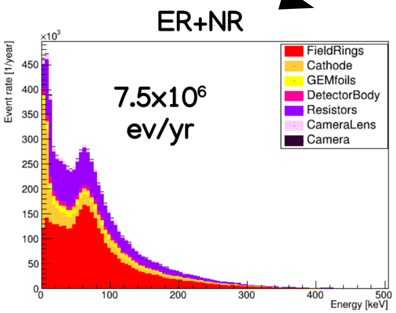

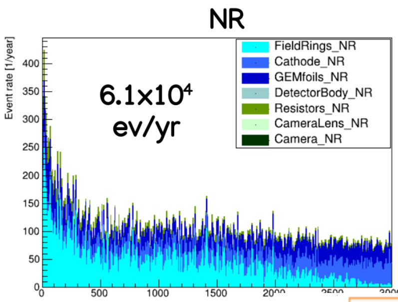

Future

CYGNO-04

- **Structure:** TPC in back-to-back configuration, 50 cm drift per side and 0,4 m^3 total volume
- **Amplification:** Triple thin GEM stack of 50x 80 cm^2 per side
- **Readout:** Optical with 2 sCMOS (Hamamatsu ORCA Quest) and 6 PMTs per side
- **Purpose:**
  - Prove the scalability of the technology to large volumes using **two cameras per side** (better than LIME)
  - Characterise internal background

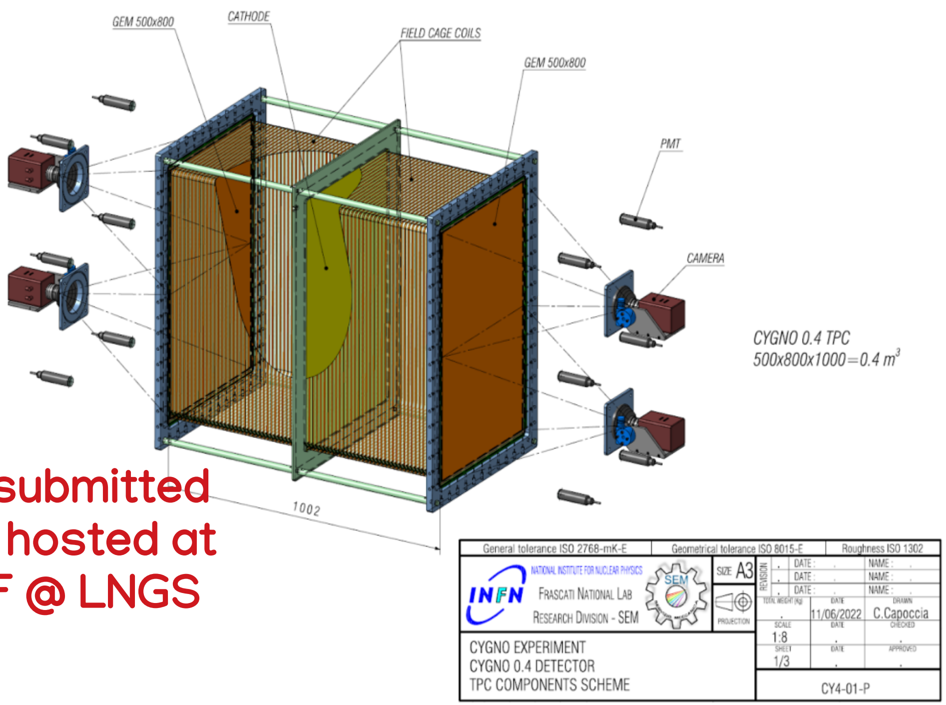

TDR submitted to be hosted at Hall F @ LNGS

CYGNO-30

- O(30) m^3 detector for the DM physics case
- It will profit of all the lesson learned in R&D phase
- Possibility of adding hydrocarbon gas component to introduce H

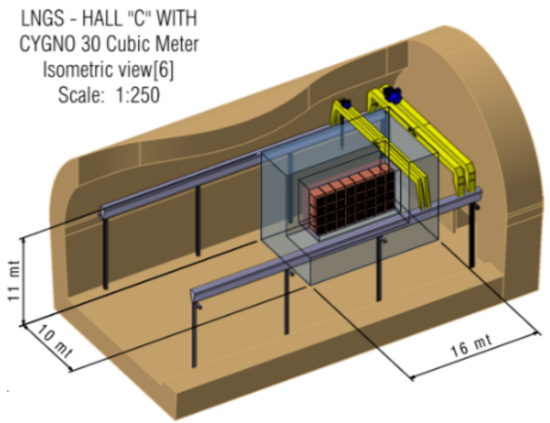

Subject of Study

- In the CYGNO context, the experimental features which can be improved are:

Energy threshold

- The energy threshold E_{thr} is of the utmost importance to probe low WIMP masses and increase sensitivity

$$E_{max}=\frac{1}{2}rm_{\chi}(v_{lab}+v_{esc})^2$$

Only m_{χ} whose E_{max} is above E_{thr} are detectable

- E_{thr} depends on the photons collected by the sensor

Optimisation of the amplification stage

Diffusion

- In imaging TPC, diffusion can spoil the original track topology, hindering the capability of track reconstruction

- In directional DM searches it is crucial as **head-tail recognition, angular resolution** and **ER to NR discrimination**

Negative Ion Drift Operation

Summary

- Directional Dark Matter (Intro)
- Amplification Stage Optimisation
- Negative Ion Drift Operation
  - Atmospheric Pressure
  - Lower Pressure
- Directionality Studies
  - CYGNO-30 Limits
  - DM Discrimination

Amplification Stage Study

- E_{thr} depends on the amount of photons collected by the sensors
- The optical readout allows to image large areas, but the solid angle covered can be as small as 10^{-4}
- **Maximising the light production** is key for low threshold
- Using more than 3 amplification stages would saturate gain
- Measurement of light enhancement with strong electric field below last GEM

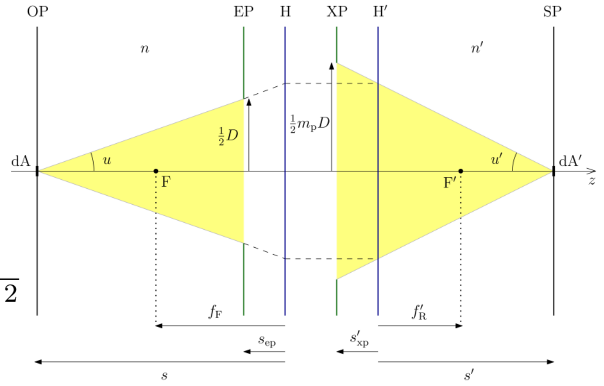

$$\Omega_f = \frac{1}{\left(4N^2\left(\frac{1}{I}+1\right)\right)^2}$$

Rowalds., book, IOP Publishing (2017)

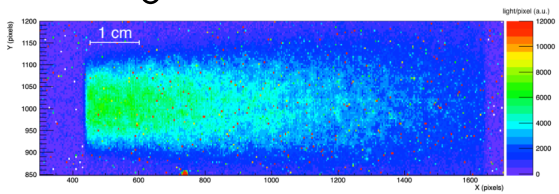

High field turned on

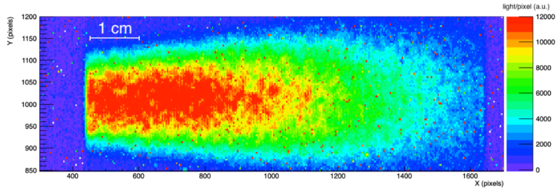

Baracchini et al., JINST, 15 (08) (2020)

SETUP

- MANGO detector used to extend the induction field study to other GEM configurations and He concentrations (60% or 70%)
- MANGO is 10x10 cm^2 readout area with variable drift gap (0.8 cm here)
- sCMOS: ORCA Fusion, effective granularity 49x49 μm^2
- Metallic mesh employed as induction electrode (T=0.55)
- ***ttt:*** Stack of 3 thin GEMs (50 μm thick, 70 μm hole diameter, 140 μm pitch)
- ***TT:*** Stack of 2 thicker GEMs (125 μm thick, 175 μm hole diameter, 350 μm pitch)
- ***Tt:*** Stack of 1 *T* GEM and a *t* one

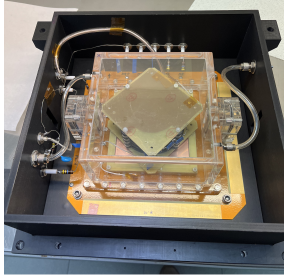

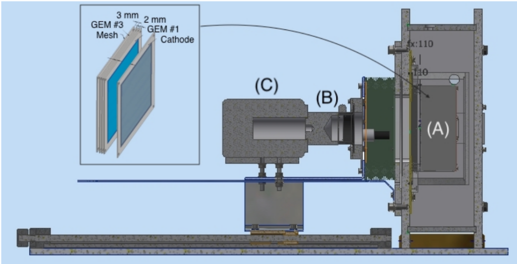

ttt

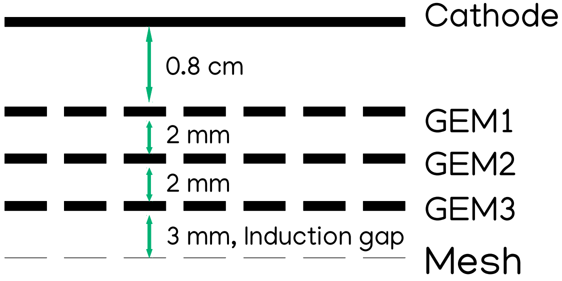

TT

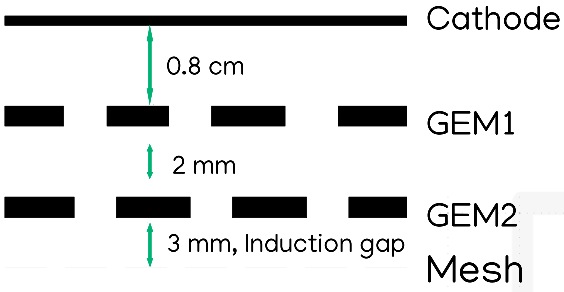

Tt

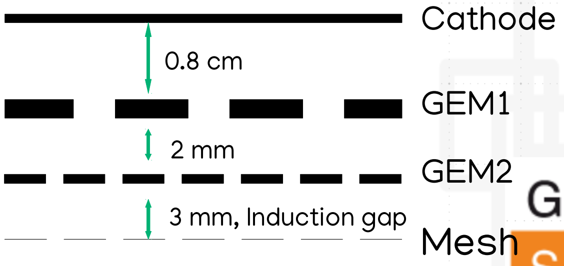

Setup

- ^{55}Fe source of 48 kBq allows an event by event analysis of the images
- Camera exposure 0.5 s exposure
- Optimisation of the amplification structure based on the analysis of **light yield, energy resolution** and **intrinsic diffusion**

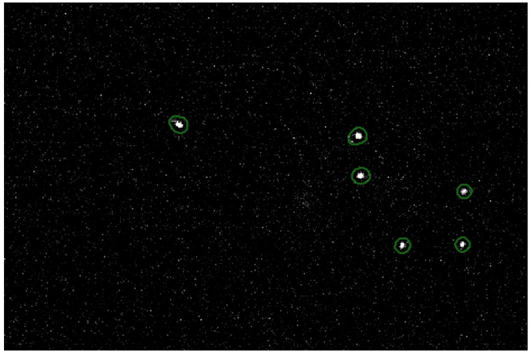

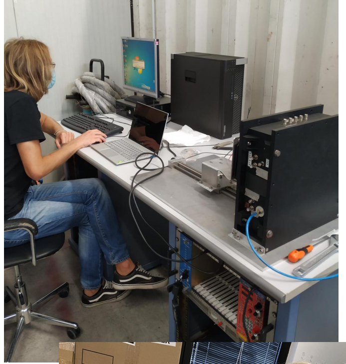

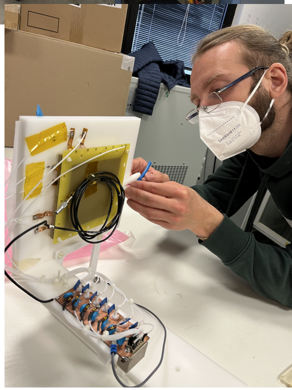

Light yield

Energy resolution $\frac{\sigma}{Mean}$

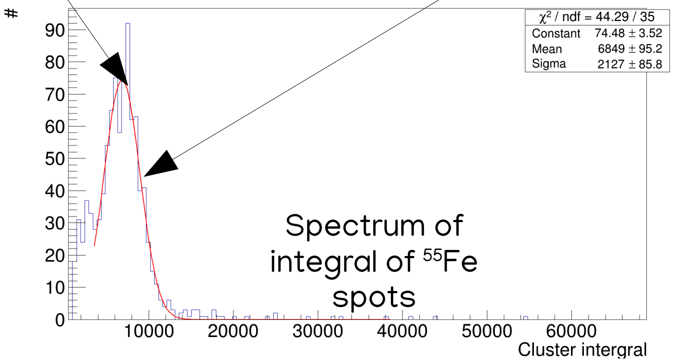

Spectrum of integral of ^{55}Fe spots

Intrinsic diffusion

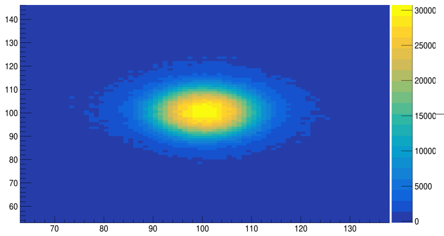

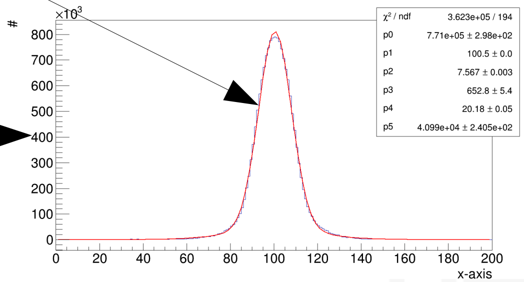

Gain

- Characterisation of the setups with regular operation

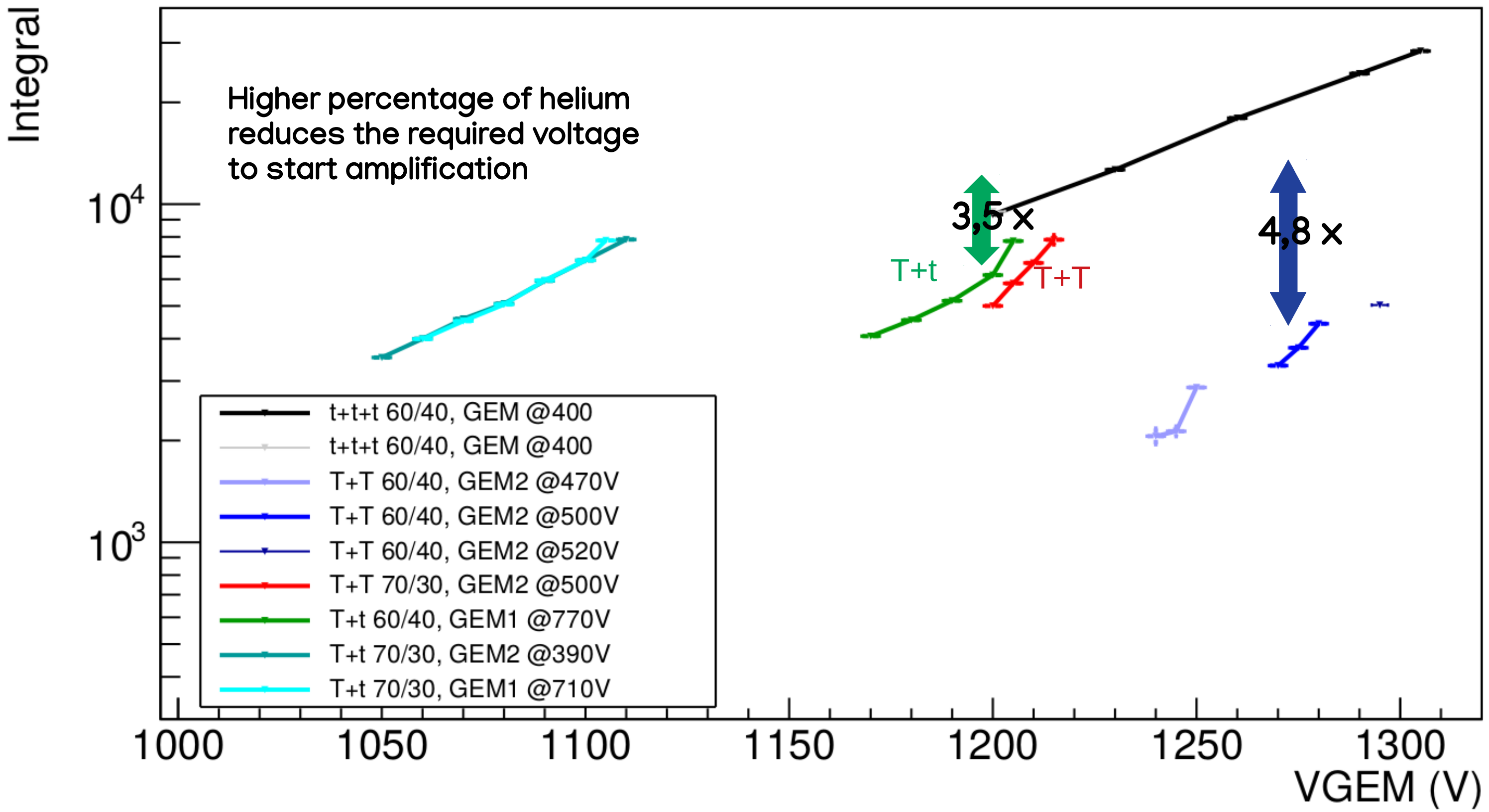

Visible light difference when not using triple stack

Gain Parametrisation

- The gain can be parametrised as a function of a *reduced field* (Σ) inside the GEM holes as (T.N. Thorpe, S.E. Vahsen, 10.1016/j.nima.2022.167438)

$$\Gamma = \frac{ln(G)}{n_g pt} = A_0 + B_0\Sigma = A_0 + \frac{B_0}{pn_g t}V_g$$

$$\Sigma = \frac{V_g}{n_g pt}$$

– (Γ) reduced gain
– **p** pressure
– n_g number of GEMs

– A_0, B_0 free parameters
– **t** thickness of GEM
– V_g sum of voltage across GEMs

- Table obtain by fitting the data of previous slide

- The consistency of the parameters suggests the parametrisation is correct within the uncertainties

- Good understanding of the multiplication process

Config	Colour	$[0]\ \frac{1}{torr \cdot cm}$	$\sigma_{[0]}\ \frac{1}{torr \cdot cm}$	$[1]\ \frac{1}{torr \cdot cm \cdot V}$	$\sigma_{[1]}\ \frac{1}{torr \cdot cm \cdot V}$
ttt 60/40	Black	-0.36	0.14	0.00106	0.00011
Tt 60/40	Green	-0.7	0.2	0.0012	0.0004
Tt 70/30	Cyan	-0.6	0.2	0.0012	0.0003
Tt 70/30	Dark Green	-0.49	0.19	0.0011	0.0002
TT 60/40	Blue	-1.6	0.9	0.0017	0.0007
TT 70/30	Red	-1.6	1.0	0.0018	0.0006

Induction Field

- Fixing the V_g and increasing the induction field (E_{Mesh})

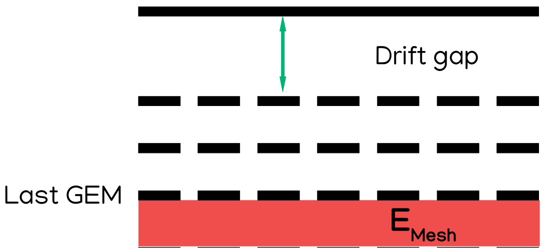

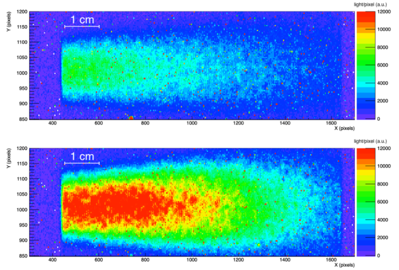

ttt case

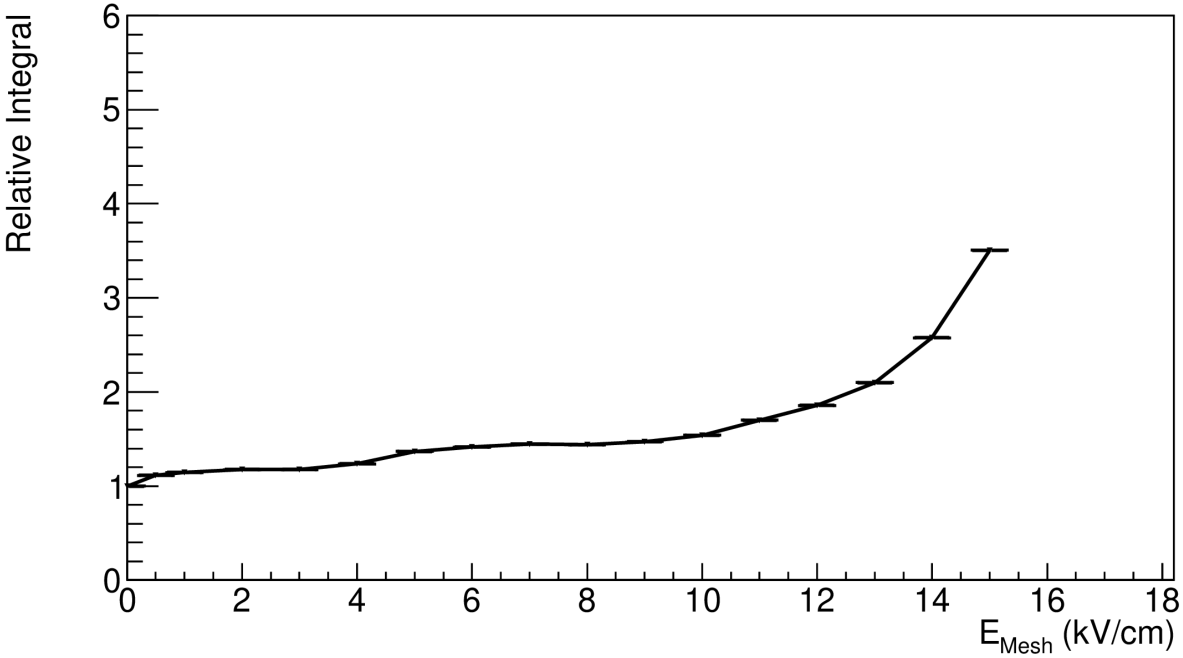

INDUCTION FIELD

- Fixing the V_g and increasing the induction field (E_{Mesh})

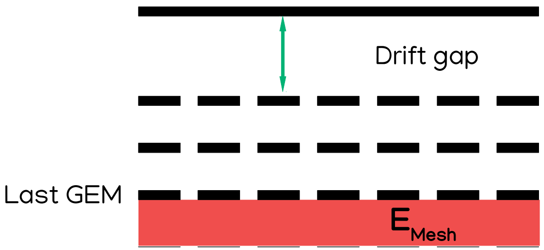

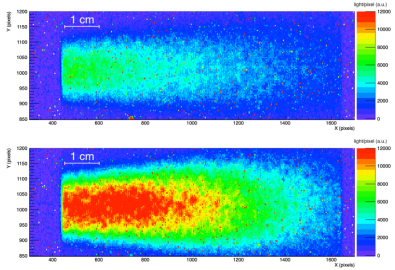

ttt case

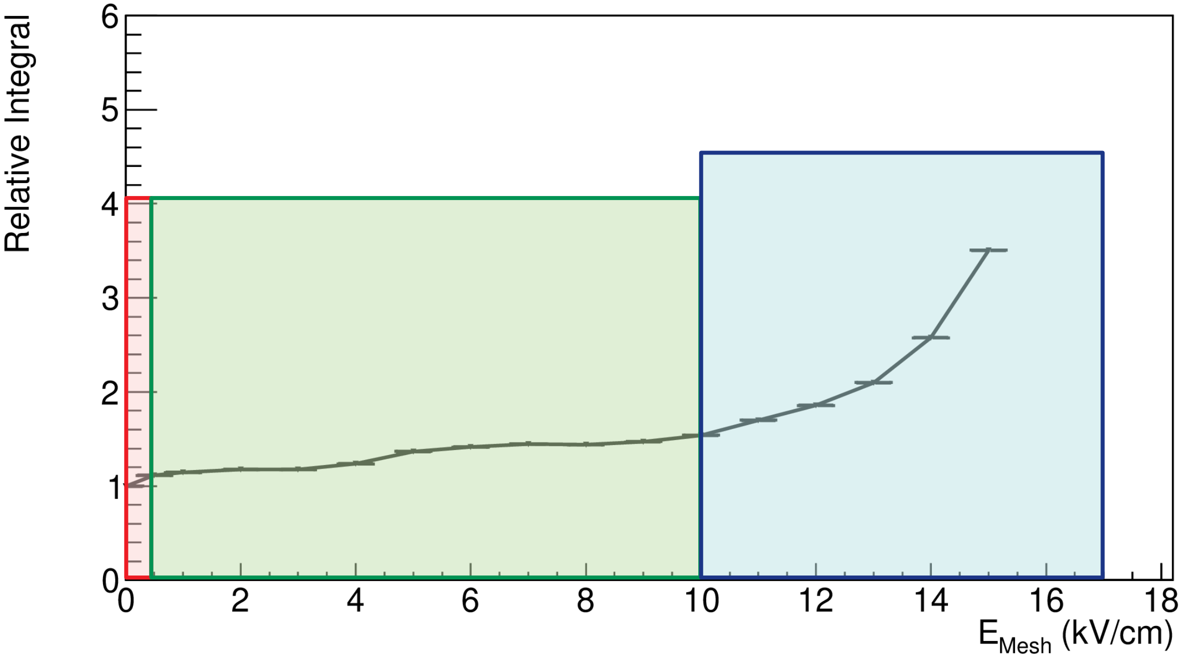

- Immediate increase
- Linear increase
- Exponential growth

Induction Field: Linear Increase

- Employing the parametrisation of the gain, the reduced field can be expanded with a term to include the influence of E_{Mesh}

$$\Sigma = \frac{1}{p}\left(\frac{V_g}{n_g t} + \alpha E_{mesh}\right)$$

Once V_g is fixed this is a constant term ([0]) which should match the terms fitted with the gain (**Condition C**)

$$\Gamma = A_0 + \frac{B_0}{p n_g t} V_g + \frac{B_0 \alpha}{p} E_{mesh}$$

[1]:
Term proportional to E_{Mesh}

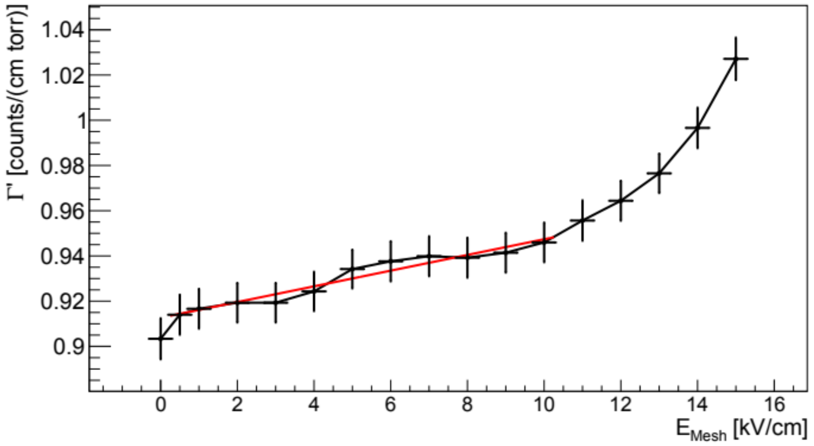

Conf	[0] $\frac{1}{torr \cdot cm}$	$\sigma_{[0]}$ $\frac{1}{torr \cdot cm}$	[1] $\frac{1}{torr \cdot kV}$	$\sigma_{[1]}$ $\frac{1}{torr \cdot kV}$	Cond. C
ttt 60/40	0.912	0.005	0.0036	0.0010	✓
Tt 60/40	0.747	0.009	0.0010	0.0009	✓
Tt 70/30	0.704	0.007	0.0029	0.0015	✓
TT 60/40	0.48	0.01	0.0025	0.0013	✓
TT 70/30	0.505	0.004	0.0016	0.0010	✓

Induction Field: Exponential Increase

- The exponential part is studied after removing the linear contribution

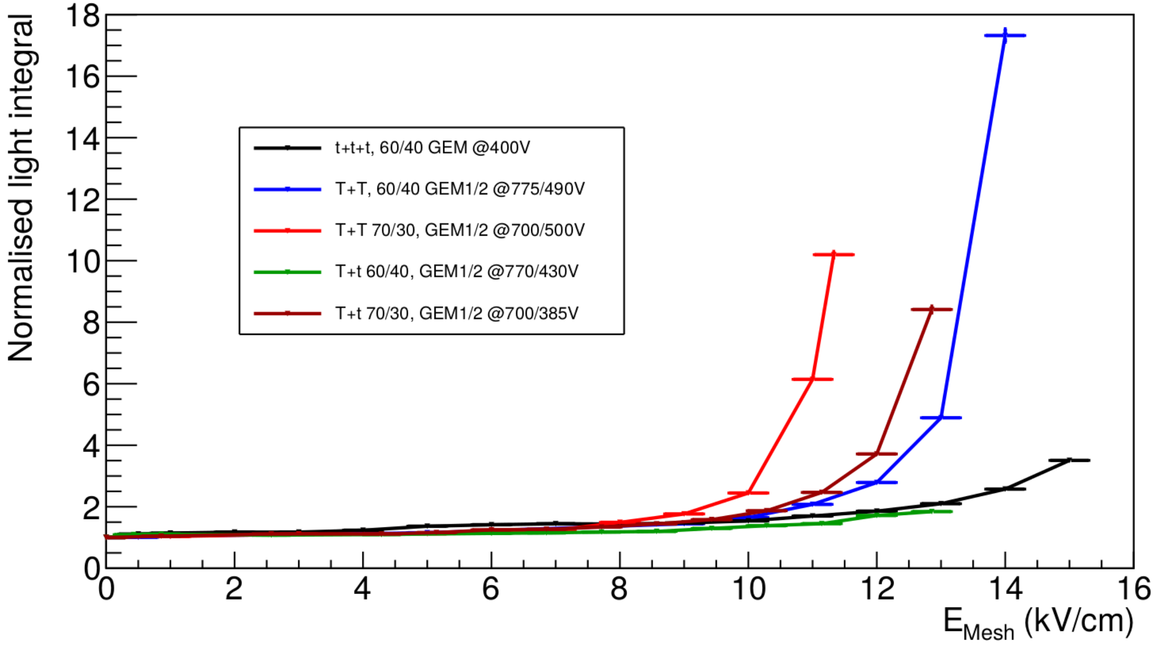

Large increment of light can be achieved (more than 10)

- The **intensity** of the light increase depends on the last GEM
- The data are fitted in order to find the breaking point of the exponential growth

$$a + b \cdot e^{cE_M - d}$$

- The helium content modifies the breaking point

$E_{break,60/40}$ = (9.7 ± 0.8) kV/cm

$E_{break,70/30}$ = (8.7 ± 0.7) kV/cm

As for the gain scan, more helium requires lower field for the phenomenon to begin

Maxwell Simulation

- Ansys Maxwell program used to simulate the electric field of the MANGO setup and GEMs
- The uniformity of the field in the gap was confirmed
- However, a hundred of micrometer away from GEM holes the fields are far from constant

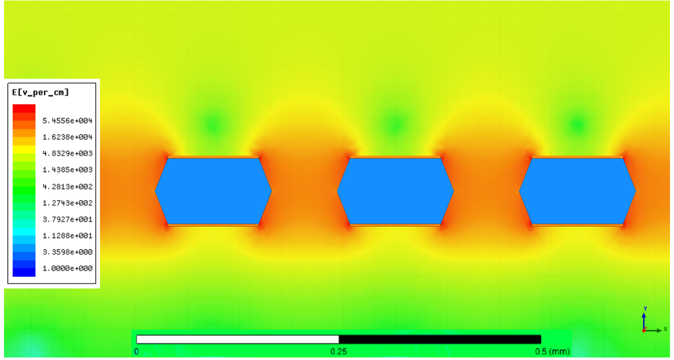

- The profile of the electric field is studied on an axis perpendicular to the GEM plane in three conditions
  - Low V_g, no induction field
  - High V_g, no induction field
  - Low V_g, high induction field

GEM Field Profile

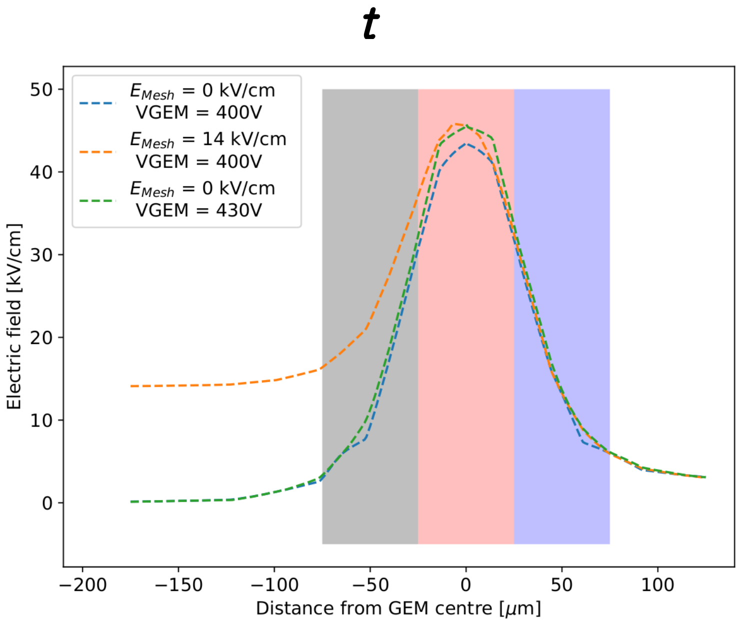

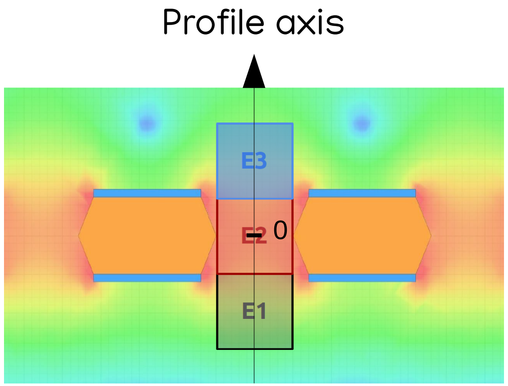

T GEM more affected

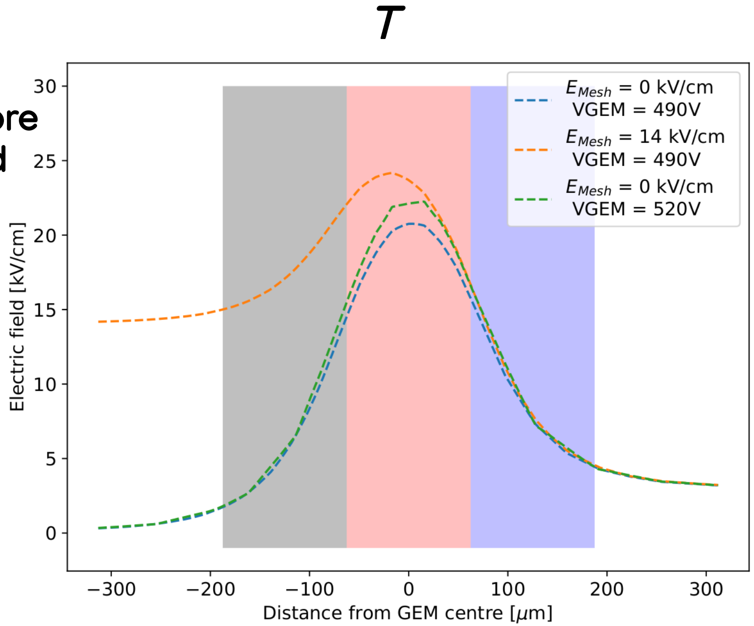

- Increasing V_g enhances the field strength without changing the structure
- A strong E_{mesh} modifies the shape of the profile generating a region below the GEM where light production and amplification can take place
- To quantify the electric field intensity, the value is averaged in 3 regions

GEM Fields Dependence

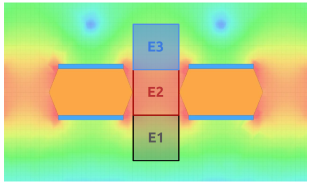

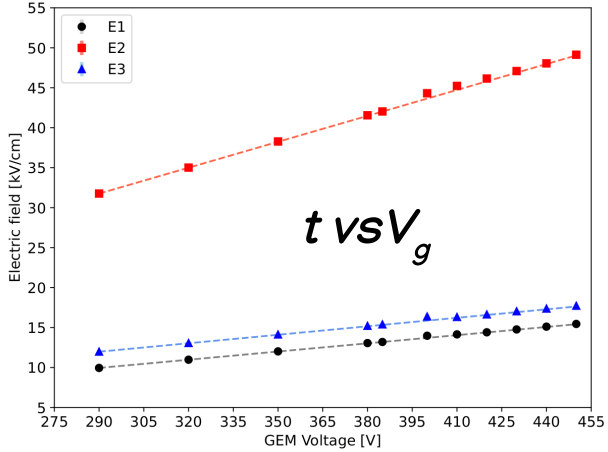

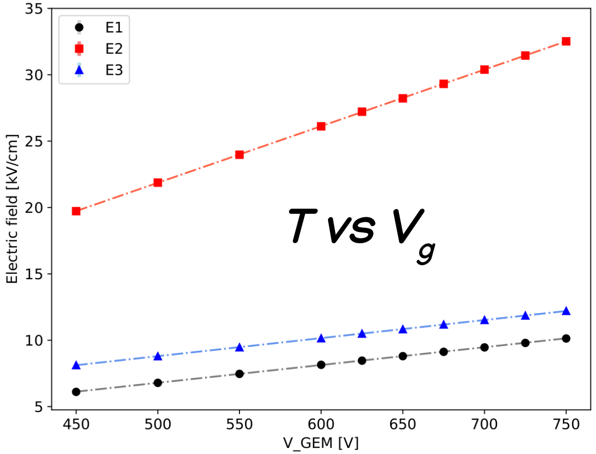

- The induction field does not affect the field above the GEM
- The induction field increses the field inside the GEM hole, but less than V_g (**Compatible with linear increase**)
- The field below the GEM is strongly enhanced up to values where amplification is achievable
- *T* GEM has intrinsically lower fields, so the induction field is relatively larger (**Compatible with *T* GEM granting larger light amplification**)

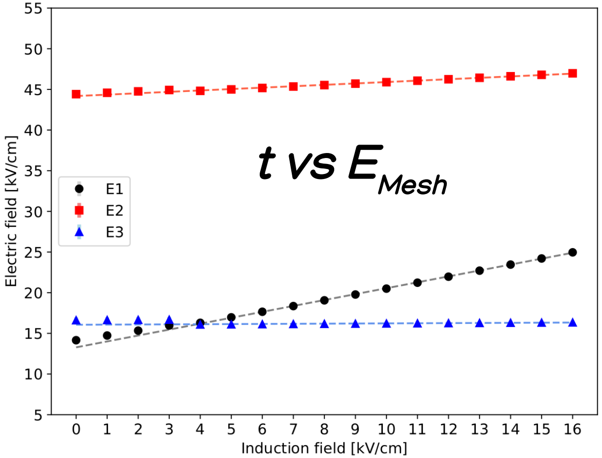

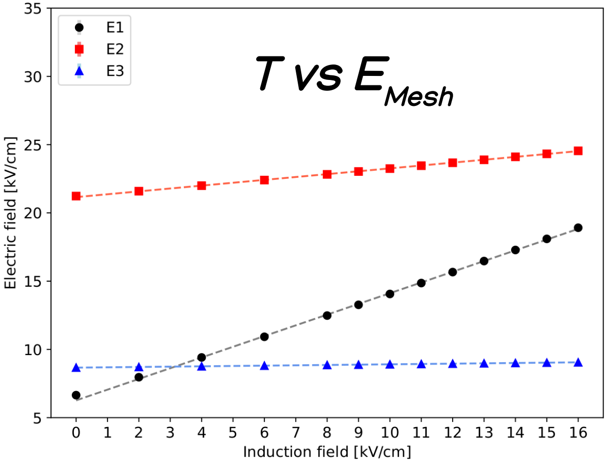

Induction Field

- Fixing the V_g and increasing the induction field (E_{Mesh})

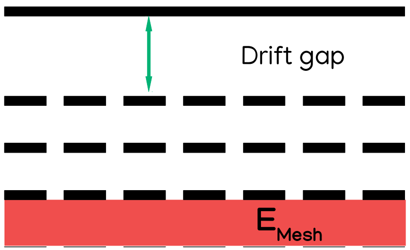

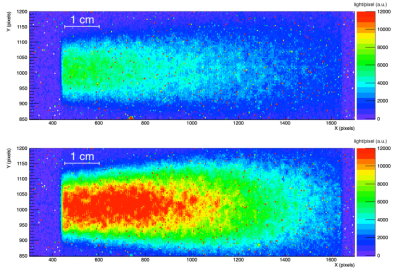

ttt case

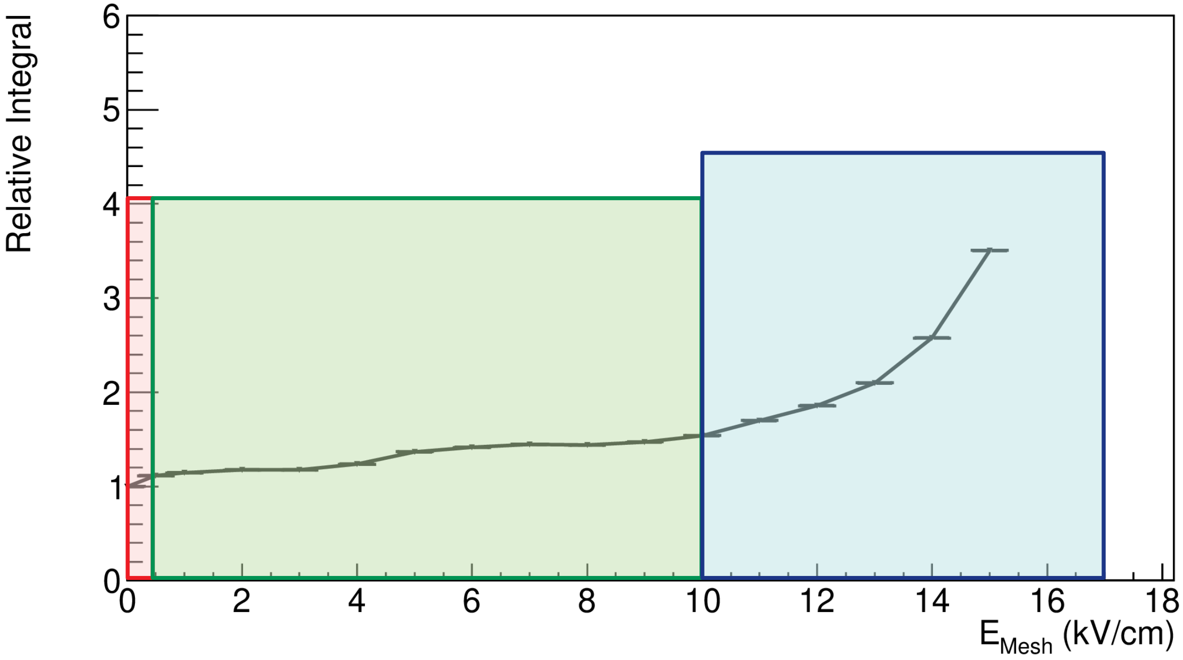

- Increase due to better defined field lines below the last GEM (Maxwell simulations)
- Linear increase due to the induction field affecting the field inside GEM
- Exponential growth due to a different phenomenon happening inside the induction gap

Energy Resolution

vs V_g

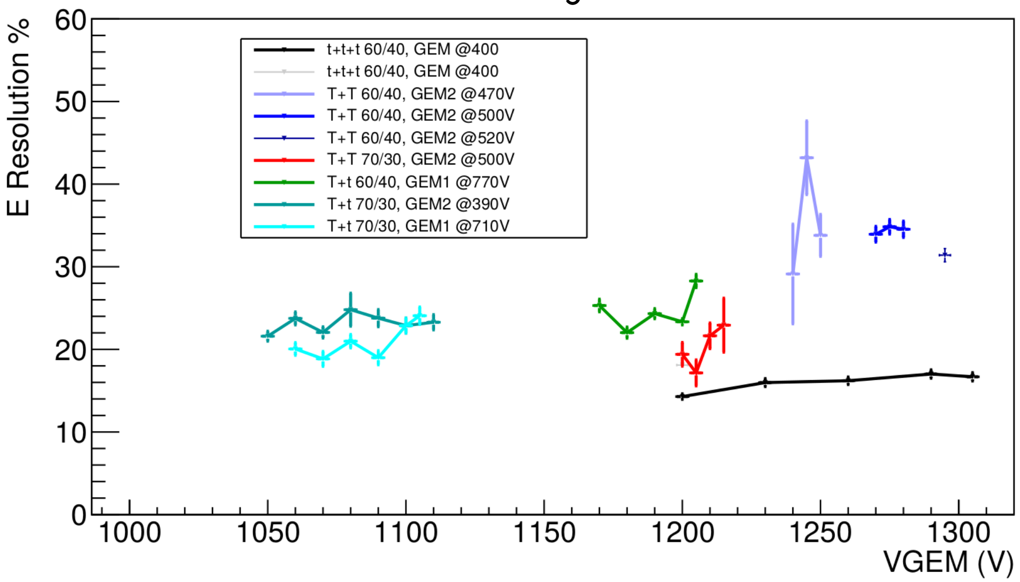

vs E_{Mesh}

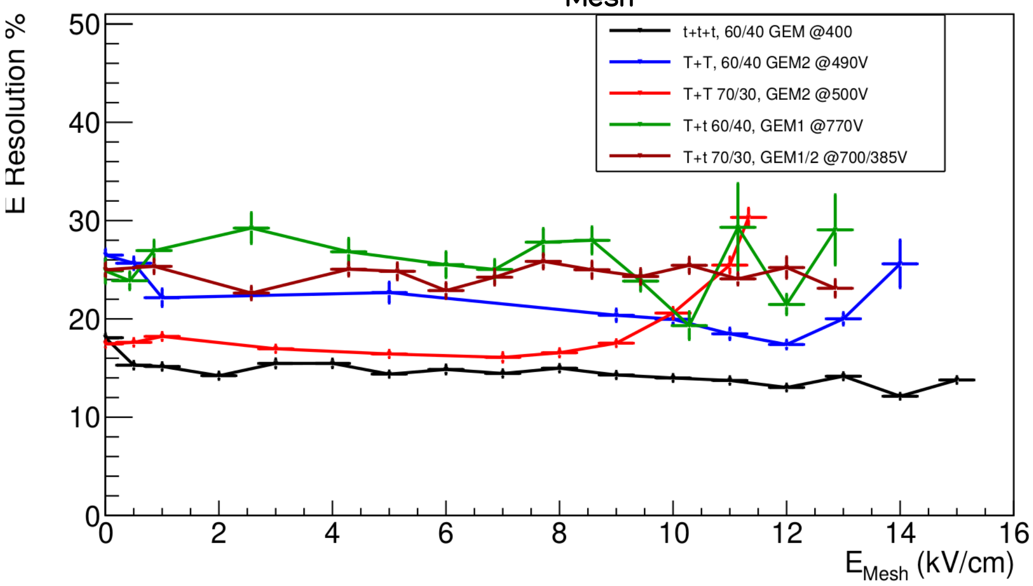

- Best energy resolution obtained with stronger fields and higher gain (*ttt*)
- Energy resolution roughly constant with V_g
- Energy resolution is constant or improves with field if the last GEM is thin
- At the breaking point the *TT* GEMs have a clear worsening of the resolution

Diffusion

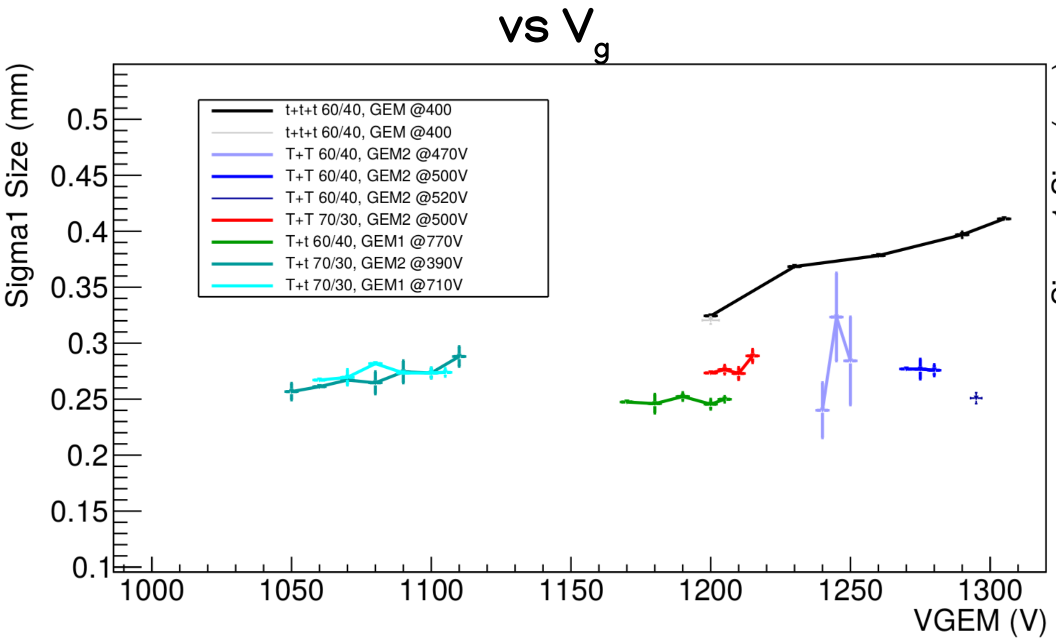

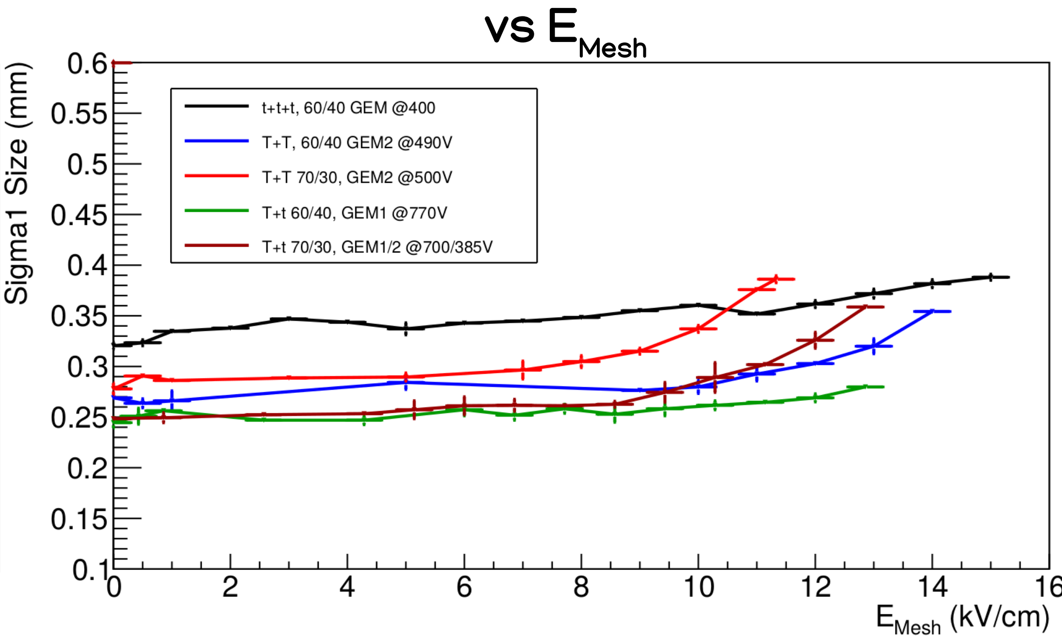

- Diffusion is in general independent of the V_g
- *ttt* clearly worsens with the applied voltage
- *Tt* has the lowest diffusion among all (only two GEMs and the granularity copes with the GEM pitch)

- From the breaking point the spot size increases
- Expected as extra light is generated out of the focus

Discussion

- Innovative way to enhance light yield with He:CF_4 mixture
- The induction field allows any structure to reach larger light yield

		Integral	E res (%)	Diff [μm]
ttt	min	9510 ± 40	16.0 ± 0.3	320 ± 4
	max V_{GEM}	28400 ± 110	16.6 ± 0.3	412 ± 5
	max E_{Mesh}	33500 ± 140	13.8 ± 0.3	388 ± 5
TT	min	3410 ± 20	28.0 ± 1.5	260 ± 3
	max V_{GEM}	5090 ± 30	31.0 ± 0.6	255 ± 3
	max E_{Mesh}	58800 ± 300	25.7 ± 0.5	356 ± 5
Tt	min	4600 ± 30	25.2 ± 0.5	245 ± 3
	max V_{GEM}	7700 ± 40	27.8 ± 0.5	245 ± 3
	max E_{Mesh}	11800 ± 50	26.8 ± 0.5	280 ± 4

Discussion

		Integral	E res (%)	Diff [μm]
ttt	min	9510 ± 40	16.0 ± 0.3	320 ± 4
	max V_{GEM}	28400 ± 110	16.6 ± 0.3	412 ± 5
	max E_{Mesh}	33500 ± 140	13.8 ± 0.3	388 ± 5
TT	min	3410 ± 20	28.0 ± 1.5	260 ± 3
	max V_{GEM}	5090 ± 30	31.0 ± 0.6	255 ± 3
	max E_{Mesh}	58800 ± 300	25.7 ± 0.5	356 ± 5
Tt	min	4600 ± 30	25.2 ± 0.5	245 ± 3
	max V_{GEM}	7700 ± 40	27.8 ± 0.5	245 ± 3
	max E_{Mesh}	11800 ± 50	26.8 ± 0.5	280 ± 4

- Innovative way to enhance light yield with He:CF_4 mixture
- The induction field allows any structure to reach larger light yield
- It is possible to reach a light yield of the *ttt* with another structure but with lower intrinsic diffusion

		E_{Mesh} [kV/cm]	Integral	E res (%)	Diff [μm]
Same light	*ttt*	3 ± 0.3	11300 ± 50	15.5 ± 0.3	347 ± 5
	TT	12.3 ± 0.4	11300 ± 50	17.9 ± 0.4	307 ± 4
	Tt	12.3 ± 0.4	11300 ± 50	25.0 ± 0.5	273 ± 4
Max E_{Mesh}	*ttt*	15 ± 0.3	33500 ± 140	13.8 ± 0.3	388 ± 5
	TT	14 ± 0.3	58800 ± 300	25.7 ± 0.5	356 ± 5
	Tt	12.8 ± 0.2	11830 ± 50	26.8 ± 0.5	280 ± 4

- Each structure excels in a particular feature
  - *ttt* Energy resolution
  - *TT* light yield
  - *Tt* intrinsic diffusion
- Application to many fields depending optimisable depending on need

Summary

- Directional Dark Matter (Intro)
- Amplification Stage Optimisation
- Negative Ion Drift Operation
    - Atmospheric Pressure
    - Lower Pressure
- Directionality Studies
    - CYGNO-30 Limits
    - DM Discrimination

Diffusion in Drift Region

- In imaging TPC, diffusion can spoil the original track topology, hindering the capability of track reconstruction
- In directional DM searches it is crucial as **head-tail recognition, angular resolution** and **ER to NR discrtimination**
- **Negative Ion Drift operation (NID)**

  In sinergy with the INITIUM project, an ERC Consolidator Grant with the goal of realising NID operation within the CYGNO optical approach

Part of this project has been funded by the European Union's Horizon 2020 research and innovation programme under the ERC Consolidator Grant Agreement No 818744

European Research Council

Established by the European Commission

CYGNUS white paper: https://arxiv.org/abs/2008.12587

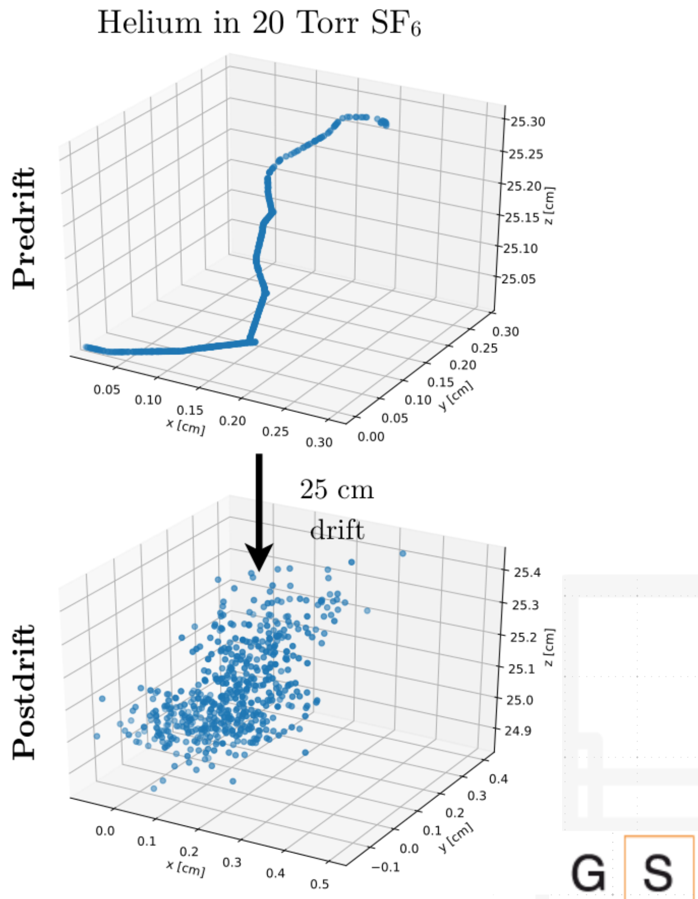

G S S I

Negative Ion Drift (NID)

- Small addition of electronegative gas (CS_2,SF_6) which captures free electrons in O(1–100) μm

Martoff et al, D.A.E., 440 (2) (2000)

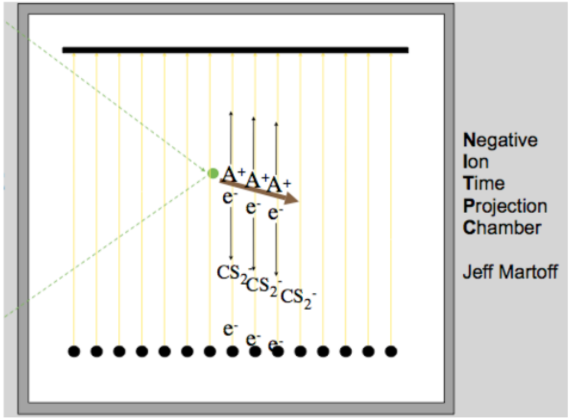

- The negative ion is carrying the information to the readout plane

- Slower drift velocity O(1) cm/ms

- Intense electric fields required to extract the electron from the negative ion

Martoff et al, D.A.E., 440 (2) (2000) Phan et al, JINST., 12 (2016)

- Pioneered by Martoff and DRIFT (CS_2) and New Mexico group (SF_6) (low pressure 10–100 Torr)

- Gas mixture of He:CF_4:SF_6 (59/39,4/1,6) was demonstrated a NID mixture with charge readout (610 Torr)

Baracchini et al,JINST, 13(04) (2018)

Negative Ion Drift (NID)

- Advantages:

Diffusion

- The large mass of ions allows better energy exchange with neutral component
- Large reduction on the diffusion during drift **(from 300 $\frac{\mu m}{\sqrt{cm}}$ of typical gas mixture to <100 $\frac{\mu m}{\sqrt{cm}}$)**

ED mix

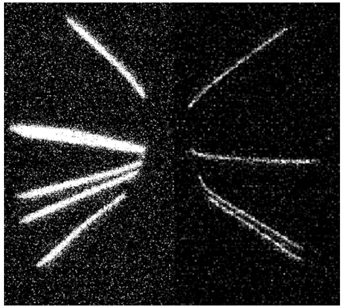

NID mix

Fiducialisation

- Different species with different masses can be generated

$$z = \frac{v_m v_M}{v_m + v_M} \Delta T$$

- Delay in arrival time allows very precise fiducialisation (130 μm res)

Iketa et al, JINST 15 (07) (2020)

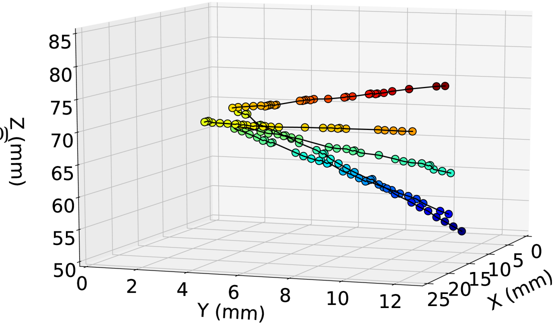

Summary

- Directional Dark Matter (Intro)
- Amplification Stage Optimisation
- Negative Ion Drift Operation
  - Atmospheric Pressure
  - Lower Pressure
- Directionality Studies
  - CYGNO-30 Limits
  - DM Discrimination

First NID with Optical Readout at High Pressure

- **$He:CF_4:SF_6$ (59/39.4/1.6) NID,** or standard $He:CF_4$ 60/40 (ED) is fluxed into MANGO detector
- Drift length increased to 5 cm with field cage
- 900 mbar (atmospheric pressure at LNGS)
- ^{241}Am source, which emits 5.4 MeV alpha particles, is positioned between the field cage rings

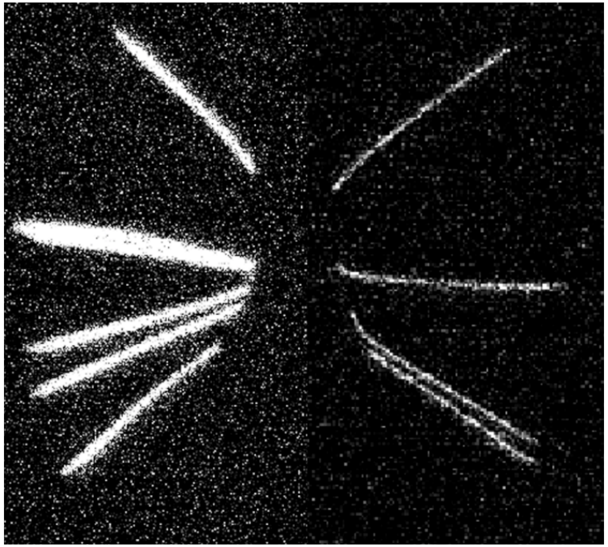

Gain Measurement

- sCMOS images analysed by reconstruction code
- Selection on the tracks:
  - Longer than 1.4 cm
  - Slimness < 0.3 (ratio of the width of a track over its length)

Distribution of light yield of reconstructed tracks

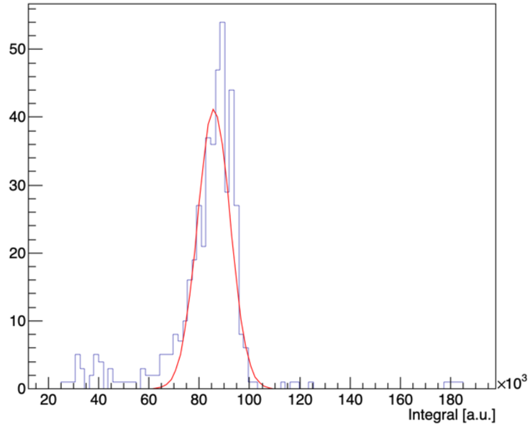

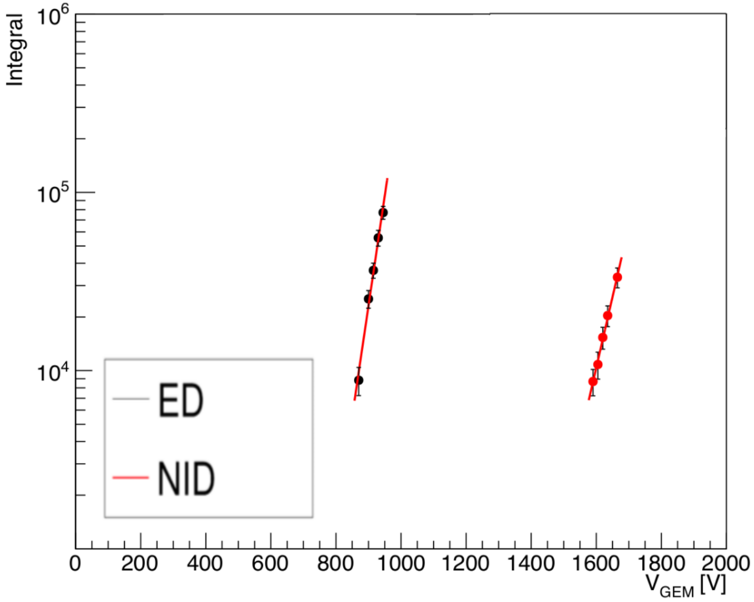

Rough estimation of the gain suggests O(10^4) achievable

Assuming the light production in the gas is similar

With charge readout it corresponds to O(1) keV_{ee} energy threshold

CYGNUS white paper:
https://arxiv.org/abs/2008.12587

Mobility Measurement

- The drift velocity cannot be measured by the drift time as the instant of interaction is unknown
- The elongation of the track along the drift direction is exploited and studied as a function of the drift field

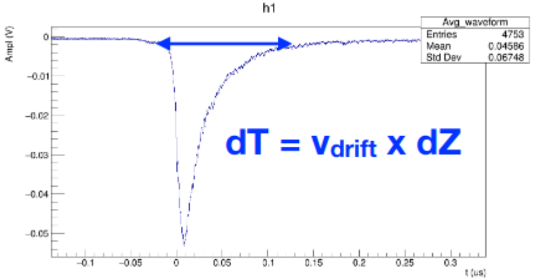

- **ED**

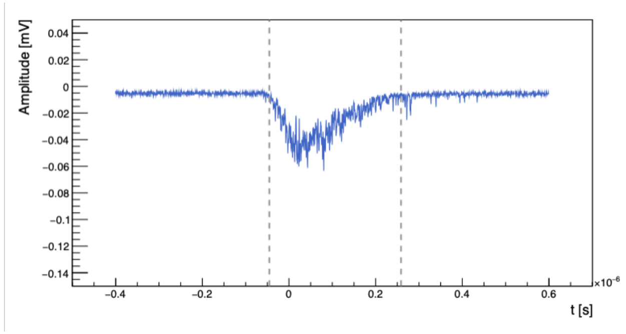

- Trigger directly on PMT
- Define start and end of the signal when the amplitude exceeds 3 times the RMS of the baseline
- Drift velocity taken from Garfield simulations

dZ = (0.7 $\pm$ 0.2) cm

Mobility Measurement

- NID

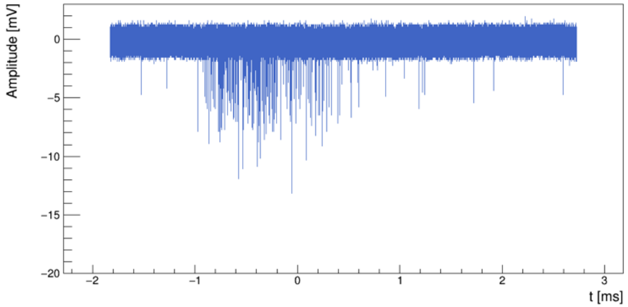

- **First ever PMT waveform of NID**
- Signal time extension of O(1) ms (as expected for typical NID mobilities)
- Sparse peaks of small intensity
- Trigger needed on the preamp signal
- Relevant peaks stored and rebinned to study the signal length

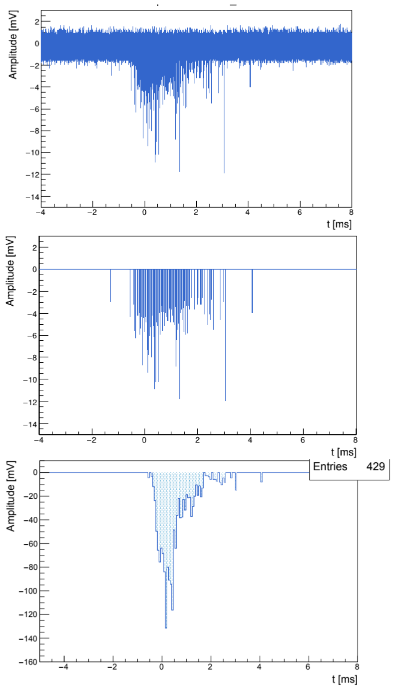

- **Reduced mobility**

$$\frac{E}{N} = \frac{E}{p} \cdot (1.0354 \cdot 10^{-2} \cdot T) \quad K_0 \equiv \mu_0 = \mu \frac{p}{p_0} \frac{T_0}{T}$$

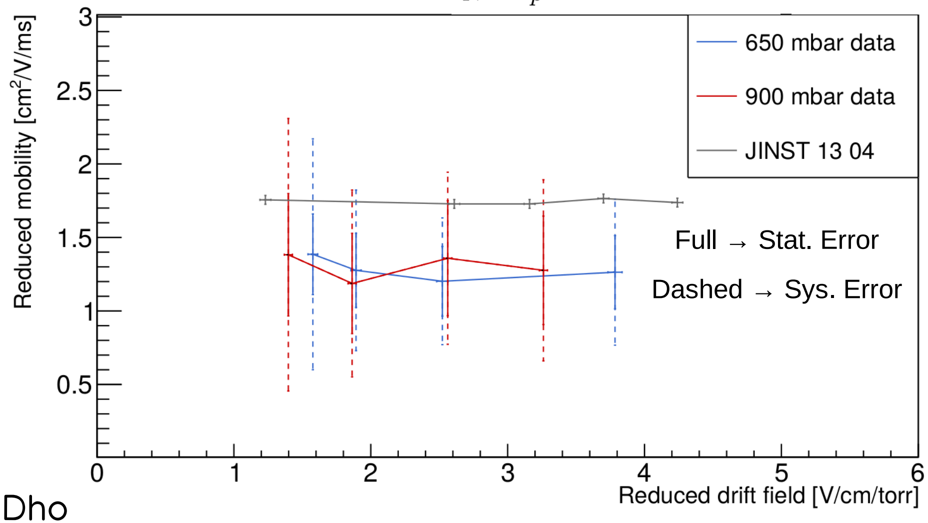

- Consistency with previous reduced mobility assessments
- Measure repeated also at lower pressure with improved collimation of the source consistent with 900 mbar data (blue points)
- NID operation confirmed

Summary

- Directional Dark Matter (Intro)
- Amplification Stage Optimisation
- Negative Ion Drift Operation
  - Atmospheric Pressure
  - Lower Pressure
- Directionality Studies
  - CYGNO-30 Limits
  - DM Discrimination

MANGOK

- To perform diffusion studies a longer field cage is needed
- 15 cm field cage implemented and installed in a vacuum vessel with quartz window
- Due to the dimensions of the vessel, the camera was positioned at arger distance than before
- To compensate for the light loss, the pressure was decreased to 650 mbar
- Alpha source was collimated and placed tilted for more precise measurements of the mobility (previous slides)
- Data taken with source placed parallel to GEM plane at different distances and with varying drift field
- The diffusion was estimated by the sigma of a Gaussian fit of the transverse profile of the tracks

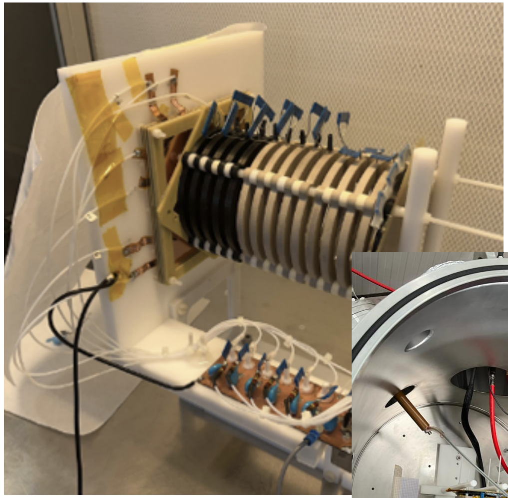

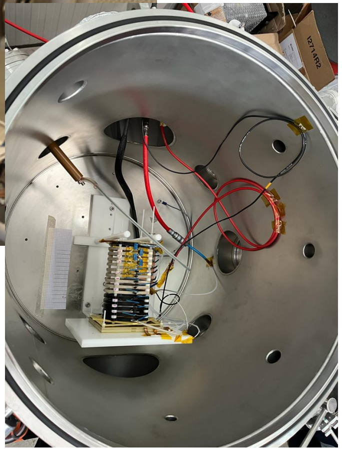

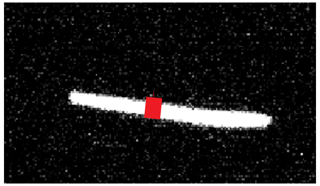

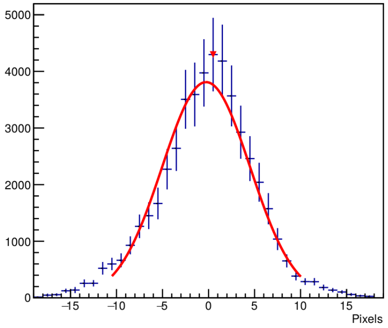

Transverse profile of alpha

TRANSVERSE DIFFUSION MEASUREMENT I

- Diffusion as a function of drift distance and drift electric field

ED

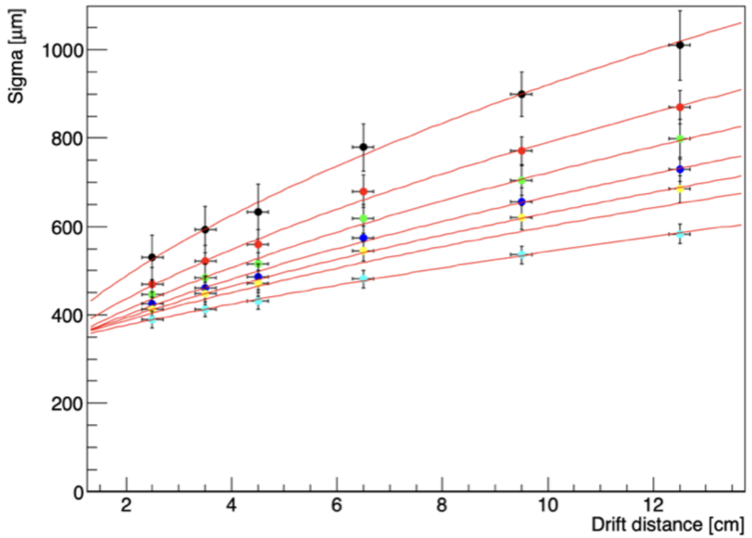

$$\sigma = \sqrt{\sigma_0^2 + \xi^2 L}$$

NID

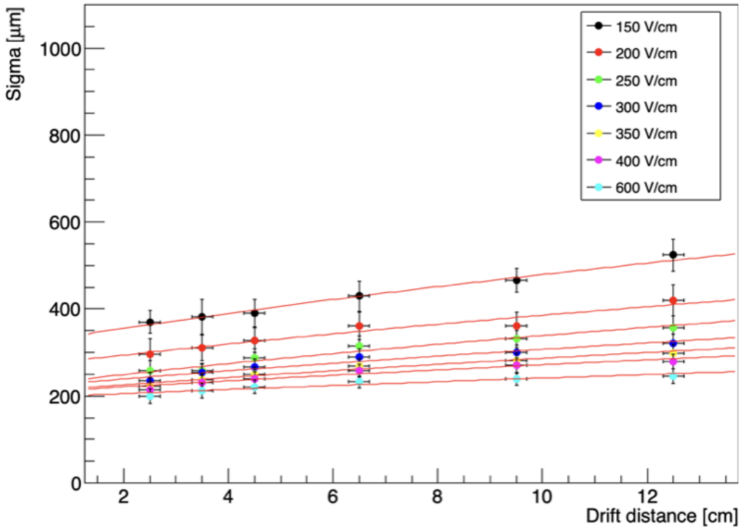

Drift field [V/cm]	σ_0^{ED} [μm]	ξ^{ED} [μm/$\sqrt{\text{cm}}$]	σ_0^{NID} [μm]	ξ^{NID} [μm/$\sqrt{\text{cm}}$]
150	300 ± 100	280 ± 20	320 ± 30	110 ± 10
200	290 ± 60	230 ± 10	260 ± 30	90 ± 20
250	290 ± 60	210 ± 10	220 ± 20	81 ± 10
300	300 ± 40	190 ± 10	220 ± 20	68 ± 10
350	300 ± 40	170 ± 10	210 ± 20	60 ± 10
400	310 ± 30	160 ± 10	210 ± 20	56 ± 9
600	320 ± 20	140 ± 10	200 ± 20	45 ± 10

Transverse Diffusion Measurement II

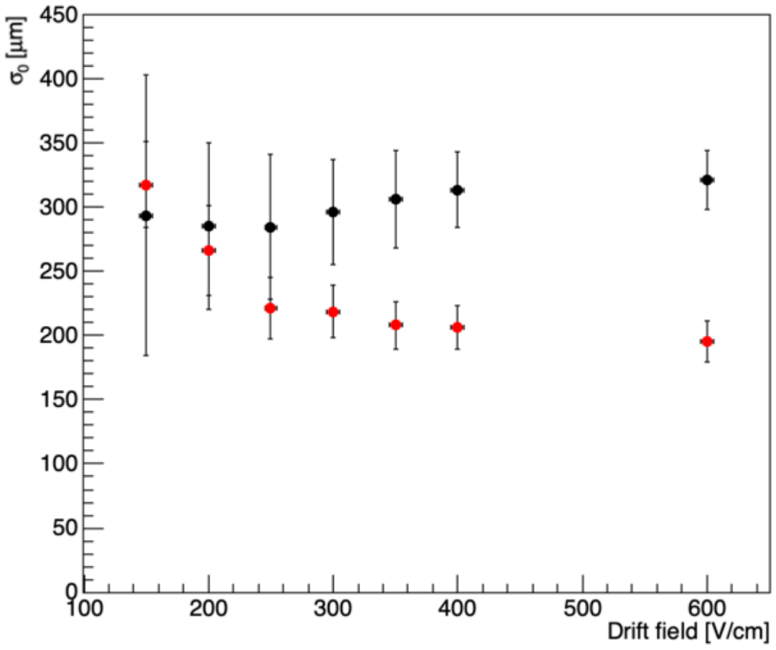

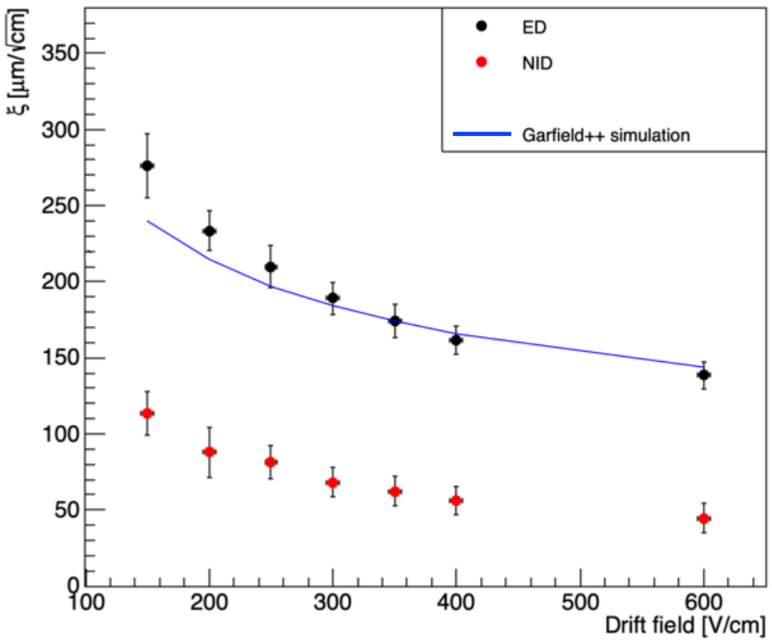

- ED measurement consistent with simulation
- Both intrinsic diffusion of the amplification stage and along drift are strongly reduced

DISCUSSION

- NID at nearly atmospheric pressure with optical readout was succesfully obtained for the first time ever
- One of the smallest ever diffusion coefficient was measured 45 $\frac{\mu m}{\sqrt{cm}}$ @ 600 V/cm ⟶ 35 $\frac{\mu m}{\sqrt{cm}}$ @ 1 kV/cm
- Compared with the 110 $\frac{\mu m}{\sqrt{cm}}$ of CYGNO standard gas mixture, it significantly improves the scalability of future directional DM detectors

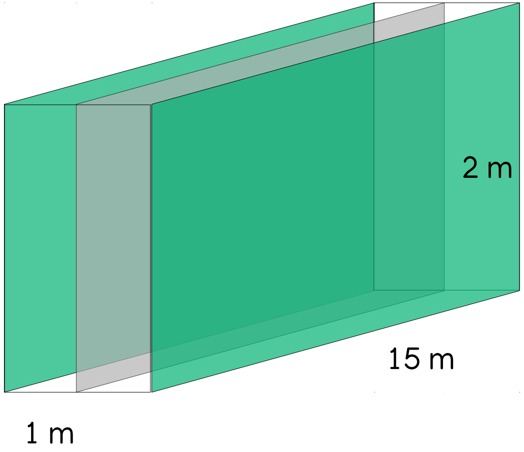

30 m^3

94 m^2

60 m^2 readout

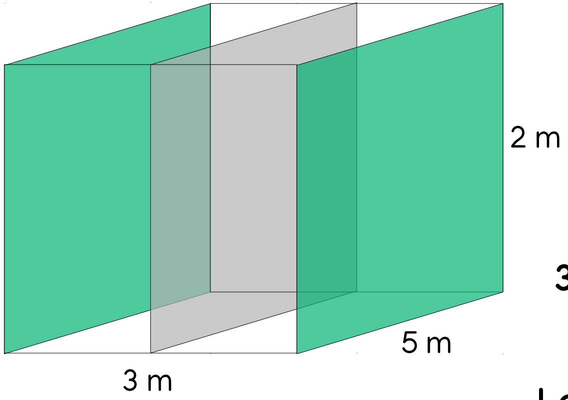

30 m^3

62 m^2

20 m^2 readout

30 m^2 less surface:
Less material (background)
Less redout sensors

- About 10^4 gain was also found, enough for detection of low energy recoils with a charge readout
- **Enables the realisation of CYGNUS**

CYGNUS white paper:
https://arxiv.org/abs/2008.12587

Summary

- Directional Dark Matter (Intro)
- Amplification Stage Optimisation
- Negative Ion Drift Operation
    - Atmospheric Pressure
    - Lower Pressure
- **Directionality Studies**
    - CYGNO-30 Limits
    - DM Discrimination

Directionality Potential

- Directionality can offer powerful means to improve the exclusion limits when searching for WIMP and the capability to identify the DM nature once a signal is found

CYGNO-30 Limits

- If no statistical significance of DM events over the background are found, limits can be placed
- Exploiting the angular distribution of the recoils more stringent limits can be estimated with respect to no angular information
- CYGNO-like detector of 30 m^3 with future expected performances is taken as an example

DM models discrimination

- Once a DM signal is found, how can we assess its nature?
- Directionality offers an additional observable to probe DM nature, that can result particularly crucial if more than one model can produce the same energy spectrum of NR
- Two models are studied to assess energy and angular capabilities in discrimination

Summary

- Directional Dark Matter (Intro)
- Amplification Stage Optimisation
- Negative Ion Drift Operation
  - Atmospheric Pressure
  - Lower Pressure
- Directionality Studies
  - CYGNO-30 Limits
  - DM Discrimination

Method and Bayesian Approach

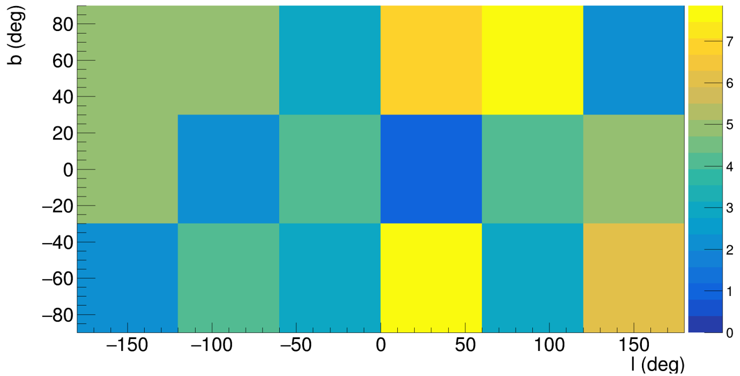

- Fake experiments are simulated with MC techniques starting from a background assumption (μ_b expected events)
- A likelihood function which includes the expected background and WIMP signal (μ_b, μ_s) is used to fit the data
- The likelihood function is profiled on the angular information to exploit it in the fitting procedure
- The Bayesian approach is employed as very sound in determination of limits close to physical boundary region
- The posterior probability on μ_s is calculated from the fitted likelihood

$$p(\vec{\mu}, \vec{\theta}|\vec{x}, H) = \frac{p(\vec{x}|\vec{\mu}, \vec{\theta}, H)\pi(\vec{\mu}, \vec{\theta}|H)}{\int_\Omega \int_D p(\vec{x}|\vec{\mu}, \vec{\theta}, H)\pi(\vec{\mu}, \vec{\theta}|H) d\vec{\mu} d\vec{\theta}}$$

- The 90% C.I. (Credible Interval) is estimated by

$$\mu_1(90\%CI) : \int_0^{\mu_1(90\%CI)} p(\mu_1|\vec{x}, H) d\mu_1 = 0.9$$

- The limit on the number of events is transformed into a limit on the WIMP cross section versus mass

Signal Model

- Only the angular distribution is considered in the study

$$\frac{dD}{d\cos\gamma} = \alpha_0 \int_{E_{thr}}^{E_{max}} S(E) \left(e^{-\frac{\left(\frac{\sqrt{2m_A E}}{2\mu_A} - v_{lab}\cos\gamma\right)^2}{v_p^2}} - e^{-\frac{v_{esc}^2}{v_p^2}} \right) dE$$

$$E_{max} = \frac{1}{2} m_\chi r (v_{lab}\cos\gamma + v_{esc})^2$$

γ = angle between recoil and Sun's opposite motion

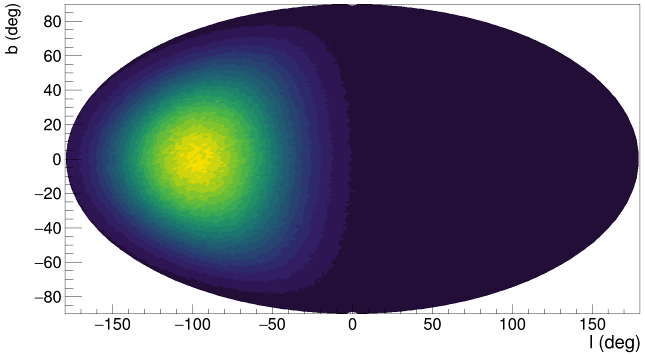

Angular performances

- **30°x30° deg** on all energy range
- Full **head-tail**

E range assumptions

- E_{max} maximum possible allowed by the escape velocity of the Galaxy
- E_{thr} taken as 1 keV_{ee} (conservative)
  0.5 keV_{ee} (realistic)

Prior assumption

- Taken flat between 0 and 1000

- The composiion of CYGNO gas mixture and the quenching factor are taken into account
  - Elements He, C, F (He:CF_4) and H (for R&D He:CF_4:iC_4H_{10})
  - Differently from electrons, nuclear recoils dissipate energy in other interactions that do not produce ionization

$$E_{ee} = QF \cdot E_{nr}$$

  - Effectively **each element has different energy threshold**

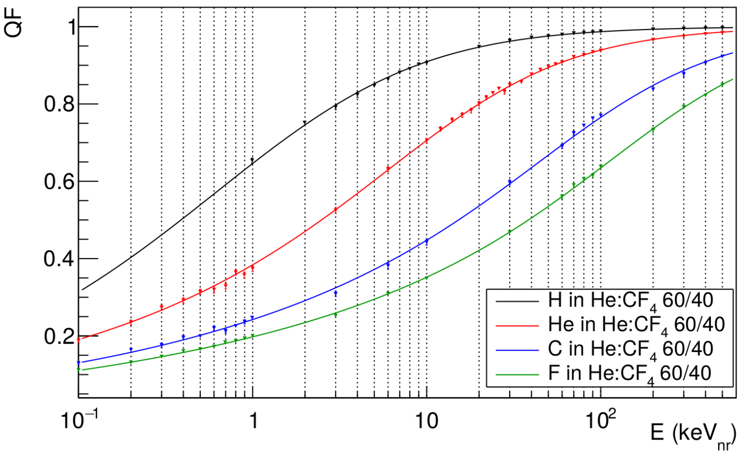

Element Recoil Probability

- With separate energy thresholds, each element has a different angular distribution

- To correctly account for the probability of each element to recoil and be detected, the total number of events is used as a weight function

$$N_{DMevt} = tV \frac{P}{P_{atm}} \frac{T_0}{T} \sum_i^{n_{mol}} \sum_j^{n_{el,i}} \rho_i k_i \frac{N_0}{A_{mol,i}} N_{at,i,j} \frac{2\rho_0 \sigma_{n,SI}}{m_\chi^2 r_j} \frac{\mu_{A,j}^2}{\mu_n^2} A_j^2 I_j^{E\gamma}(m_\chi, E_{thr,j})$$

$I^{E\gamma}_i$ integral of the velocity distribution

$$P_X = \frac{N_{DMevt,X}}{N_{DMevt}} = \frac{\sum_i^{n_{mo}} F_{i,X}}{\sum_i^{n_{mo}} \sum_j^{n_{el,i}} F_{i,j}}$$

$F_{i,j}$ term of the total event which depends on the gas *jth* atom in the *ith* molecule

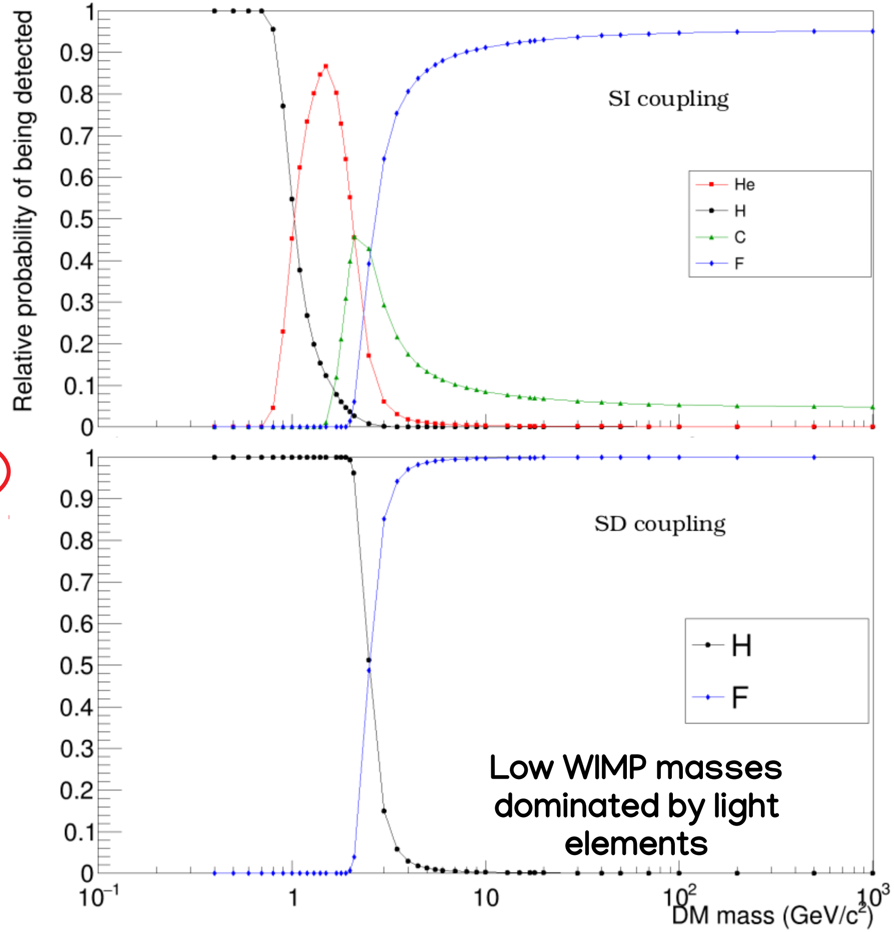

Different thresholds represent different WIMP mass threshold sensitivity

	1 keV$_{ee}$		0.5 keV$_{ee}$	
	$E_{thr,nr}$ (keV$_{nr}$)	Min DM mass (GeV/c^2)	$E_{thr,nr}$ (keV$_{nr}$)	Min DM mass (GeV/c^2)
H	1.4	0.5	0.8	0.3
He	2.1	1.0	1.2	0.7
C	3.1	1.9	1.8	1.4
F	3.8	2.5	2.2	1.9

Background Model

Angular distribution

- Considered flat as in Galactic coordinate it is expected to be (at first order)

Intensity

- Geant4 MC simulations predicts for CYGNO-04 a background of the order of 10-100 evt/y in the range 1-20 keV (after rejection of Ers)
- Given the uncertainty on how exactly CYGNO-30 will be realised and on what the experience on CYGNO-04 will teach us, three background scenarios are considered in this study $\mu_b = 10^2 \quad 10^3, \quad 10^4$ evt/y

Prior

- The background will be measured and highly simulated

- Poissonian distribution taken centred on the μ_b used

LIKELIHOOD

- Likelihood include both signal and background
- Based on a profiled event bin likelihood

$$\mathcal{L}(\vec{x}|\mu_s, \mu_b, H_1) = (\mu_b + \mu_s)^{N_{evt}} e^{-(\mu_b+\mu_s)} \prod_{i=1}^{N_{\text{bins}}} \left[\left(\frac{\mu_b}{\mu_b + \mu_s} P_{i,b} + \frac{\mu_s}{\mu_b + \mu_s} P_{i,s} \right)^{n_i} \frac{1}{n_i!} \right]$$

Poissonian fluctuation of total events

Product on all the bin of the histogram

Probability of event to end in the *ith* bin weighted on signal to background proportion

Weighting factor

Likelihood

- Likelihood include both signal and background
- Based on a profiled event bin likelihood

$$\mathcal{L}(\vec{x}|\mu_s, \mu_b, H_1) = (\mu_b + \mu_s)^{N_{evt}} e^{-(\mu_b+\mu_s)} \prod_{i=1}^{N_{\text{bins}}} \left[\left(\frac{\mu_b}{\mu_b + \mu_s} P_{i,b} + \frac{\mu_s}{\mu_b + \mu_s} P_{i,s} \right)^{n_i} \frac{1}{n_i!} \right]$$

Poissonian fluctuation of total events

Product on all the bin of the histogram

Probability of event to end in the *ith* bin weighted on signal to background proportion

Weighting factor

- Probability to end up in a bin

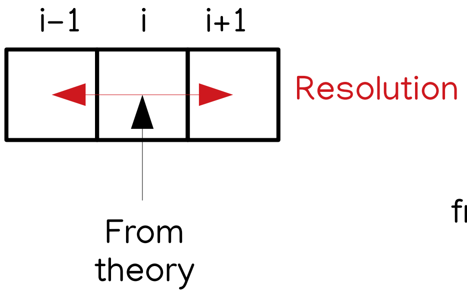

$$P_{i,x} = \sum_{j=i}^{N_{adjacent}} \left[P^{\text{migrate}}_{j\to i} \sum_{k}^{n_{el}} P^{theo}_{k,j,x} P^{el}_{k,x} \right]$$

Estimated from element probability

Migration probability from one bin to another due to resolution

From theoretical distribution

Effect of Directionality

- 90% C.I. evaluated with and without profiling on the angular distribution

$$\mathcal{L}(\vec{x}|\mu_s,\mu_b,H_1) = \frac{(\mu_b+\mu_s)^{N_{evt}}}{N_{evt}!}e^{-(\mu_b+\mu_s)}$$

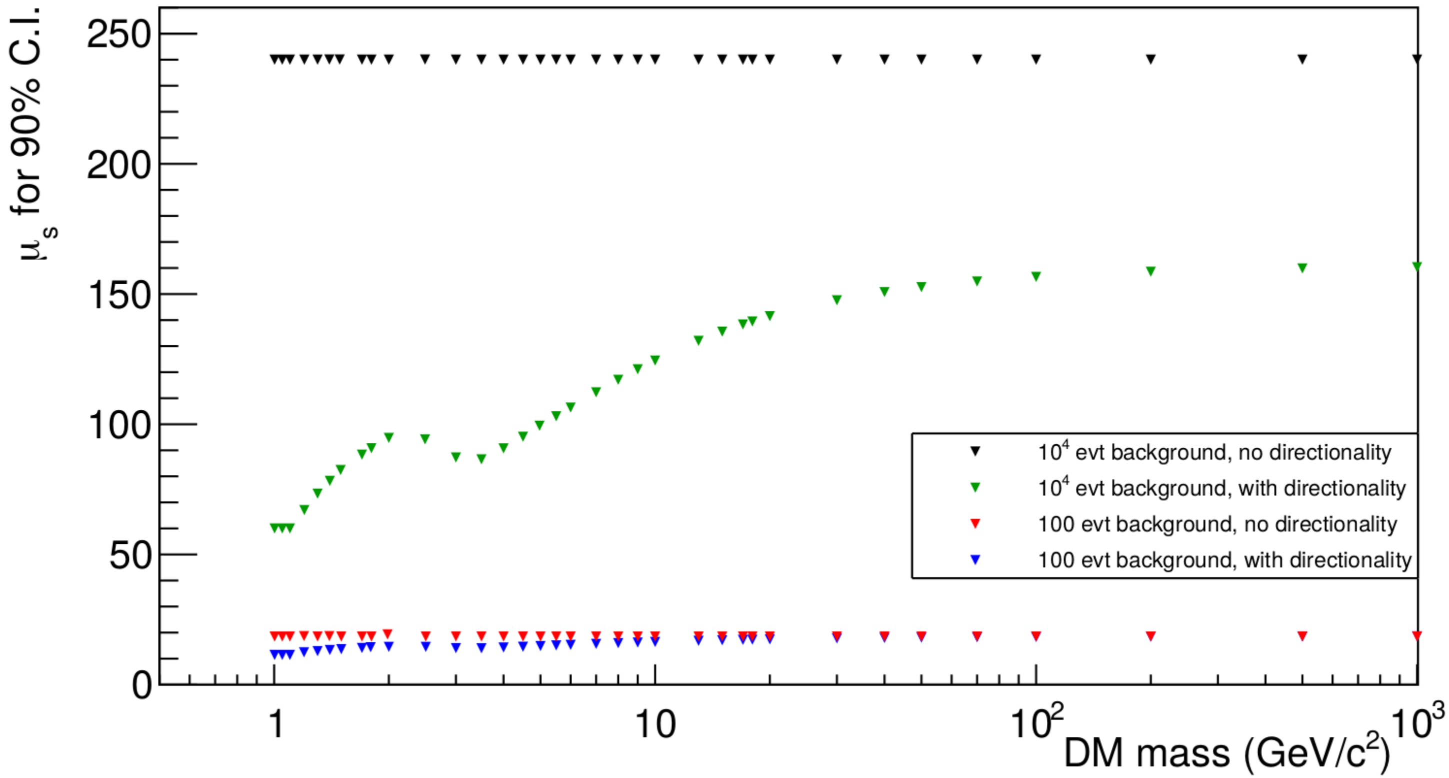

Direction more effective with more background

↓

For directional detectors, sensitivity improves with backgrounds

Stronger effect when the angular distribution is more peaked

CYGNO-30 Limits

Solid lines	**current limits**
Dotted lines	**future limits**

Amaro et al, Instruments 6 (1) (2022)

SI

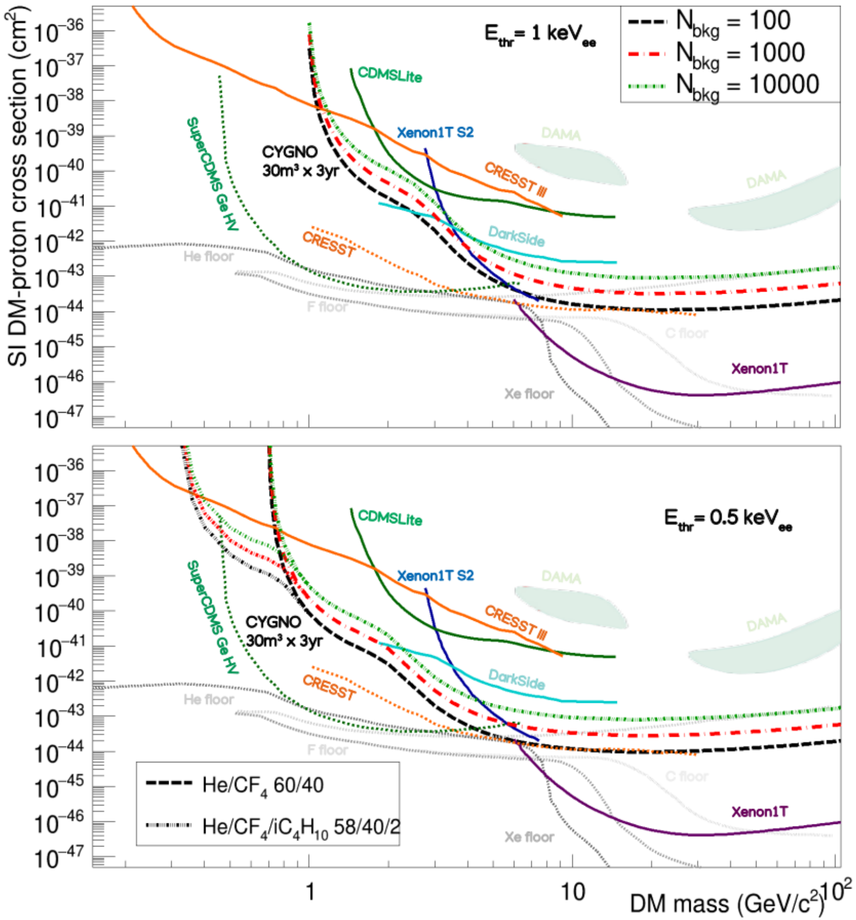

SD

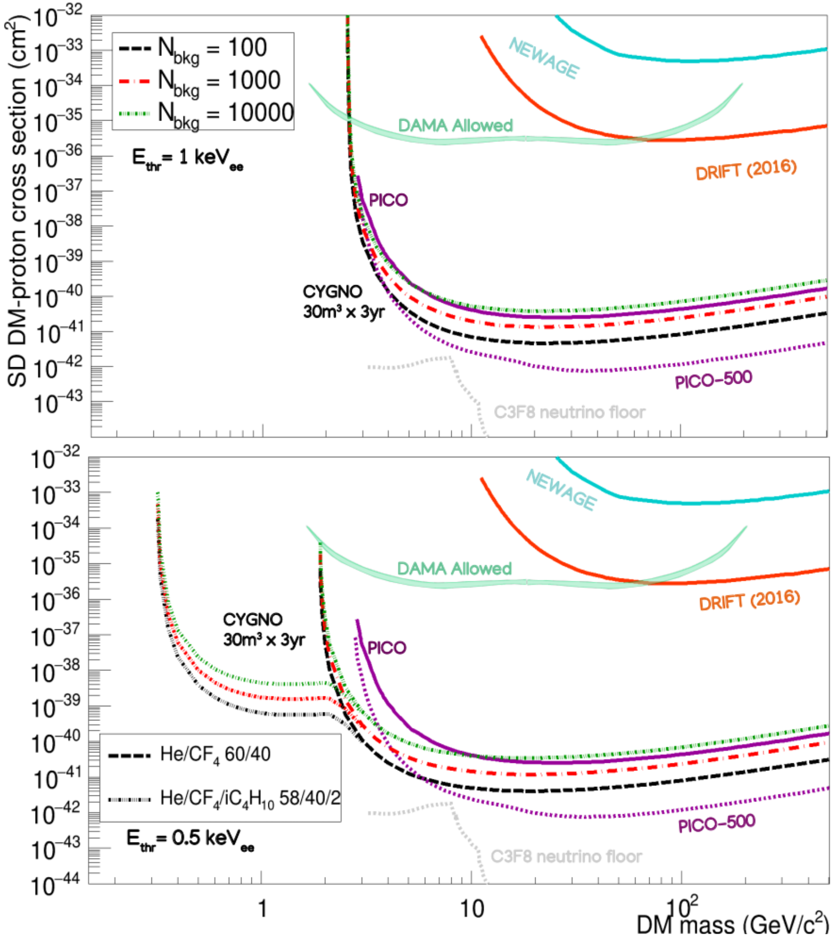

Summary

- Directional Dark Matter (Intro)
- Amplification Stage Optimisation
- Negative Ion Drift Operation
    - Atmospheric Pressure
    - Lower Pressure
- Directionality Studies
    - CYGNO-30 Limits
    - DM Discrimination

Method and Frequentist Approach

- Two DM models are compared (WIMP and SNDM) which can induce nuclear recoils of comparable energy
- The main assumption is that μ_n events induced by DM are unequivocally detected
- A frequentist approach is used based on a loglikelihood ratio test
- The likelihoods and fake experiments are profiled on one single measurable quantity at a time: **energy, 1D angle, 2D angle**
- **Goal:** find for each observable the minimum number of events to discriminate the two models
- Distributions *g* of likeliood ratios are built with the different MC truths
- **Discrimination:** when type I and II errors are 5%

Hypothesis
WIMP = H_0
SNDM = H_1

MC truth
z = WIMP, SNDM

$$\lambda_z = \frac{\mathcal{L}_{z|H_1}}{\mathcal{L}_{z|H_0}}$$

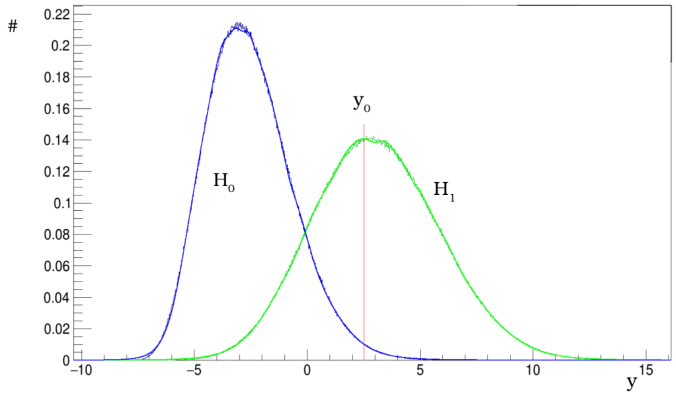

$$\text{Error Type I: } a_I = \int_{y_0}^{+\infty} g_{H_0}(y)dy$$

$$\text{Error Type II: } a_{II} = \int_{-\infty}^{y_0} g_{H_1}(y)dy$$

Supernova Dark Matter (SNDM)

- Dark fermion of O(1–100) MeV/c² mass coupled to SM via dark photon

$$\mathcal{L} \supset \frac{e\epsilon g_d}{\Lambda^2}\bar{\chi}\gamma_\mu\chi J^\mu_{\rm em}$$

- Could be generated in SN explosion and couple to electrons

DeRocco et al, PRD, 100 (7) (2019)

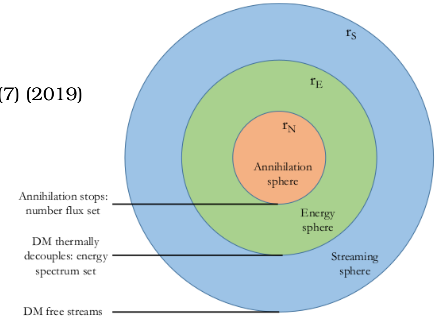

Flux of DM **MeV** particles with **semirelativistic** velocity → **can induce keV recoils on nuclei**

- The Maxwell-Boltzmann distribution of their velocity induces a spread in time of arrival → **Diffuse flux from Galaxy**

- Most of SN are in the centre of the Galaxy

Baracchini et al, PRD, 102 (7) (2020)

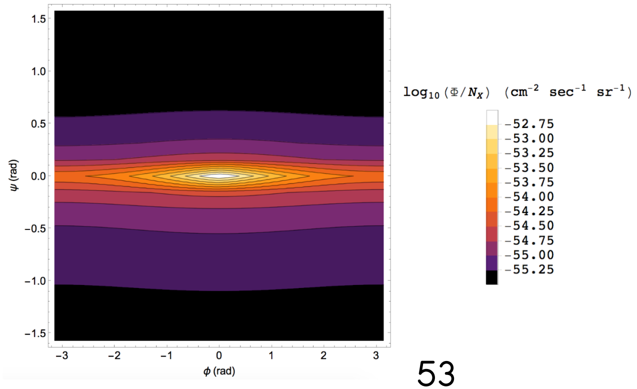

anisotropic flux

Experimental Assumptions

Target material

- **^{131}Xe, ^{19}F, ^{4}He** for sensitivity of large and small WIMP mass comparing classical, tonne-scale direct DM search experiment to directional ones

Energy range

- Xenon experiment has **[4.9, 40.9] keV** for WIMP search for efficiency and expected WIMP signal Aprile et al., PRD, 100 (5) (2019)
- Using the same conditions the energy range for He and F is transformed to **[5.9, 100] keV**

Energy resolution

- For Xe, taken from Xenon experiment → $\sigma_E = \frac{a}{\sqrt{E}} + b$ Aprile et al., PRD, 97 (9) (2018)
- For F and He, assumed in a gas detector → $\sigma_E = \sqrt{c^2 + \frac{d^2}{E}}$ Vahsen et al., NIM A, 788 (2015)

Angular resolution

- Variable from 2° deg (better than perfect) up to 45° (worst than foreseen)
- Full head-tail

NO BACKGROUND

Energy and Angular Spectra

- Different scenarios of WIMP and SNDM parameters are tested for a total of 6 scenarios

Low and large WIMP masses

Scenario	Target	WIMP Mass [GeV/c^2]	SNDM Mass [MeV/c^2]	T [MeV]	$\log_{10} y$	Φ
1	^{4}He	10	5	0.31	-13.3	0.006
2	^{19}F	10	7	1.0	-14.3	0.02
3	^{131}Xe	10	9	1.6	-14.6	0.03
4	^{4}He	100	5	0.52	-14.0	0.01
5	^{19}F	100	14	3.0	-15.0	0.07
6	^{131}Xe	100	38	13.4	-16.0	0.1

SNDM parameters chosen so that average recoil momentum is equal

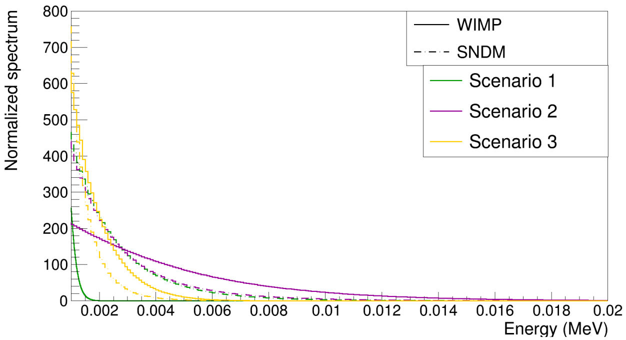

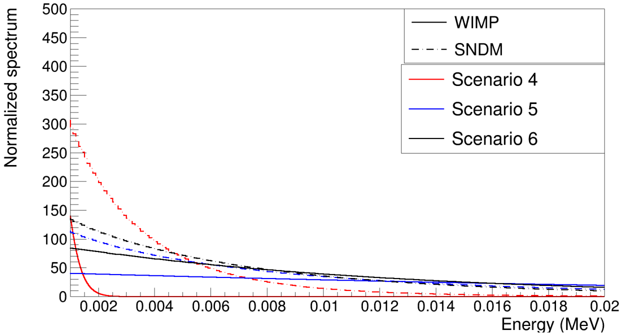

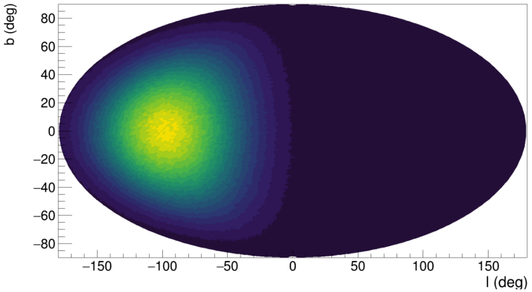

WIMP

Scenario 2

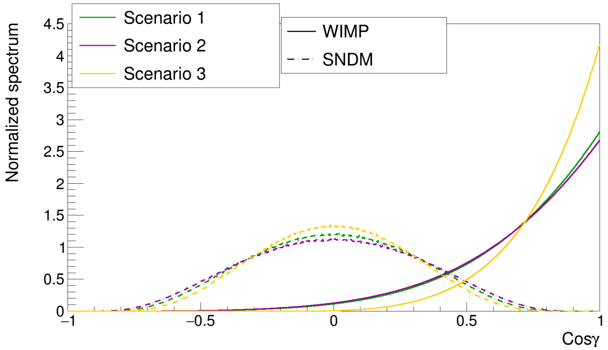

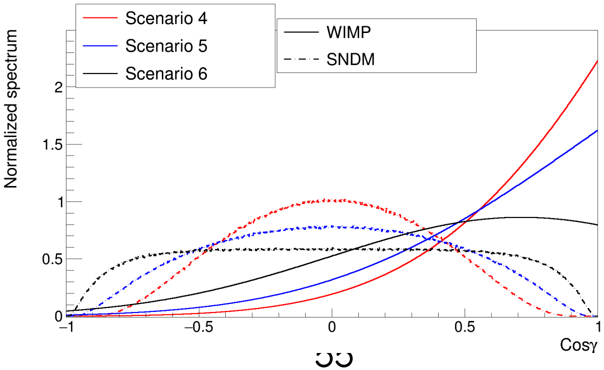

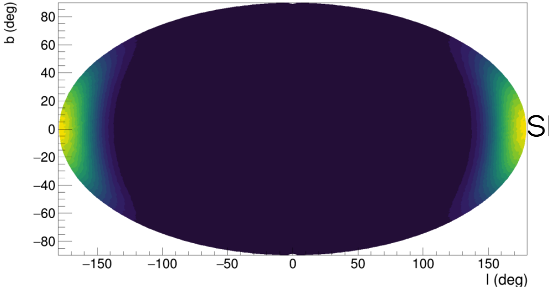

SNDM

Results

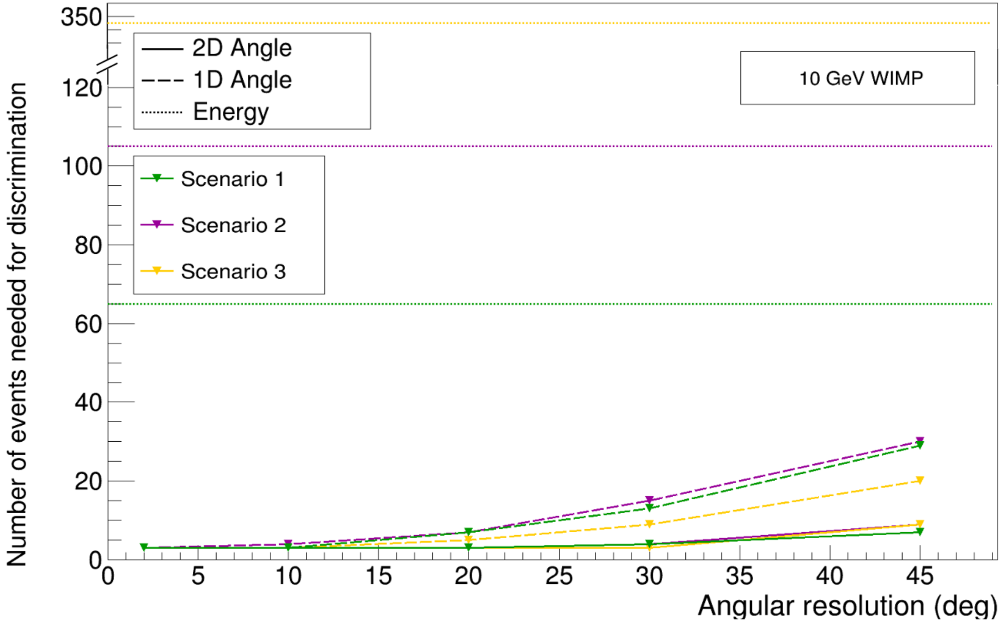

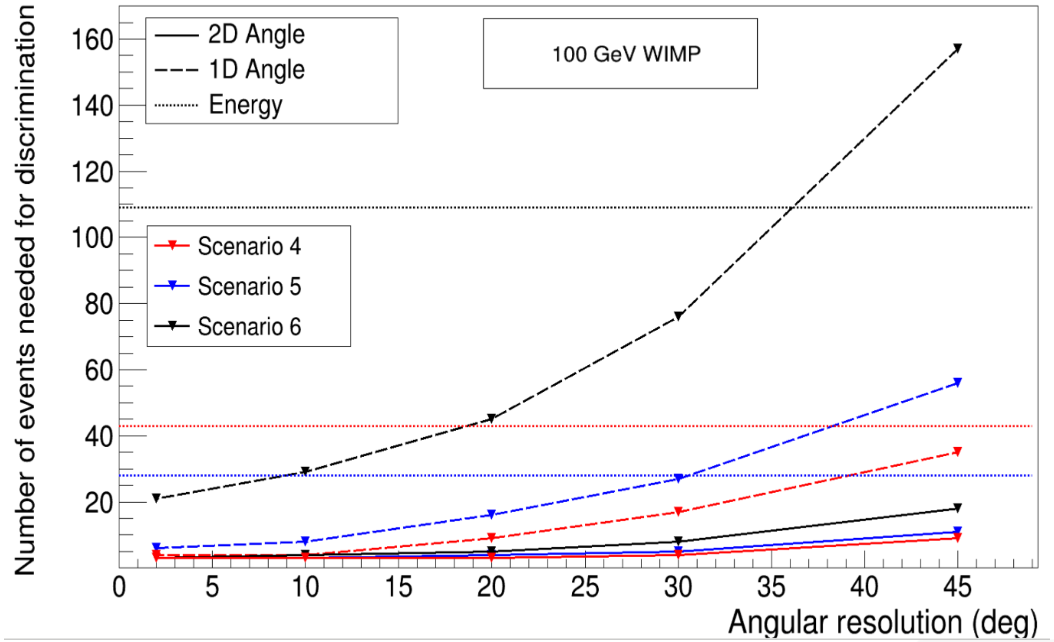

- Better discrimination with 1D angle with better than 30° angular resolution
- 3D angular information improves discrimination by orders of magnitude

PHYSICAL REVIEW D **102,** 075036 (2020)

Discovering supernova-produced dark matter with directional detectors

Elisabetta Baracchini,[1,2] William DeRocco,[3] and Giorgio Dho[1,2]
[1] *Gran Sasso Science Institute, I-67100, L'Aquila, Italy*
[2] *Istituto Nazionale di Fisica Nucleare Laboratori Nazionali del Gran Sasso, I-67100 Assergi, Italy*
[3] *Stanford Institute for Theoretical Physics, Stanford University, Stanford, California 94305, USA*

(Received 18 September 2020; accepted 12 October 2020; published 27 October 2020)

Conclusions

- Dark matter is one of the most relevant topics in modern physics
- Directional search is key for:
  - improved search within neutrino fog
  - Claim of positive discovery of DM
- Future WIMP DM searches will require directional detectors
- The CYGNO experiment aims to build a large, O(30–100) m^3, directional detector for rare event searches
- CYGNO employs a TPC filled with He:CF_4 with GEM amplification and optical readout

Conclusions

- Fundamental observables for DM directional detectors based on gaseous TPCs are
  - Energy threshold
  - Topological structure of the recoils

- The study and optimisation of the amplification stage to increase the light yield without degrading the intrinsic diffusion was performed with CYGNO prototypes
- The addition of an extra electrode below the last GEM allowed to enhance the light yield and in combination with other GEM structures proved to be versatile improving the detector characteristics

- Small amount of SF_6 gas was added to the CYGNO gas mixture and NID operation was successfully obtained at almost atmospheric pressure with optical readout
- The 45 $\frac{\mu m}{\sqrt{cm}}$ diffusion coefficient measured is one of the smallest ever measure at 600 V/cm, opening possibilities for new imaging detectors

- The potential of directionality was studied in the limit estimation for a CYGNO-like of 30 m^3 detector allowing a factor 4-5 improvement with large background
- The capabilities in DM models discrimination was put under test with a simple analysis which showed how directionality can outperform the energy information by orders of magnitude

Future Prospects

- The extra electrode in the amplification stage proved to be extremely useful. It would be interesting to develop an amplfication structure tailored to exploit this process with a compactified geometry

- Extensive studies on the NID gas composition which allowed such low diffusion to be achieved. It includes

    - Different concentrations of He, CF_4, SF_6 and different gases (CH_3NO_2) to explore the phenomenon and gas mixtures with the gaol of further minimising diffusion

    - Employ diverse amplification structures (COBRA, MMTHGEM) to improve the absolute NID gain

- These optimisation studies improve imaging TPCs beyond the case of DM, with potential application to Solar neutrino spectroscopy, x-ray polarimetry and Migdal effect

- Following LIME underground operation, exploit the measured background to perfection the limit estimation of a 30 m^3 CYGNO directional detector

BACKUP

Spectrum Calculation

- The differential rate per unit mass can be formulated from

$$\frac{dR}{dq^2 d\Omega} = \frac{N_0}{A_{mol}} \frac{\rho_0}{m_\chi} \int_{v_{min}(q)} \frac{d\sigma}{dq^2 d\Omega} v f(\vec{v}) d^3 v$$

Kinematics

$$\frac{dR}{dq^2 d\Omega} = \frac{N_0}{A_{mol}} \frac{\rho_0}{m_\chi} \frac{d\sigma}{dq^2} \frac{1}{2\pi} \int \delta\left(\cos\theta - \frac{q}{2\mu_A v}\right) v f(\vec{v}) d^3 v$$

Cross section

$$\frac{d\sigma}{dq^2} = \frac{1}{\pi v^2} |\mathcal{M}|^2 = \frac{\sigma_{WA} S(q)}{4\mu_A^2 v^2}$$

$$\sigma_{WA} = \sigma_{WA,SI} + \sigma_{WA,SD}$$

$$\begin{cases} \sigma_{WA} = \frac{4\mu_A^2}{\pi}\left[Z f_p + (A-Z) f_n\right]^2 \\ \sigma_{WA,SD} = \frac{32 G_F^2 \mu_A^2}{\pi} \frac{J+1}{J} \left(a_p \langle S_p \rangle + a_n \langle S_n \rangle\right) \end{cases}$$

$$\sigma_{WA} = \sigma_{n,SI} \frac{\mu_A^2}{\mu_p^2} A^2 + \sigma_{p,SD} \frac{\mu_A^2}{\mu_p^2} \frac{4 \langle S_p \rangle (J+1)}{3J}$$

SHM velocity distr

$$f(\vec{v}) = \begin{cases} \alpha e^{-\frac{v^2}{v_p^2}} & \text{if } |\vec{v}| < v_{esc} \\ 0 & \text{if } |\vec{v}| > v_{esc} \end{cases}$$

Radon transform with v_{lab}

$$\frac{dR(t)}{dE\, d\cos\gamma} = \frac{N_0}{A_{mol}} \frac{2\rho_0 \sigma_{n,SI} S(E)}{m_\chi^2 r} \frac{\mu_A^2}{\mu_n^2} A^2 \pi \frac{v_p^3}{v_{lab}(t)} \alpha' \times$$

$$\times \left(e^{-\frac{\left(\frac{\sqrt{2 m_A E}}{2\mu_A} - v_{lab}(t)\cos\gamma\right)^2}{v_p^2}} - e^{-\frac{v_{esc}^2}{v_p^2}} \right) \Theta\left(\cos\gamma - \frac{\frac{\sqrt{2 m_A E}}{2\mu_A} - v_{esc}}{v_{lab}(t)} \right)$$

Dependence of the Spectrum

- The spectrum depends on 3 main observables:

$$\frac{dR(t)}{dEd\cos\gamma} = \frac{N_0}{A_{mol}}\frac{2\rho_0\sigma_{n,SI}S(E)}{m_\chi^2 r}\frac{\mu_A^2}{\mu_n^2}A^2\pi\frac{v_p^3}{v_{lab}(t)}\alpha'\times$$

$$\times\left(e^{-\frac{\left(\frac{\sqrt{2m_AE}}{2\mu_A}-v_{lab}(t)\cos\gamma\right)^2}{v_p^2}} - e^{-\frac{v_{esc}^2}{v_p^2}}\right)\Theta\left(\cos\gamma - \frac{\frac{\sqrt{2m_AE}}{2\mu_A}-v_{esc}}{v_{lab}(t)}\right)$$

Energy

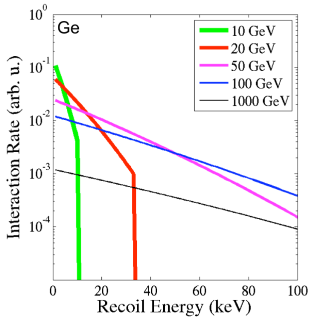

Schnee, World Scientific (2011)

Time

$$\frac{dR}{dE} \simeq R_0 + R_m\cos(\omega(t-t_0))$$

Angle

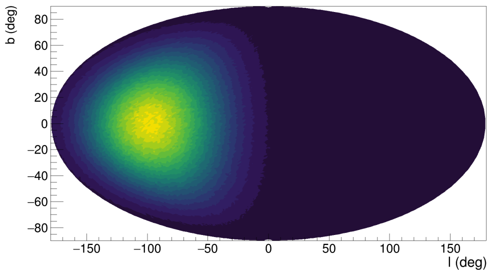

Neutrino Fog

- Previously different definition of neutrino floor: **insurmountable obstacle to DM search**
- New definition independent on the experiment (just on the target material)
- Energy recoil spectra of neutrino or DM induced recoils differ

$$n = -\left(\frac{d\ln\sigma_{n,SI}}{d\ln N}\right)^{-1}$$

How the discovery potential improves with larger exposures

No background n=1

Known subtractable background n=2

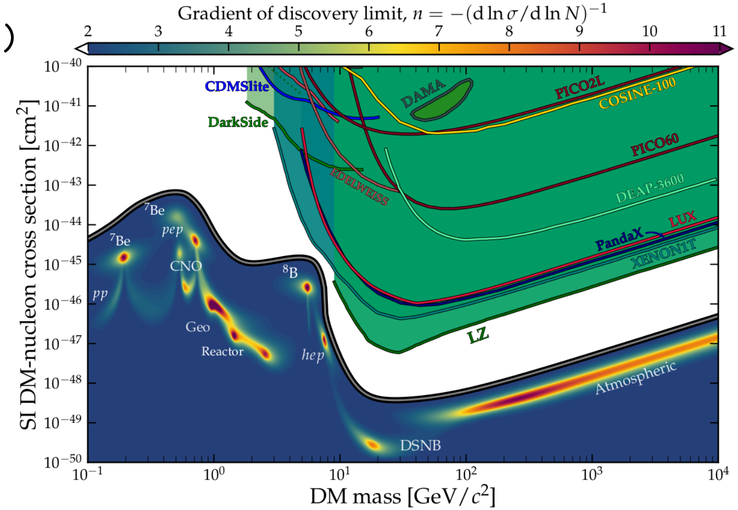

ν floor: when n crosses 2

- The investment of only-energy-sensitive detectors in exposure is not worth it

Directionality can sidestep the problem

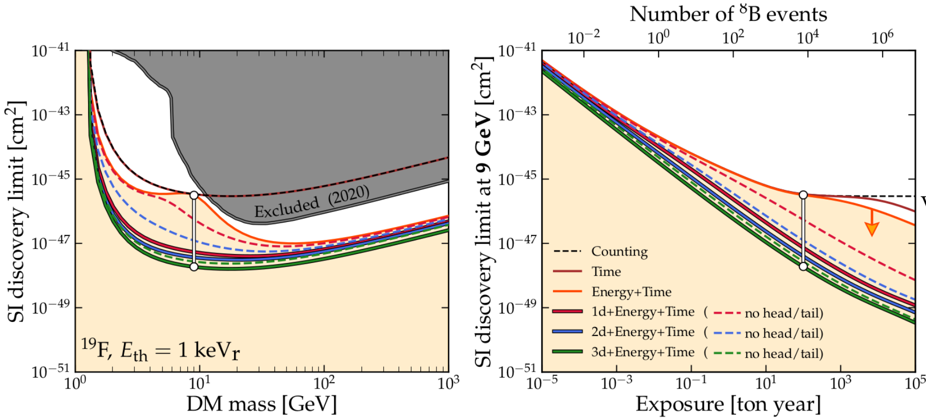

Vahsen et al, A.R., 71 (1) (2021)

REJECTION CAPABILITIES

- **Background rejection** capabilities were tested with LEMOn prototype

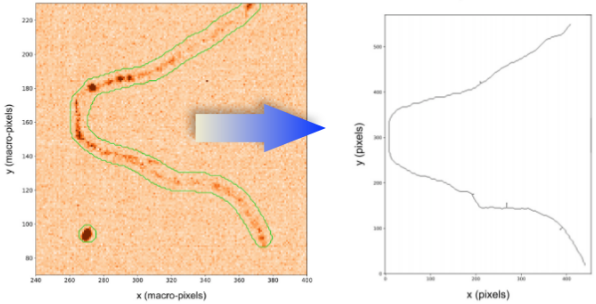

- Algorithm based on DBSCAN recognizes the tracks and allows topogical studies
- A simple cut on the photon density per pixel of the sCMOS pictures allows to reject 96% of background at 6 keV keeping about 40% signal efficiency
- Machine learning techniques exploiting more topological information are under development

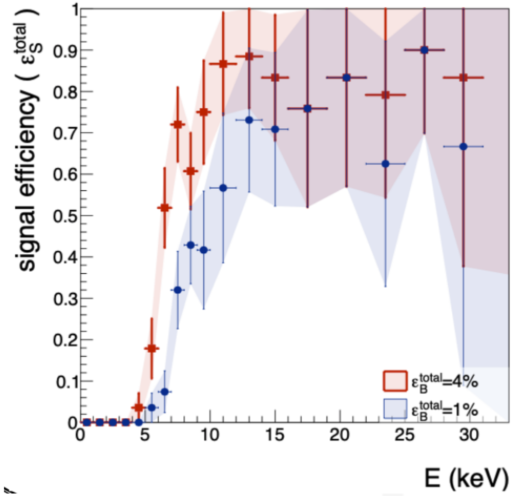

FIDUCIALISATION CYGNO

- Electron transverse diffusion can be exploited to infer the track Z coord.
- Track transverse light profile measured to have gaussian shape which enlarges linearly with Z
- Measured with both:

450 MeV e⁻

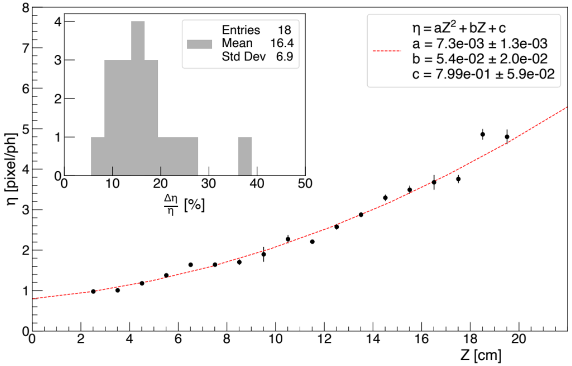

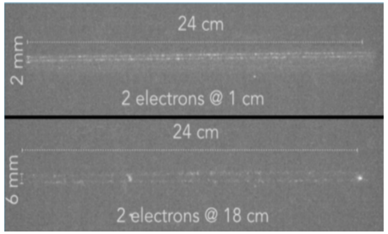

5.9 keV e⁻

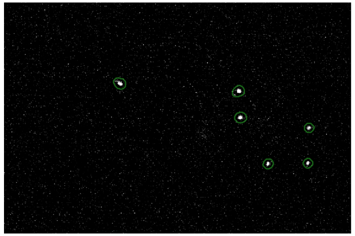

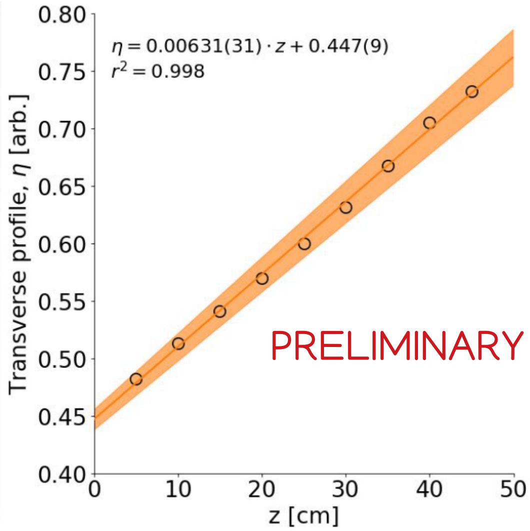

15% z resolution

5 cm z resolution

LIME Underground Plan

Shield	External		Internal		Total	
	ER/yr	NR/yr	ER/yr	NR/yr	ER/yr	NR/yr
No shield	$1.13\ 10^9$	1450	$7.26\ 10^6$	$6.11\ 10^4$	$1.14\ 10^9$	$6.25\ 10^4$
4cm Cu	$2.64\ 10^7$	850	$7.26\ 10^6$	$6.11\ 10^4$	$3.43\ 10^7$	$6.19\ 10^4$
10cm Cu	$1.95\ 10^6$	915	$7.26\ 10^6$	$6.11\ 10^4$	$9.78\ 10^6$	$6.20\ 10^4$
10cm Cu + cuts	N.A.	772	N.A.	16	N.A.	788
40cm H_2O +10 Cu	$5.09\ 10^5$	2.0	$7.26\ 10^6$	$6.11\ 10^4$	$8.34\ 10^6$	$6.11\ 10^4$
40cm H_2O +10 Cu + cuts	$2.0\ 10^4$	2.0	$2.8\ 10^5$	17	$3.3\ 10^5$	19

No shield configuration

- Characterization of the detector with ^{55}Fe sources
- **External background studies**, to cross-check simulation

2 months

4 cm copper

- **External background studies**, to cross-check simulations
- ^{55}Fe calibration

1 month

10 cm copper

- **External background studies**,to cross-check simulations, ^{241}AmBe measurements
- **Measurement of underground neutron flux.** Expected **200** events above **20 keV** in 4 months

4 months

10 cm copper and 40 water

- **Internal background studies** for final MC validation, when internal and external background are expected to have the same intensity

10 months

Relevenat Parameters for Discovery Potential

- Billard, Mayet, Santos (Physical Review D ,85(3) (2012)) found out the most relevant parameters for a limit or discovery potential of WIMP:

Energy threshold **Background level** **Head-tail** **3D** **angular res** **energy res**

Only directional

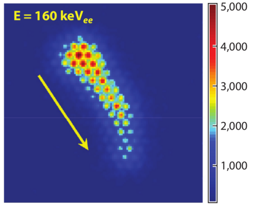

Vahsen et al., Annual review

- The WIMP masses which can induce detectable recoils depend on the E_{thr}

$$E_{max} = \frac{1}{2} m_\chi r (v_{lab} \cos\gamma + v_{esc})^2$$

	1 keV$_{ee}$		0.5 keV$_{ee}$	
	$E_{thr,\mathrm{nr}}$ (keV$_{\mathrm{nr}}$)	Min DM mass (GeV/c^2)	$E_{thr,\mathrm{nr}}$ (keV$_{\mathrm{nr}}$)	Min DM mass (GeV/c^2)
H	1.4	0.5	0.8	0.3
He	2.1	1.0	1.2	0.7
C	3.1	1.9	1.8	1.4
F	3.8	2.5	2.2	1.9

THRESHOLD 1 OR 0.5 keV_{EE}

- The WIMP masses which can induce detectable recoils depend on the E_{thr}

$$E_{max} = \frac{1}{2} m_\chi r (v_{lab} \cos\gamma + v_{esc})^2$$

	1 keV_{ee}		0.5 keV_{ee}	
	$E_{thr,nr}$ (keV_{nr})	Min DM mass (GeV/c^2)	$E_{thr,nr}$ (keV_{nr})	Min DM mass (GeV/c^2)
H	1.4	0.5	0.8	0.3
He	2.1	1.0	1.2	0.7
C	3.1	1.9	1.8	1.4
F	3.8	2.5	2.2	1.9

- Also it modifies the part of the velocity distribution which can cause a recoil

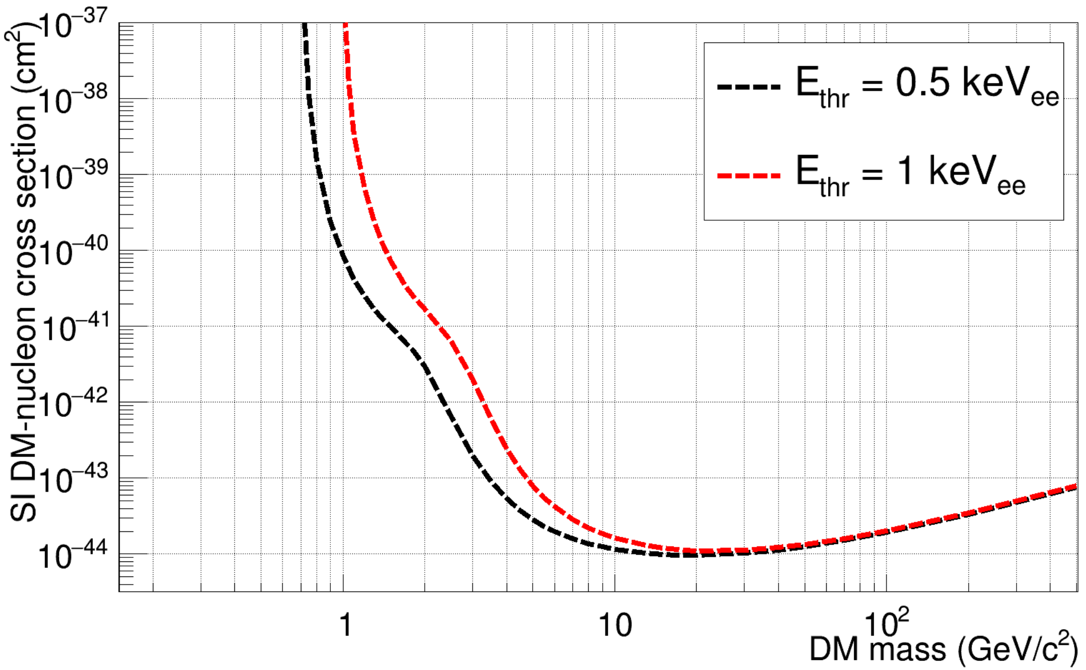

$He:CF_4$ gas in CYGNO-like 30 m^3

Light Analysis

- LEMOn detector: 20x24 cm^2 readout area and 20 cm drift, effective granularity 125 x 125 μm^2)
- Studies on the light amplification induced by electric field below the last GEM extended with LEMOn prototype and an ITO glass (T=0.9)
- ORCA Fusion camera employed (2304x2304 pixels, 0.7 e^- RMS)
- ^{55}Fe source (5.9 keV X-ray) of 115 MBq produces current signals well above the sensitivity of the LEMOn current reader (10 nA)
- The light measurements used 1 s exposure and average light output on different areas (after noise pedestal subtraction)

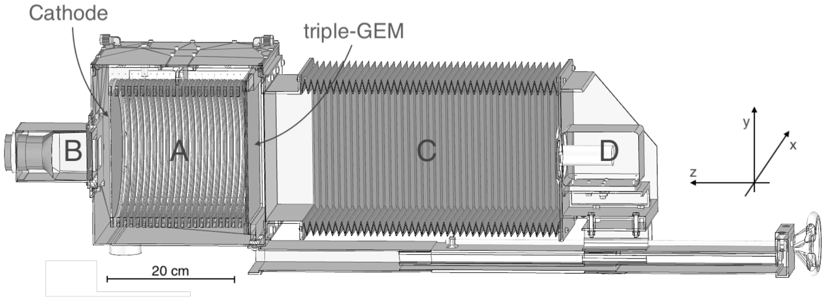

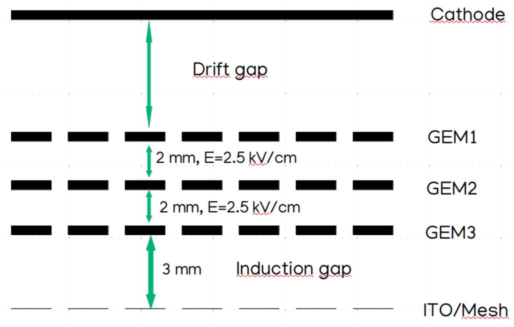

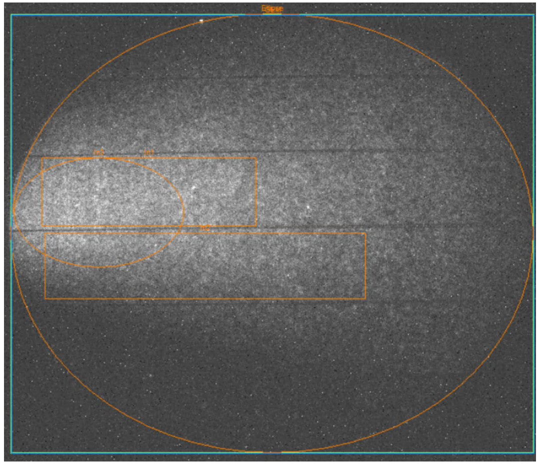

Charge Analysis

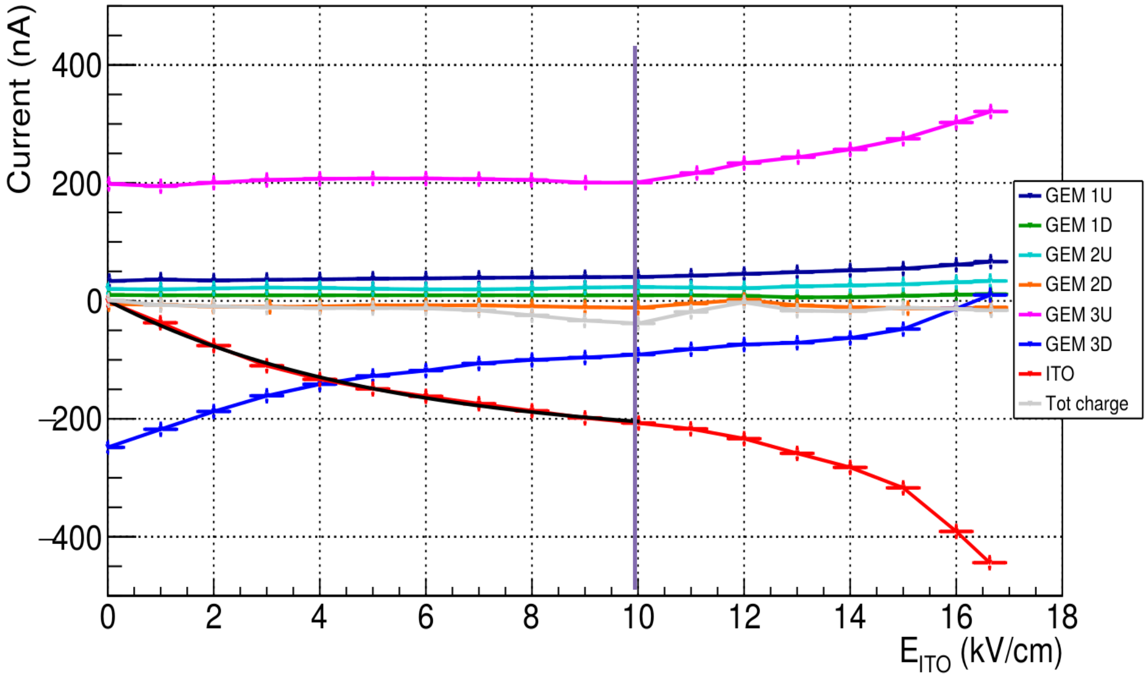

- Total sum of the charge is zero (gray)
- 3U collects ions from 3rd stage of amplification (magenta)
- ITO (red) and 3D (blue) share the electrons generated by the amplification

Charge Analysis

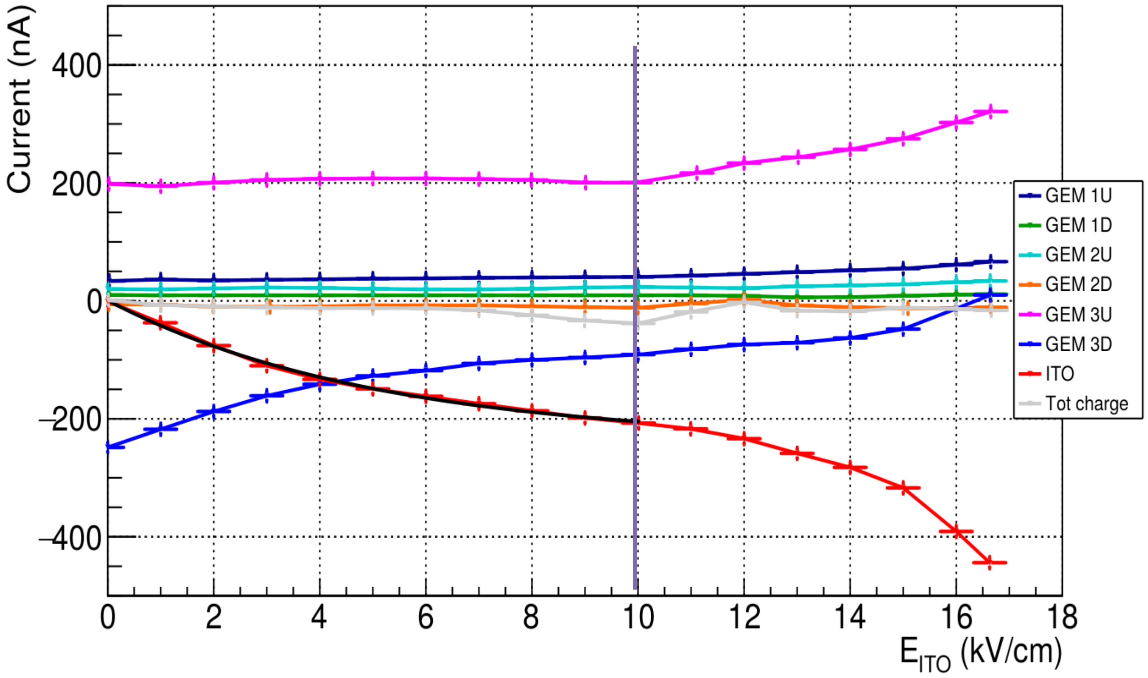

- Total sum of the charge is zero (gray)
- 3U collects ions from 3rd stage of amplification (magenta)
- ITO (red) and 3D (blue) share the electrons generated by the amplification
- If any new charge is generated in the induction:
  - 3D and 3U collect the ions
  - ITO only collects electrons

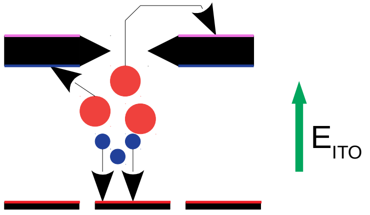

Charge Analysis

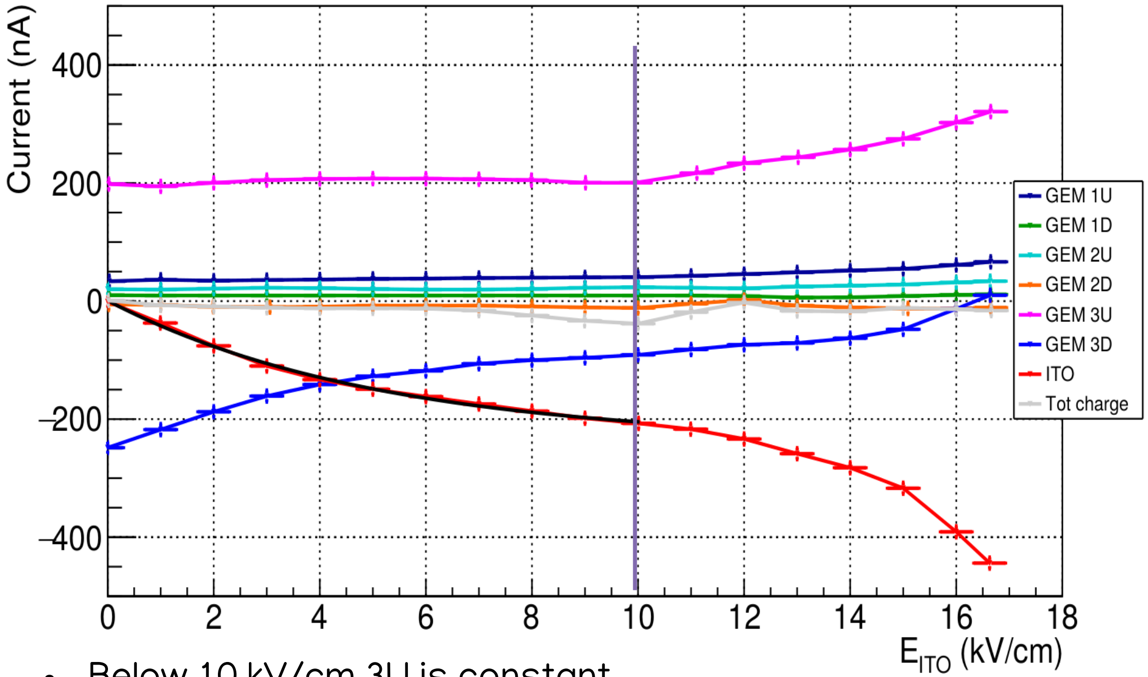

- Below 10 kV/cm 3U is constant
- Above 10 there is a rise in charge → **Charge is produced**
- The amount of charge created can be evaluated from the ITO after taking into account for the sharing of electrons between 3D and mesh

- Total sum of the charge is zero (gray)
- 3U collects ions from 3rd stage of amplification (magenta)
- ITO (red) and 3D (blue) share the electrons generated by the amplification
- If any new charge is generated in the induction:
  - 3D and 3U collect the ions
  - ITO only collects electrons

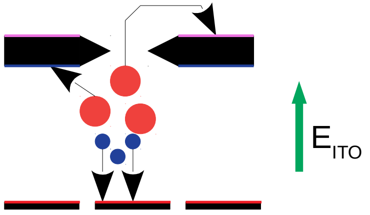

Result

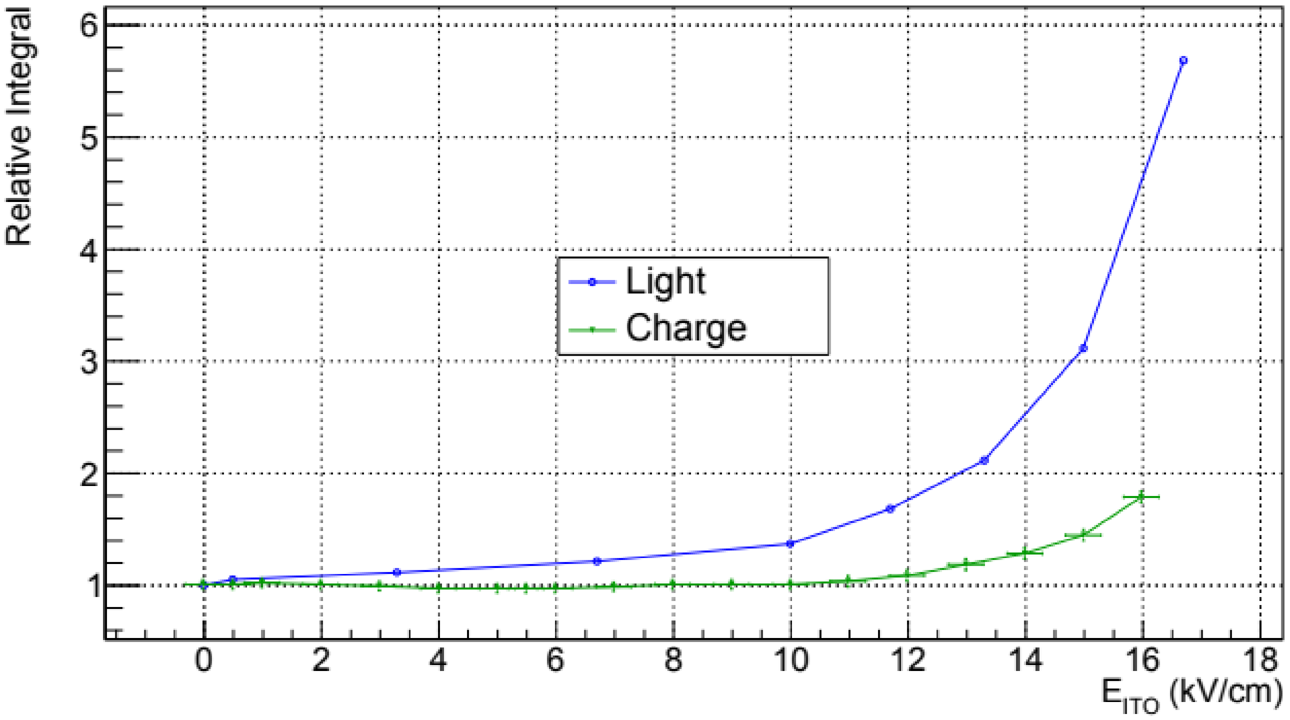

- Clear increase in light yield
- Since 10 kV/cm charge is produced but it is considerably less than the light

Light increment far exceeds the extra charge produced

Induction Field

- Fixing the voltage across the GEMs and increasing the induction field

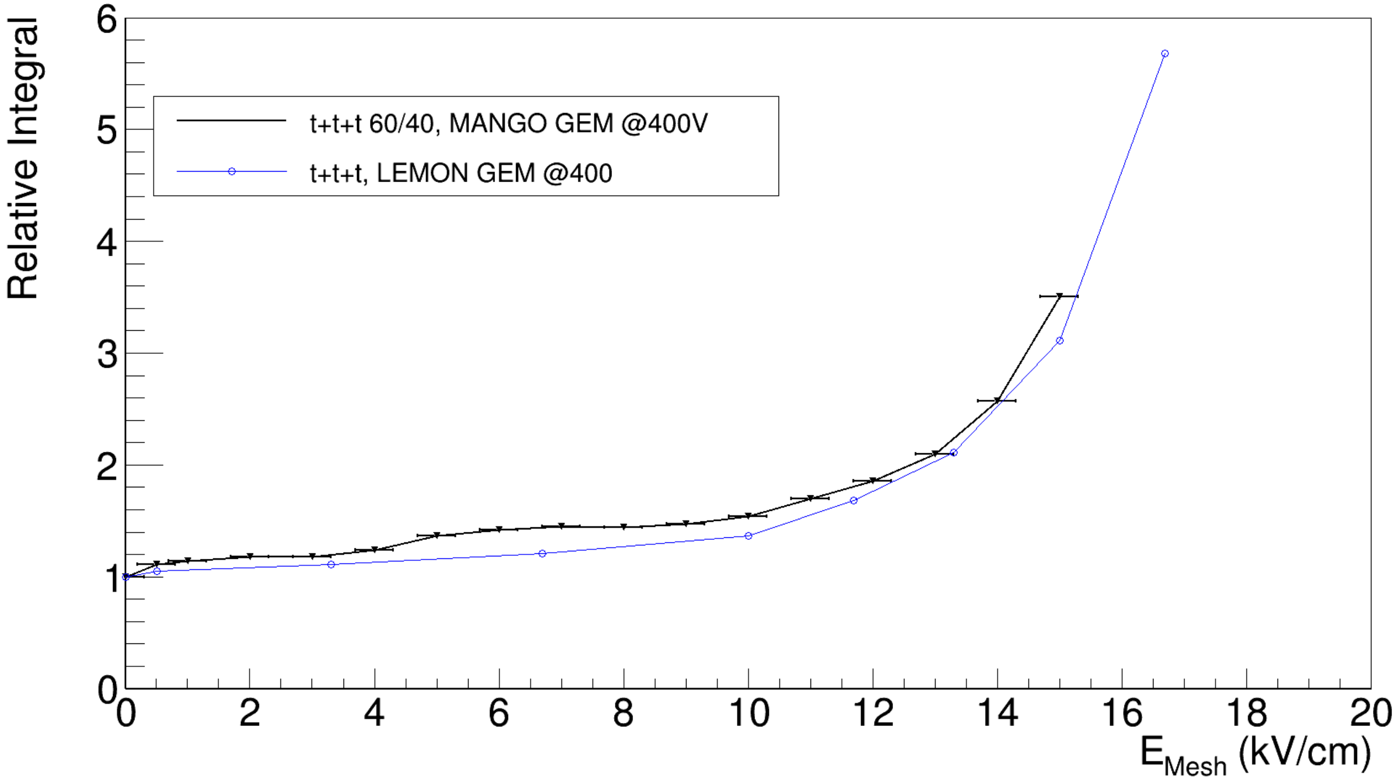

Nice consistency between the two detectors

Diffusion Measurement

- ^{55}Fe emits X-rays of 5.9 keV which induce ERs travelling for O(100) μm in the gas
- The diffusion contribution prevails over the topology of the original track → Round spots on camera images
- Given the extremely small drift gap, the intrinsic diffusion of the **amplification stage dominates**
- A double Gaussian fit is applied to the spatial distribution of the overlap of all the ^{55}Fe signal once their barycentres are aligned
- Method independent of the light intensity

Average spatial projection of the superimposed ^{55}Fe spots

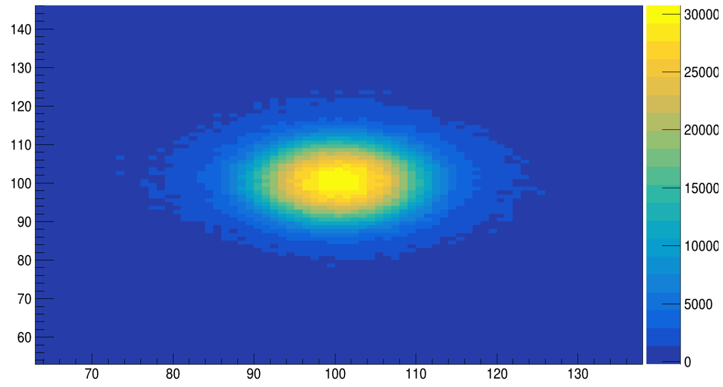

Primary sigma taken as the estimation of diffusion

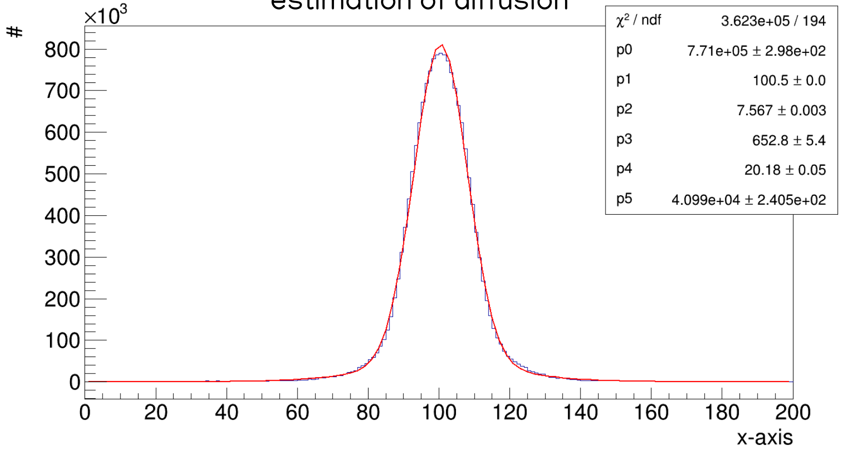

Increase at Low Field

Increase due to better defined field lines below the last GEM (Maxwell)

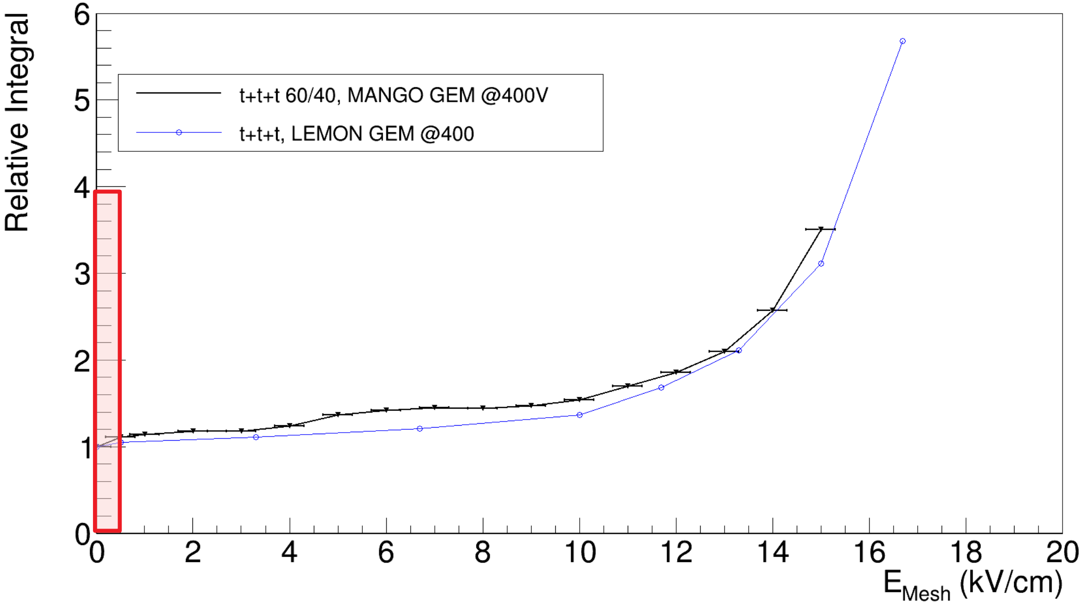

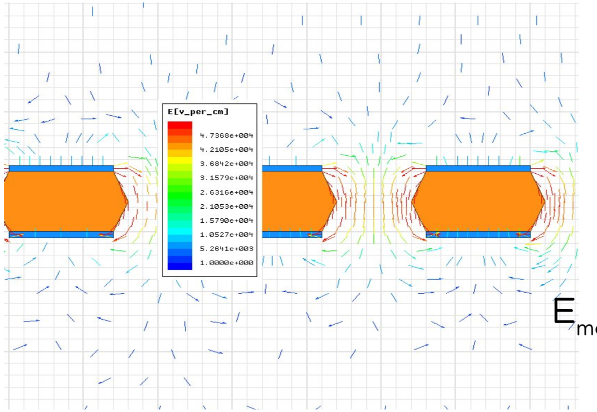

E_{mesh} = 0 kV/cm

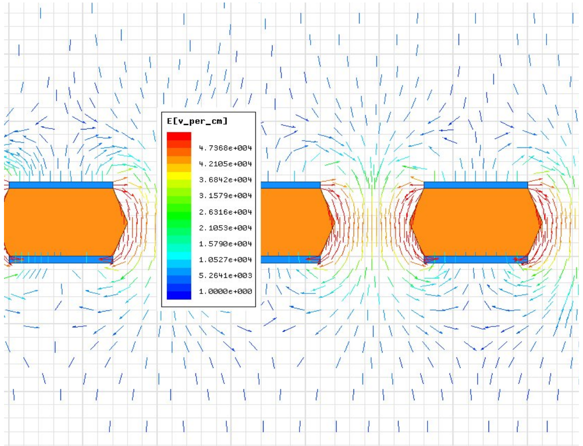

E_{mesh} = 1 kV/cm

ENERGY RESOLUTION

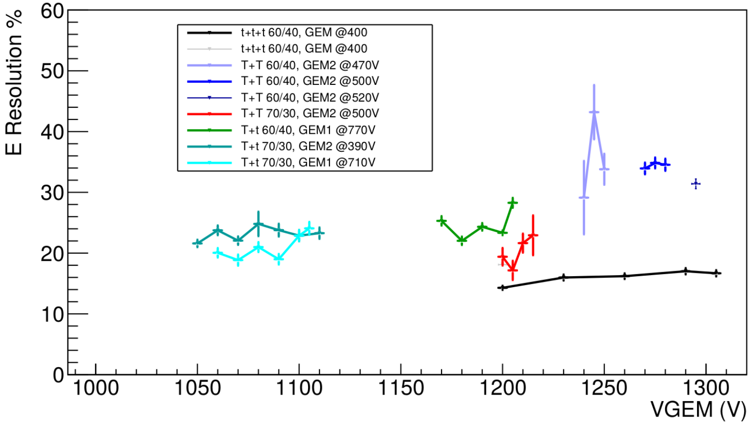

$$\sigma_E^2 = \left(\frac{\sigma_{n_0}}{n_0}\right)^2 + \frac{1}{n_0}\left(\frac{\sigma_A}{\bar{A}}\right)^2 = \left(\frac{F}{n_0}\right) + \frac{1}{n_0}\left(\frac{\sigma_A}{\bar{A}}\right)^2$$

Depends on a function χ: Alkhazov, NIM, 89 (1970)

the larger χ, the smaller σ_A

Favours large reduced fields: *ttt*

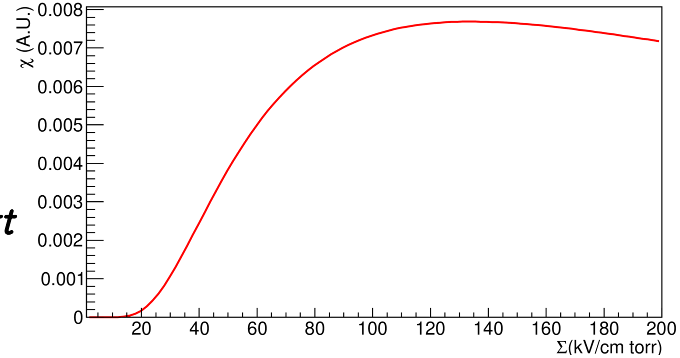

LIGHT AND CHARGE GENERATION

- The induction field modifies the structure of the electric field inside the GEM hole allowing light and charge production in a larger region

- Why more light than charge?

- Light produced by neutral fragmentation, charge from ionising fragmentation

Process	Threshold (eV)	Energy loss (eV)
Direct vibrational excitation ν_4 ν_3	0.078 0.159	0.078 0.159
Indirect vibrational excitation	4.0	0.4
Electron attachment	4.3	4.3
Electronic excitation (dissociation into neutral fragments)†	12.5 (10)	12.5 (10)
Dissociative ionization†	15.9	15.9

Neutral Fragmentation (14)
First ionisation (7)

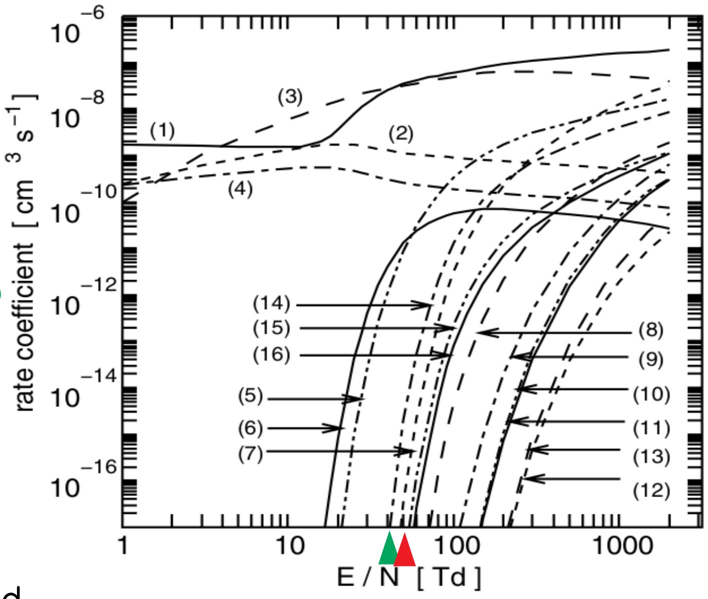

Kurihara et al, JPD, 33 (17) (2000)

- Cross section of pure CF_4
- It may change with He
- Large difference in energy threshold among CF_4 and He

- Passing from 0 to high field, light is first produced

SF$_6$ Properties

Christophorou et al, JPC, 29 (3) (2000)

- Given the high electronegativity electron are capture within 1 μm from liberation point and generate SF_6^{*-}

$$SF_6^{-*} \rightarrow SF_6 + e^- \qquad \text{(auto-detachment)}$$

Auto-detachment half life O(1–10^3) μs

$$SF_6^{-*} + SF_6 \rightarrow SF_6^- + SF_6 \qquad \text{(collisional stabilisation)}$$

$$SF_6^{-*} \rightarrow SF_5^- + F \qquad \text{(auto-dissociation)}$$

Minority carriers

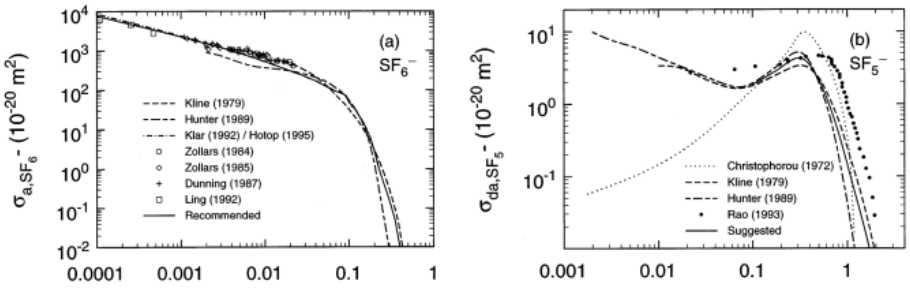

- To extract electrons

$$SF_6^- + SF_6 \rightarrow SF_6 + SF_6 + e$$

High threshold 90 eV (c.m.)

$$SF_6^- + SF_6 \rightarrow SF_6 + SF_5^- + F$$

$$SF_5^- + SF_6 \rightarrow SF_5 + SF_6 + e$$

Threshold of ~30 eV (c.m.)

$$SF_6^- + SF_6 \rightarrow F^- + SF_5 + SF_6$$

$$F^- + SF_6 \rightarrow F + SF_6 + e$$

Threshold of ~8 eV (c.m.)

Collisions at high field (375 Td) generate fluorine ions which can more easily lose an electron

Setup Crosscheck

- The σ_0 term is not always constant in NID analysis
- Can it affect the ξ measurement?
- Test with ED mixture keeping same drift field and modifying the voltage across GEMs

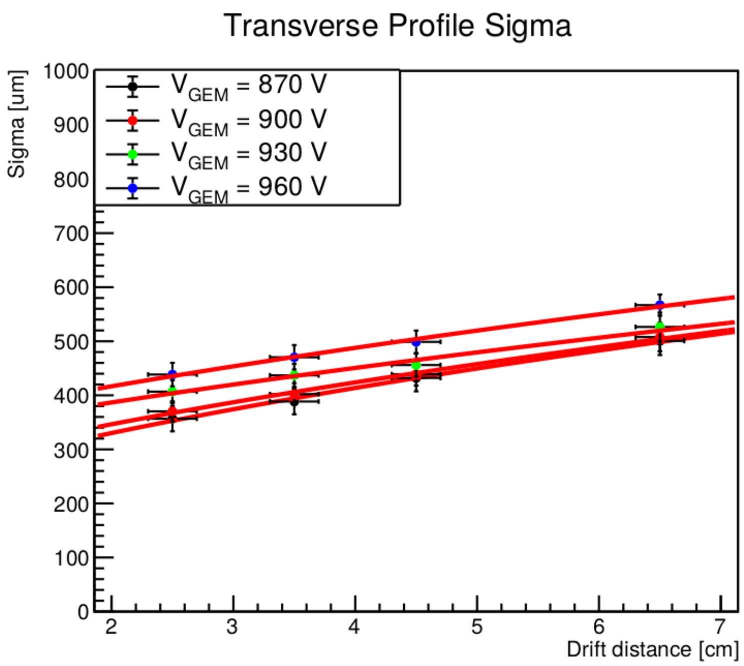

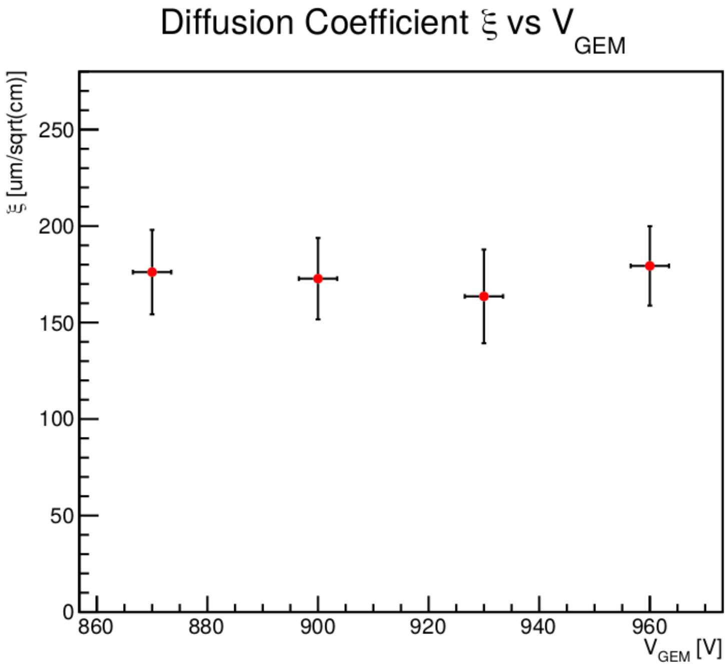

Thermal Limit

- Blum, Rolandi, Riegler book and the free path theory of *Kinetic Theory of Mobility and Diffusion* (John Wiley) suggest the thermal limit of any ion or electron to be:

$$\sigma^2 = \frac{2k_B T L}{eE}$$

- Our results are sound, but appear well below thermal limit

- The approximations on the cross section between ions are key as inelastic terms can induce an effective temperature below room temperature

- Calculating these cross section is extremely hard (molecular gases with vibrational energy levels)

- Some other experimental results showed how light gases could *reduce* the temperature of the drifting particles

Martoff et al, D.A.E., 440 (2) (2000)

Ohnuki et al, NIM A, 463 (2001)

Dion PhD thesis

- More studies planned

GSI

Element Probability Calculation

$$N_{DMevt,i} = tV\frac{P}{P_{atm}}\frac{T_0}{T}\rho_i\frac{N_0}{A_{mol,i}}\frac{2\rho_0\sigma_{n,SI}}{m_\chi^2 r_i}\frac{\mu_{A,i}^2}{\mu_n^2}A_i^2 I_i^{E\gamma}(m_\chi, E_{thr,i})$$

$$I^{E\gamma}(m_\chi, E_{thr}) = \int_{E_{thr}}^{E_{max}} dE \int_{-1}^{1} d\cos\gamma S(E)\pi\frac{v_p^3}{v_{lab}}\alpha' \times \left(e^{-\frac{\left(\frac{\sqrt{2m_A E}}{2\mu_A} - v_{lab}\cos\gamma\right)^2}{v_p^2}} - e^{-\frac{v_{esc}^2}{v_p^2}}\right)$$

- t the time of exposure;
- V the volume of the detector;
- P the working pressure of the gas;
- P_{atm} the atmospheric pressure;
- T the working temperature expressed in Kelvin;
- T_0 the temperature of 0 degrees Celsius expressed in Kelvin;
- ρ_i the gas density at atmospheric pressure and 0 degrees Celsius;
- N_0 the Avogadro number;
- $A_{mol,i}$ the molar mass of the gas;
- ρ_0 the local DM density (Section 2.1);
- $\mu_{A,i}$ the reduced mass between the WIMP mass and the mass of the nucleus A defined as in Equation 2.5;
- μ_n the reduced mass between the WIMP mass and the mass of the nucleon;
- A_i the atomic mass of the nucleus;
- $I_i^{E\gamma}(m_\chi, E_{thr,i})$ the velocity distribution integrated in the velocity, energy and angle after the Radon transformation (see Section 2.1.5).

Considering gas mixtures with poliatomic gases

$$N_{DMevt} = tV\frac{P}{P_{atm}}\frac{T_0}{T}\sum_i^{n_{mol}}\sum_j^{n_{el,i}}\rho_i k_i\frac{N_0}{A_{mol,i}}N_{at,i,j}\frac{2\rho_0\sigma_{n,SI}}{m_\chi^2 r_j}\frac{\mu_{A,j}^2}{\mu_n^2}A_j^2 I_j^{E\gamma}(m_\chi, E_{thr,j})$$

- k — portion of *ith* gas in gas mixture
- j — runs on atoms
- i — runs on molecules
- $N_{a,i,j}$ — number of j atoms in molecule i

$$F_{i,j} = \rho_i k_i\frac{N_{at,i,j}}{A_{mol,i}}\frac{2}{r_j}\mu_{A,j}^2 A_j^2 I_j^{E\gamma}(m_\chi, E_{thr,j})$$

$$P_X = \frac{N_{DMevt,X}}{N_{DMevt}} = \frac{\sum_i^{n_{mo}} F_{i,X}}{\sum_i^{n_{mo}}\sum_j^{n_{el,i}} F_{i,j}}$$

GSSI

SUPERNOVA DARK MATTER (SNDM)

$$\mathcal{L} \supset \frac{e\epsilon g_d}{\Lambda^2}\bar{\chi}\gamma_\mu\chi J^\mu_{\rm em}$$

- Dark fermion of O(1–100) MeV/c² mass coupled to SM via dark photon
- Could be generated in SN explosion and couple to electrons

DeRocco et al, PRD, 100 (7) (2019)

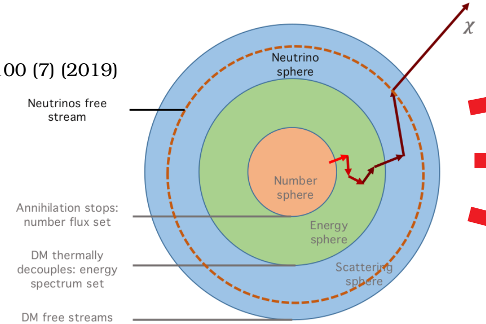

Flux of DM **MeV** particles with **semirelativistic** velocity → **can induce keV recoils on nuclei**

- The Maxwell–Boltzmann distribution of their velocity induces a spread in time of arrival → **Diffuse flux from Galaxy**
- Most of SN are in the centre of the Galaxy

Negligible contribution from extragalactic SN

Baracchini et al, PRD, 102 (7) (2020)

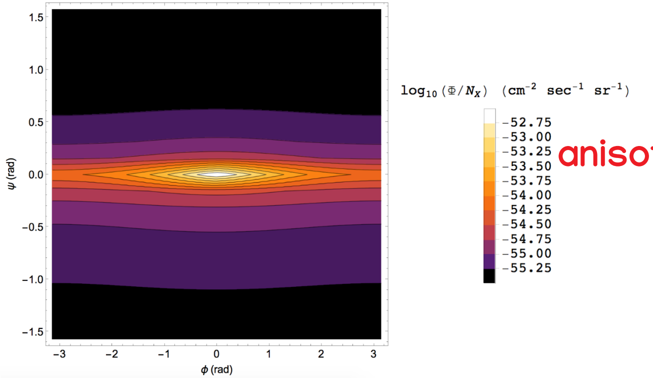

anisotropic flux

Mass of the particle — Equilibrium temperature at the decoupling — Proportional to coupling constant — Gravitational redshiftRedshift

SNDM Mass [MeV/c²]	T [MeV]	$\log_{10} y$	Φ
5	0.31	-13.3	0.006
7	1.0	-14.3	0.02
9	1.6	-14.6	0.03
5	0.52	-14.0	0.01
14	3.0	-15.0	0.07
38	13.4	-16.0	0.1

Scenarios 2D Angle